UNIVERSIDADE FEDEREAL DE SANTA CATARINA
CENTRO DE CIÊNCIAS DA SAÚDE
PROGRAMA DE PÓS-GRADUAÇÃO EM FARMÁCIA

Bianca da Costa Bernardo Port

Estudos de formulações com dapsona: caracterização de cristais em géis comerciais e desenvolvimento de nanoemulsões

Florianópolis
2022

Bianca da Costa Bernardo Port

Estudos de formulações com dapsona: caracterização de cristais em géis comerciais e desenvolvimento de nanoemulsões

Dissertação submetida ao Programa de Pós-Graduação em Farmácia da Universidade Federal de Santa Catarina como requisito parcial para a obtenção do título de título de Mestra em Farmácia

Orientador: Prof. Thiago Caon, Dr.

Florianópolis – SC

2022

Ficha de identificação da obra elaborada pelo autor,
através do Programa de Geração Automática da Biblioteca Universitária da UFSC.

Port, Bianca da Costa Bernardo
Estudos de formulações com dapsona: caracterização de cristais em géis comerciais e desenvolvimento de nanoemulsões / Bianca da Costa Bernardo Port ; orientador, Thiago Caon, 2023.
145 p.

Dissertação (mestrado) - Universidade Federal de Santa Catarina, Centro de Ciências da Saúde, Programa de Pós Graduação em Farmácia, Florianópolis, 2023.

Inclui referências.

1. Farmácia. 2. Dapsona. 3. Cristais. 4. Nanoemulsão. I. Caon, Thiago . II. Universidade Federal de Santa Catarina. Programa de Pós-Graduação em Farmácia. III. Título.

Bianca da Costa Bernardo Port

Estudos de formulações com dapsona: caracterização de cristais em géis comerciais e desenvolvimento de nanoemulsões

O presente trabalho em nível de mestrado foi avaliado e aprovado, em 16 de dezembro de 2022, pela banca examinadora composta pelos seguintes membros:

Prof. Luis Felipe Costa Silva, Dr.
Universidade Federal de Santa Catarina

Prof.(a) Tatiane Cogo Machado, Dr.(a)
Faculty of Medical Sciences, Newcastle University

Certificamos que esta é a **versão original e final** do trabalho de conclusão que foi julgado adequado para obtenção do título de Mestra em Farmácia pelo Programa de Pós-Graduação em Farmácia.

Profa. Thaís Cristine Marques Sincero. Dra
Coordenação do Programa de Pós-Graduação

ICP-Edu
Documento assinado digitalmente
Thiago Caon
Data: 06/03/2023 23:44:10-0300
CPF: ***.048.259-**
Verifique as assinaturas em https://v.ufsc.br

Prof. Thiago Caon, Dr.
Orientador

Florianópolis - SC, 2022.

AGRADECIMENTOS

Agradeço primeiramente a Deus por ter me proporcionado oportunidades para chegar até aqui, e me guiado durante toda minha jornada acadêmica.

À minha família, meu marido Leonardo Port, meus pais Ana Paula e Elson Bernardo e minha irmã Beatriz Bernardo, por todo apoio e motivação para superar as dificuldades, pela dedicação e paciência contribuindo diretamente para que pudesse ter uma jornada mais leve e por entenderem minha ausência em diversos momentos importantes.

Ao Prof. Dr. Thiago Caon, pela orientação, pela disposição em ajudar e contribuir para um melhor aprendizado e pela confiança depositada, me estimulando na busca de novos conhecimentos.

À Drª Débora Fretes Argenta, pela sua disponibilidade e paciência, pelos seus ensinamentos e correções, e por todo incentivo e auxílio necessário para a elaboração desse trabalho.

À Drª Gabriela pelo suporte, ensinamentos e constante incentivo durante todas as etapas deste trabalho, particularmente durante a pandemia.

Aos colegas de mestrado Nicole, Júlia, Izi e Douglas, pelo apoio e por serem sempre solícitos.

À Fundação para o Remédio Popular pela doação do fármaco para a pesquisa e a empresa Lipid Ingredientes & Technologies que gentilmente forneceu o Phosal 50+®.

A todos os colegas do Laboratório de Farmacotécnica pelo convívio e apoio.

À Isabela Di Pá e a Prof. Dra. Izabella Thaís da Silva pela disponibilidade e suporte nos ensaios biológicos.

À banca examinadora pela disponibilidade e contribuições.

À CAPES e CNPQ pela bolsa e apoio financeiro deste projeto. À UFSC e ao PGFar por disponibilizarem toda a infraestrutura necessária para a execução deste projeto.

A todos que direta ou indiretamente colaboraram na execução deste trabalho e na minha formação acadêmica e que não foram aqui mencionados.

RESUMO

A administração da dapsona na pele (DAP) tem sido considerada a fim de eliminar efeitos adversos sistêmicos. Géis tópicos indicados para acne já são disponíveis comercialmente. Estas formulações têm como particularmente a presença de fármaco solúvel e insolúvel em um mesmo sistema. Tendo em vista que a patente destas formulações não traz detalhes a respeito da proporção de fármaco dissolvido/não dissolvido, bem como da fase sólida presente, a primeira etapa deste estudo visou responder a estes questionamentos. Géis de DAP foram preparados misturando-se uma solução orgânica contendo DAP com uma solução aquosa contendo polímeros e conservantes. Os agentes solubilizantes selecionados foram o etoxidiglicol (DEGEE), polietilenoglicol (PEG) e 1-metil-2-pirrolidona (MPR). A forma sólida foi identificada por difração de raios X (DRX) e técnicas microscópicas. A DAP dissolvida nas formulações foi quantificada por espectrofotometria UV/Vis. Diferentes formas cristalinas foram identificadas dependendo do agente solubilizante utilizado. Na presença de DEGEE e PEG, as formas cristalinas prevalentes foram hidrato e solvato de PEG, respectivamente. Na presença de MPR, uma mistura de hidrato e solvato foi encontrada. A análise microscópica dos géis mostrou partículas com hábitos cristalinos heterogêneos. Para a formulação com MPR (FMP), observou-se quantidade de DAP dissolvida quatro vezes maior em relação às outras formulações. Géis com maior quantidade de cristais mostraram maior acúmulo na região dos folículos pilosos. Frente a estes resultados, sugere-se cautela com relação à substituição do agente solubilizante em géis tópicos, particularmente quando há fármaco na forma sólida, pois isto pode alterar a quantidade de cristais, forma cristalina do fármaco, com impacto direto na performance do produto. A segunda etapa deste estudo envolveu o desenvolvimento de nanoemulsões tópicas de DAP e óleo de chaulmoogra (CH) pela técnica de emulsificação espontânea. A combinação destes ativos é vantajosa no tratamento da hanseníase pela possibilidade de um sinergismo de ação. As nanoemulsões ótimas mostraram um tamanho de partícula médio de 146,76 ± 0,2 nm, índice de polidispersão de 0,171 ± 0,1, potencial zeta de -38,3 ± 0,1 e pH 4,5. As nanoemulsões não apresentaram modificações significativas destes parâmetros ao final de 60 dias a 25 ºC, e o no estudo de estabilidade acelerada, NEs com CH se mostraram mais estáveis. A presença do CH também aumentou a permeação/retenção de DAP em pele humana, sendo que este efeito pode estar associado a ácidos graxos presentes no óleo, os quais atuariam como promotores de absorção. De fato, maior desordem de regiões lipídicas da pele foi confirmada pela análise de FT-IR após tratamento com a formulação com maior proporção de CH. Na avaliação do efeito cicatrizante pelo ensaio de "scratch", tanto a forma livre quanto nanoencapsulada do CH mostraram melhorias significativas nos eventos de migração celular. Estes resultados sugerem que a inclusão do CH em nanoemulsões de DAP pode conferir vários benefícios: (1) aumento da atividade; (2) melhora da estabilidade e (3) de processos cicatriciais (comum em pacientes com hanseníase). Estudos *in vivo* ainda são necessários para confirmar os benefícios aqui encontrados.

Palavras chaves: dapsona; óleo de chaulmoogra; géis; caracterização no estado sólido; nanoemulsões.

ABSTRACT

The percutaneous administration of dapsone (DAP) has been considered in order to avoid or reduce systemic adverse effects. Topical gels indicated for acne are already commercially available. These formulations are characterized by the presence of soluble and insoluble drug in a same system. Considering that the patent of these formulations does not provide details on the proportion of dissolved/crystalline drug, as well as the solid phase present, the first step of this study aimed to investigate these aspects. DAP gel formulations were prepared by mixing an organic solution containing DAP with an aqueous solution containing polymers and preservatives. The solubilizing agents selected were ethoxydiglycol (DEGEE), polyethylene glycol (PEG) and 1-methyl-2-pyrrolidone (MPR). The solid forms were identified by X-ray diffraction pattern analysis (PDRX) and microscopic techniques. The DAP in the dissolved form was quantified in a UV/Vis spectrophotometer. Different crystalline phases/forms were identified depending on the solubilizing agent used. In the presence of DEGEE and PEG, the prevalent crystalline forms were PEG hydrate and solvate, respectively. In MPR, a mixture of hydrate and solvate was found. Microscopic analysis of the gels showed crystals with heterogeneous crystalline habits. For the gel with MPR (FMP), a four times greater amount of dissolved DAP was observed. Gel formulations with a greater number of crystals showed a preferential accumulation in the region of hair follicles. Therefore, the substitution of the solubilizing agent in topical gels should be carefully performed as it can affect the number of crystals, the crystalline form of the drug, which impact on the performance of the product. The second step of this study involved the development of topical nanoemulsions of DAP and chaulmoogra oil (CH) by the spontaneous emulsification technique. The combination of these actives is advantageous in the treatment of leprosy due to the possibility of a synergistic action. The optimal nanoemulsions showed an average particle size of 146.76 ± 0.2 nm, polydispersity index of 0.171 ± 0.1, zeta potential of -38, 3 ± 0.1 and pH 4.5. The nanoemulsions did not show significant changes in these parameters after 60 days at 25 ºC. In the accelerated stability study, NEs with CH were more stable. The presence of CH also increased the permeation/retention of DAP in human skin, and this effect may be associated with the action of fatty acids from the CH, which would act as chemical penetration enhancers. In fact, greater disorder of skin lipid domains was confirmed by the FT-IR analysis of the skin after treatment with the formulations prepared with the highest CH content. During the evaluation of the healing effect by the scratch assay, both the free and nanoencapsulated CH significantly improved cell migration events. These results suggest that the inclusion of CH in DAP nanoemulsions may provide several benefits: (1) increased activity; (2) enhanced stability and (3) improved healing processes (cutaneous lesions are common in leprosy patients). *In vivo* studies should be performed to confirm these benefits found here.

Keywords: dapsone, chaulmoogra oil, gel formulation, solid-state characterization, nanoemulsions.

LISTA DE FIGURAS

Capítulo I - Revisão Bibliográfica

Capítulo II – Artigo publicado

Capítulo III – Artigo a ser submetido para avaliação

LISTA DE TABELAS

Capítulo II – Caracterização de cristais em géis comerciais de dapsona

Capítulo III – Desenvolvimento de nanocarreadores com óleo de chaulmoogra e investigação do efeito cicatrizante

LISTA DE ABREVIATURAS E SIGLAS

API - *Active pharmaceutical ingredient*

AUC – Área sob a curva

CH - Chaulmoogra

CLN – Carreados nanoestruturado lipídico

C_{max} – Concentração máxima do fármaco no sangue

DAP – Dapsona / *Dapsone*

DEGEE – Etoxidiglicol / *Ethoxydiglycol*

DHF - Diidrofolato

DHP - Diidropteroato

DPHS – Diidropteroato sintase

FDA – Food and drug administration

G6PD – Glicose-6-fosfato desidrogenase / *Glucose-6-phosphate dehydrogenase*

MB – Multibacilar

ME – Microemulsão

MPR – 1-metil-2-pirrolidona / *1-methyl-2-pirrolidone*

NE – Nanoemulsão

NLS – Nanopartícula lipídica sólida

OMS – Organização Mundial da Saúde

PABA - Ácido para-aminobenzóico

PB – Paucibacilar

PBPK - *Physiologically based pharmacokinetics*

PHO - Phosal

PXRD - *Powder X-ray Diffraction*

PEG – Polietilenolglicol / *Polyethylene glycol*

T_{max} – Tempo necessário para atingir a C_{max}

THF – Tetaidrofólico

SUMÁRIO

1 INTRODUÇÃO

A dapsona é uma sulfona sintética que tem ação anti-inflamatória e antimicrobiana, fato que tem contribuído para sua permanência no mercado por décadas. Sua atividade antibiótica é explicada principalmente pela inibição competitiva do ácido para-aminobenzóico (PABA), substrato da enzima dihidropteroato sintase, essencial na produção de folato bacteriano (BARAN et al., 2011; GEORGE, 2020). Seu efeito anti-inflamatório está associado à inibição da interleucina 8 (IL-8), impedindo a aderência dos neutrófilos nos tecidos inflamados bem como diminuição da produção de espécies reativas de oxigênio geradas a partir da enzima mieloperoxidase (WOZEL; BLASUM, 2014; MOLINELLI et al., 2019). Embora a síntese deste composto tenha ocorrido em 1908, somente depois de três décadas é que seu potencial terapêutico foi explorado. Desde então, a DAP vem sendo utilizada no tratamento de desordens tais como hanseníase, acnes vulgar e dermatite herpetiforme (WOZEL, 2010).

A acne é uma doença de pele comum que afeta cerca de 79 a 95% dos adolescentes e 40 a 54% dos adultos acima de 25 anos (CORDAIN et al., 1998). A fisiopatologia da acne envolve a inflamação das unidades pilosebáces, hiperqueratinização dos folículos, excesso de secreção de sebo e colonização do *Propionibacterium acnes.* Como consequência, lesões inflamatórias e não inflamatórias acabam afetando principalmente o rosto, mas também a região das costas e o peito (MOHIUDDIN, 2019). O aspecto das lesões juntamente com os sintomas clínicos serve como base para a classificação da doença em acne leve, moderada e grave (POCHI et al., 1991; DAWSON; DELLAVALLE, 2013). Esta classificação é utilizada para ajudar a definir o tratamento, que pode incluir medicamentos orais e tópicos como anti-inflamatórios, antibióticos, retinoides, estrogênios e antiandrogênios (KERI; SHIMAN, 2009). Devido as suas atividades biológicas anteriormente descritas, a DAP tem se mostrado eficaz no tratamento da acne inflamatória (SARDANA et al., 2015).

A hanseníase, por sua vez, é uma doença causada pela infecção do *Mycobacterium leprae* com sintomas que se manifestam na pele e no sistema nervoso periférico. Foi considerada como uma doença incurável por anos, porém, este cenário foi se modificando com o advento das sulfanilamidas em 1940 (KAR; GUPTA, 2015). Antes mesmo de se difundir o uso desses compostos sintéticos, a lepra era tratada com o óleo de chaulmoogra (PARASCANDOLA, 2003). Atualmente, cepas resistentes têm sido encontradas, o que levou a OMS a definir um esquema terapêutico polimedicamentoso com doses diárias de dapsona e clofazimina, ambos autoadministrados, e doses mensais de rifampicina e clofazimina com administração supervisionada (OMS, 2018). As doses diárias recomendadas para a DAP é 100

mg para adultos e entre 50 a 100 mg para crianças (LOCKWOOD et al., 2010). Após a administração oral, cerca de 86% do fármaco é absorvido no intestino, alcançando a circulação entero-hepática (AHMAD; ROGERS, 1980). No fígado, a DAP é metabolizada por reações de acetilação e hidroxilação. Esta última reação gera metabólitos responsáveis pelos efeitos adversos hematológicos tais como anemia hemolítica e metemoglobinemia (EZHILARASAN, 2021). Além disto, efeitos gastrointestinais tais como dor abdominal, náusea e vômito podem ser observados (MOLINELLI et al., 2019).

Para reduzir estes efeitos colaterais, evitar o metabolismo de primeira passagem no fígado e garantir um maior controle da liberação da dapsona, sua aplicação através da pele pode ser considerada. Pacientes com hanseníase apresentam várias complicações dermatológicas (pápulas, tubérculos, nódulos) uma vez que o bacilo de Hansen tem preferência por áreas mais frias, o que torna ainda mais interessante o uso desta rota. No caso da acne, não há necessidade de expor os pacientes a riscos sistêmicos já que a pele é o principal local afetado. Formulações tópicas de DAP para o tratamento da acne já se encontram disponíveis comercialmente. Trata-se de géis aquosos, os quais são constituídos de uma fração solúvel (dissolvida) e outra fração insolúvel (não dissolvida) do fármaco, que alcançam o alvo folicular por mecanismos distintos. A fração dissolvida da DAP é particionada do estrato córneo da epiderme para as camadas mais profundas da pele; alcançando o folículo de modo inespecífico (região de interesse na acne). A fração não dissolvida, por sua vez, onde a DAP aparece na forma de microcristais, é direcionada ao folículo e forma reservatórios para uma entrega sustentada do ativo. Para o preparo destas formulações, soluções orgânicas de DAP são misturadas a uma solução aquosa contendo polímeros e conservantes (STOTLAND et al., 2009; AL-SALAMA; DEEKS, 2017; FDA, 2020). Patentes mencionam proporções variadas de água: solvente orgânico, bem como o uso de diferentes solventes orgânicos para solubilizar a DAP, sem qualquer estudo detalhado da fase sólida obtida. Assim, a primeira parte deste estudo investigou como a variação da composição do veículo de tais formulações afetam a forma sólida, bem como tamanho e morfologia dos microcristais. A hipótese inicial era que, de fato, a natureza e a concentração dos excipientes são críticas, uma vez que a DAP tem inúmeras formas cristalinas já descritas na literatura (polimorfos, hidrato e vários solvatos).

Nanopartículas também tem sido considerada como veículo para a DAP em vários estudos recentes ((MAHORE et al., 2017; ELMOWAFY et al., 2019). Como vantagens, estes sistemas são capazes de aumentar a solubilidade, absorção, estabilidade físico-química e garantir um maior controle da liberação de fármacos (MULLER et al., 2000). Nanoemulsões tem sido um dos veículos mais tradicionalmente estudados (MONTEIRO et al., 2012; BORGES

et al., 2013). Caracterizam-se como sistemas bifásicos (uma fase oleosa e outra aquosa), estabilizados por tensoativos e co-tensoativos. A interface lipídica destes sistemas apresenta alta afinidade por membranas biológicas, as quais também são constituídas majoritariamente por lipídeos, proporcionando alta biocompatibilidade e interação (MASON et al., 2006). Frente a isto, a segunda proposta deste estudo consistiu no desenvolvimento de nanoemulsões de DAP. Em relação a outros sistemas nanoemulsionados disponíveis na literatura, o diferencial do sistema proposto é a inclusão do óleo de chaulmoogra na fase oleosa. Além de atuar como promotor químico de absorção, este óleo possui atividade antimicrobiana frente ao *Mycobacterium leprae* já descrita (NORTON, 1994) bem como efeito pró-cicatrizante em lesões cutâneas (Oommen et al., 1999; Oommen et al., 2000). A inclusão de um ativo adicional é particularmente relevante nos casos de resistência da doença e para reduzir a concentração de fármacos que apresentam problemas de toxicidade relacionados a dose. Diferentemente de combinações de fármacos sintéticos, a seleção de materiais vegetais traz impactos relevantes em termos de segurança.

2 OBJETIVOS

2.2 Objetivo geral

Avaliar o impacto de diferentes agentes solubilizantes no hábito cristalino, tamanho e morfologia de microcristais de dapsona veiculada em géis e desenvolver nanoemulsões contendo este fármaco combinado com óleo de chaulmoogra para aplicação na pele.

2.2 Objetivos específicos

- *Avaliar a solubilidade termodinâmica da DAP em diferentes proporções de agentes solubilizantes (DEGEE, MPR e PEG) através do método de agitação em frascos;*
- *Caracterizar a forma sólida da DAP presente em meios contendo diferentes proporções de agentes solubilizantes através da difração de raios-X (DRX);*
- *Reproduzir/preparar as formulações descritas nas patentes;*
- *Avaliar a solubilidade da DAP nas formulações reproduzidas;*
- *Caracterizar a forma sólida da dapsona presente nestas formulações através difração de raios-X (DRX) e análise microscópica;*
- *Avaliar a distribuição dos cristais em pele humana abdominal;*
- *Desenvolver nanoemulsões com DAP e óleo de chaulmoogra através do método de emulsificação espontânea;*
- *Avaliar o efeito da concentração dos agentes emulsionantes e do óleo de chaulmoogra nas características das nanoemulsões;*
- *Caracterizar as nanoemulsões quanto ao tamanho de partícula, carga de superfície, índice de polidispersão (PDI), teor e eficiência de encapsulação;*
- *Avaliar a estabilidade das nanoemulsões;*
- *Avaliar o perfil de liberação do fármaco a partir das nanoemulsões otimizadas utilizando o modelo do saco de diálise;*
- *Avaliar o impacto da nanoencapsulação na permeação/retenção cutânea da DAP através do modelo de difusão em câmara de Franz;*
- *Avaliar a citotoxicidade in vitro do óleo de chaulmoogra antes e após a sua nanoencapsulação através do ensaio da sulforrodamina B;*

- *Avaliar o efeito pró-cicatrizante do óleo de chaulmoogra antes e após a sua nanoencapsulação pelo método de "scratch".*

3 CAPÍTULO I - REVISÃO BIBLIOGRÁFICA

3.1 Dapsona

3.1.1 Características físico-químicas

A dapsona é uma amina aromática pertencente à família das sulfonas. É quimicamente denominada como 4,4-sulfonilbisbenzenamina, apresenta fórmula molecular $C_{12}H_{12}N_2O_2S$ (Figura 1) e massa molar de 248,30 g mol^{-1} (ANVISA, 2019a).

Figura 1. Estrutura molecular da dapsona.

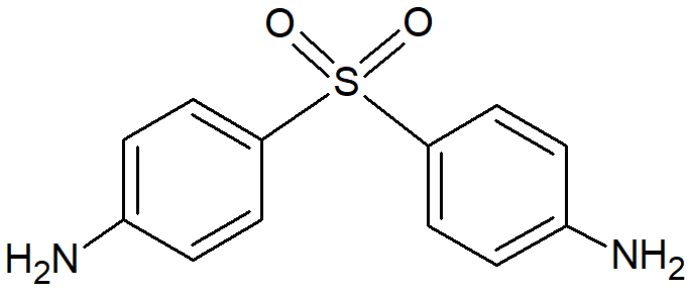

Apresenta-se como um pó cristalino branco ou levemente amarelado, com intervalo de fusão de 175-181ºC. Kuhnert-Brandstätter e Moser, em 1979, identificaram quatro formas anidras para a dapsona. A forma I apresenta ponto de fusão em 179°C, a forma II em 177ºC e a forma IV funde a 170ºC. A forma III é enantiotropicamente relacionada à forma II com temperatura de transição por volta de 80ºC (KUHNERT-BRANDSTATTER; MOSER, 1979; BRAUN et al., 2017). O anidrato III era considerado a forma sólida mais estável a temperatura ambiente, no entanto, Doris e Griesser (2018), durante um estudo sobre o hidrato de DAP, descobriram um novo polimorfo, que foi denominado forma V (BRAUN; GRIESSER, 2018). Após analisarem o novo anidrato, observaram que este é monotropicamente relacionado à forma III, além de ser mais estável. Entretanto, sua descoberta se deu tardiamente pois a transformação da fase III para a V é muito lenta, uma vez que o anidrato III possui uma estabilidade cinética muito alta. Além disso, o surgimento preferencial da forma III se dá por consequência de sua rápida taxa de nucleação e crescimento (BRAUN; VICKERS; et al., 2019)
.

Além das formas anidras, há relatos de uma forma hidrato de proporção molar 1:3 (i.e. DAP·3H2O) (BRAUN; GRIESSER, 2018) e de formas sólidas multicomponentes com alguns solventes como acetonitrila (2DAP·ACN), 1,4-dioxano (DAP·DIOX), nitrometano (2DAP·NIT), diclorometano (2DAP·DCM) e tetrahidrofurano (DAP·THF) (LEMMER et al., 2012; BRAUN; GELBRICH; et al., 2019). Um estudo realizado por Chappa et al. (2018) mostrou a formação de cristais multicomponentes de dapsona com PEG na estequiometria 1:1 (DAP·1PEG). Estes cristais mostraram-se estáveis à temperatura e a umidade o que foi atribuído as interações de hidrogênio entre os componentes (CHAPPA et al., 2018).

De acordo com a 6ª edição da Farmacopeia Brasileira (ANVISA, 2019b), a DAP é pouco solúvel aquosa e ligeiramente solúvel em álcool etílico. Estudos experimentais mostraram que a solubilidade da dapsona em água é em torno de 0,20 mg mL^{-1} (25 ºC), entretanto, não há qualquer menção da forma sólida aqui considerada (RYTTING et al., 2005). O fármaco possui um valor de log P de 0,94 e, desta forma, possui uma lipofilicidade intermediária. Seu pKa é de 2,4, característico de um base fraca. No Sistema de Classificação Biofarmacêutica (BCS), a dapsona é considerada sendo de classe II, apresentando baixa solubilidade e alta permeabilidade (LINDENBERG et al., 2004; SANTOS et al., 2012; MAKULA et al., 2017).

3.1.2 Mecanismo de ação

A DAP é um fármaco que apresenta tanto atividade bacteriostática quanto anti-inflamatória (GHAOUI et al., 2020). Sua atividade bacteriostática ocorre através da inibição da síntese de folato utilizado na produção de ácidos nucleicos e de proteínas (Figura 2). Por ter uma estrutura análoga ao PABA, é capaz de agir como antagonista competitivo da enzima diidropteroato sintase (DPHS), responsável por catalisar o PABA em diidropteroato (DHP), percussor do diidrofolato (DHF). Este, por sua vez, é transformado em tetaidrofólico (THF) pela enzima diidrofolato redutase. O THF participa da síntese do DNA e RNA bacteriano, ou seja, quando a dapsona se liga à DPHS, o THF não é sintetizado e, consequentemente, ocorre uma inibição da produção do DNA necessário para a replicação celular bacteriana (BARAN et al., 2011). O mecanismo de ação anti-inflamatório para a DAP ainda não foi completamente esclarecido. Alguns estudos indicam que a dapsona pode inibir a produção da IL-8, um agente quimiotático para neutrófilos, interferindo na aderência destas células nos tecidos inflamados. Além disso, a DAP pode inibir a produção de agentes oxidantes como o ácido hipocloroso, um composto produzido pela enzima mieloperoxidase que causa danos teciduais (MOLINELLI et al., 2019).

Figura 2. Mecanismo de ação bacteriostático da dapsona.

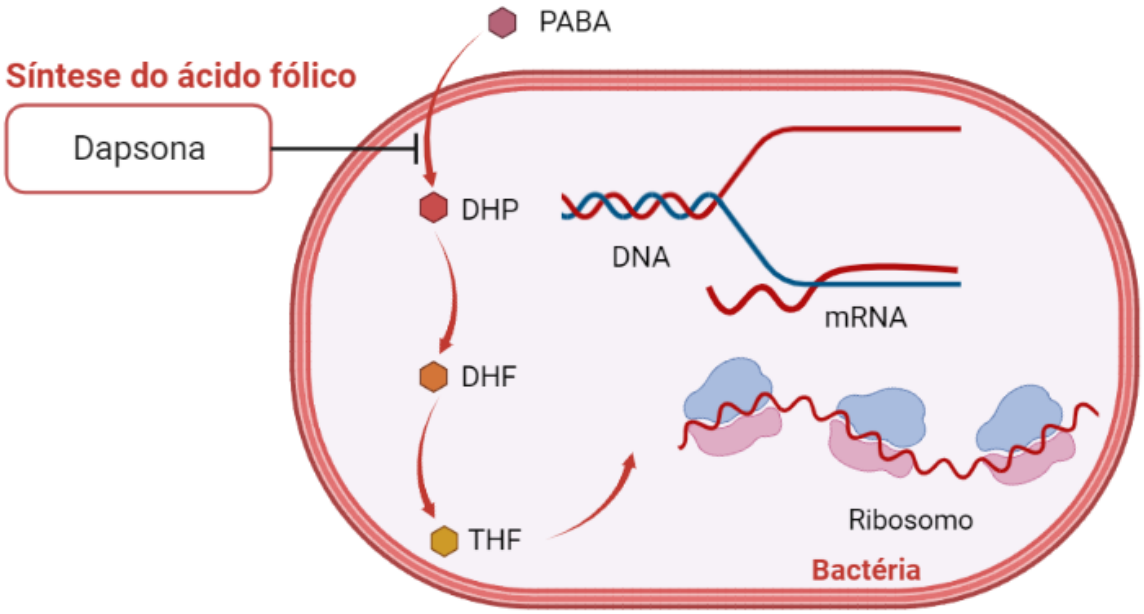

Fonte: Criado no Biorender (2021).

3.1.3 Farmacocinética

A DAP é quase que completamente absorvida pelo trato gastrointestinal, com um acúmulo preferencial na pele, fígado, rins e músculo. Após a administração oral de 100 mg, a absorção é cerca de 70 a 80%, porém, sua taxa (constante K_a) e meia vida de absorção são de, respectivamente, 0,6 h^{-1} e 1,1 h, o que permite aferir que a absorção do fármaco é lenta (ZUIDEMA et al., 1986). A concentração plasmática máxima em indivíduos saudáveis, varia entre 1,10 e 2,33 mg L^{-1}, podendo ser alcançada entre 2 e 6 h. Por apresentar um tempo de meia vida longo, em torno de 30 h, 24 h após a ingestão de 100 mg do fármaco, pode-se encontrar cerca de 0,4 a 1,2 mg L^{-1} de DAP no plasma (PIETERS; ZUIDEMA, 1986). Um estudo realizado por Thiboutot *et al*. (2007) avaliou alguns parâmetros farmacocinéticos de uma formulação "tópica" de dapsona a 5%. No primeiro dia de tratamento, observou-se que o C_{max} atingiu um valor de 5,4 ng mL^{-1} em 25,2 h, resultando em uma AUC_{24} de 88,7 ng h mL^{-1}. Após 14 dias de tratamento, esses mesmos parâmetros foram mensurados e obtiveram-se os seguintes resultados: C_{max} de 19,7 ng mL^{-1}, t_{max} de 6 h e AUC_{24} de 415 ng h mL^{-1}. Neste mesmo estudo, avaliaram-se também estes parâmetros para uma formulação "oral" de 100 mg em dose única, obtendo-se um C_{max}, t_{max} e AUC_{24} de 1375 ng mL^{-1}, 3,8 h e 22.783 ng h mL^{-1}, respectivamente

(THIBOUTOT et al., 2007). Baseado nestes dados, pode-se afirmar que as propriedades de barreira da pele são maiores que a mucosa intestinal.

Aproximadamente 70% da DAP encontra-se ligada a proteínas plasmáticas, sendo amplamente distribuída pelo corpo já que possui um volume de distribuição de 1,5 L kg^{-1}. Além disto, é capaz de atravessar a barreira hematoencefálica e a placenta e, por esta razão, deve ser utilizada com cautela por mulheres grávidas (MOLINELLI et al., 2019). Após sua absorção, a dapsona é transportada para o fígado onde é metabolizada por duas principais vias: *N*-acetilação a partir da *N*-acetiltransferase e *N*-hidroxilação através de algumas isoformas das enzimas do citocromo P450. A primeira via metabólica converte o fármaco em suas formas mono- e diacetiladas, sendo que a taxa de acetilação varia entre 0,1 a 2,0 dependendo do indivíduo. Indivíduos com uma proporção menor que 0,35 são considerados acetiladores "lentos", enquanto que os acetiladores denominados "rápidos" possuem uma proporção maior que 0,35. A dapsona acetilada pode ser desacetilada em dapsona novamente ou ser excretada pela via renal (GEORGE, 2020). Já a segunda via é responsável pelos efeitos colaterais hematológicos. Os metabólitos gerados nesta via são as hidroxilaminas, que são altamente oxidantes e capazes de consumir a glutationa presente nos glóbulos vermelhos, levando a produção indesejada de metemoglobina e hemólise (WOLF et al., 2000). A dapsona possui um *clearence* de 0,038 L/h/kg, pode ser conjugada com ácido glucurônico para ser excretada, sendo que 85% da sua excreção ocorre pelos rins e 10% pela bile (ZUIDEMA et al., 1986; ZHU; STILLER, 2001).

3.1.4 Efeitos adversos

A faixa de concentração terapêutica sérica da DAP varia entre 0,5 e 5 µg/mL. Embora estas concentrações sejam toleráveis, efeitos adversos podem ser encontrados devido a lenta metabolização do fármaco (ZUIDEMA et al., 1986). Os principais sistemas envolvidos nos efeitos adversos são os hematológicos e gastrointestinais. No sistema hematológico, os efeitos colaterais mais relatados são a metemoglobina, anemia hemolítica e agranulocitose (ZHU; STILLER, 2001). Para a anemia hemolítica e agranulocitose, os mecanismos envolvidos ainda são desconhecidos, porém, a metemoglobina ocorre devido aos metabólitos gerados na hidroxilação da dapsona que acabam oxidando a glutationa presente nas hemácias. Quando a concentração de metemoglobina é maior do que 1% nos eritrócitos, pode resultar em anemia funcional e hipóxia celular ocasionando sintomas como dor de cabeça, fadiga, taquicardia e tonturas (OLIVEIRA et al., 2014). Este quadro pode ser ainda pior em crianças, idosos ou pacientes que possuem deficiência na enzima glicose-6-fosfato desidrogenase (G6PD) (ZHU; STILLER, 2001). Efeitos gastrointestinais associados ao uso da dapsona incluem dor

abdominal, náusea e vômitos (MOLINELLI et al., 2019). Um estudo realizado por Bernardes Goulart *et al.* (2002) observou que a gastrite era o sintoma mais relatado dentre os 80 pacientes tratados com o fármaco. Cerca de 15,9% dos pacientes tratados com 100 mg de DAP por dia relataram a ocorrência deste efeito (BERNADES GOULART et al., 2002).

3.1.5 Indicações terapêuticas

Em 1908, a dapsona foi sintetizada pela primeira vez pelo professor alemão de química orgânica Emil Fromm e seu colega Jakob Wittman. Naquele momento, o interesse da molécula era voltado à produção de tintas para tecidos. Por três décadas, o potencial terapêutico da DAP foi ignorado, até que, em 1939, a atenção científica foi voltada para as propriedades medicinais das sulfas (WOZEL, 1989; MOLINELLI et al., 2019). A partir de então, a DAP passou a ser utilizada no tratamento de várias doenças infecciosas, integrando um regime multi-medicamentoso recomendado pela OMS para tratar hanseníase. Logo em seguida, foi amplamente utilizada na área dermatológica em doenças não infecciosas. Apesar da ampla utilização, as indicações terapêuticas aprovadas pela FDA se restringem à lepra, dermatite herpetiforme e acne vulgaris. *Off-label*, tem sido considerada para tratar lúpus eritematoso cutâneo e psoríase, além de ser empregada no tratamento e profilaxia da pneumonia e toxoplasmose (ZHU; STILLER, 2001; OLIVEIRA et al., 2014; GHAOUI et al., 2020). A dose recomendada de DAP varia conforme a doença. Em geral, a dosagem em adultos é iniciada com 50 a 100 mg por dia e se o objetivo do tratamento não for alcançado após algumas semanas, uma dosagem mais alta (entre 150-300 mg ao dia) pode ser testada (WOZEL, 2010). No mercado internacional, a DAP é encontrada nas apresentações de comprimidos simples de 25 e 100 mg bem como géis com 5 e 7,5% de fármaco (AGUINAGA-INURRIAGA et al., 2020). No Brasil, é disponibilizada na forma de comprimidos simples de 100 mg pela Fundação para o Remédio Popular e pelo Laboratório Farmacêutico da Marinha (ANVISA, 2021).

3.2 Acne

A acne é uma doença de pele que acomete principalmente os adolescentes. Afeta a unidade pilossebácea, que consiste no folículo piloso associado a uma glândula sebácea, podendo ou não ser inflamatória (PAIK, 2020). É difícil definir um perfil epidemiológico para acne, porém, estima-se que até 90% dos adolescentes podem ser afetados. Embora seja prevalente em adolescentes, em alguns indivíduos, pode persistir até a fase adulta (COSTA et al., 2008). O quadro clínico da acne pode variar entre manifestações leves como comedões até

inflamações mais severas e formações de abcessos em várias partes do corpo, particularmente no rosto (DEGITZ et al., 2007). Como consequência, os indivíduos afetados muitas vezes desenvolvem uma carga psicológica negativa, com insatisfação na aparência, autoestima e autoconfiança (SAMUELS et al., 2020). Tanto medicamentos tópicos quanto sistêmicos podem ser considerados no tratamento, com a possibilidade de se utilizarem associações dos mesmos. Embora muitos acreditem que a acne represente a passagem da adolescência para a fase adulta, não necessitando de tratamento, alguns dermatologistas afirmam que quando não tratada, pode deixar cicatrizes físicas e emocionais (KERI; SHIMAN, 2009).

3.2.1 Etiologia

A acne possui uma patogenia complexa, multifatorial e seu desenvolvimento está relacionado a quatro principais fatores: (i) produção excessiva de sebo que, por muitas vezes, pode vir acompanhada de alterações quali- e quantitativas na composição do mesmo (KASSIR et al., 2020); (ii) hiperqueratinização anormal no ducto pilossebáceo devido ao aumento dos andrógenos; (iii) colonização e proliferação de bactérias no ducto pilossebáceo tais como o *Propionibacterium acnes* e (iv) a resposta do sistema imunológico do hospedeiro (MOHIUDDIN, 2019). Estes fatores não podem ser vistos isoladamente já que atuam sinergicamente estimulando a patogênese da acne. A hiperprodução de sebo e hiperqueratinização pilossébacea produz um ambiente favorável para o *P. acnes*, encontrado na microbiota da pele e que, em circunstâncias fisiológicas, não é patogênico (RIBEIRO et al., 2015). O microrganismo transforma os triglicerídeos presentes na pele em ácidos graxos através da enzima lipase, promovendo assim a formação de comedões. Além disto, o *P. acnes* induz a uma reposta inflamatória do sistema imune do hospedeiro, ocasionando os sintomas exacerbados no desenvolvimento da doença (RIBEIRO et al., 2015; PAIK, 2020).

3.2.2 Sinais e sintomas

As características clínicas da acne são representadas por unidades pilossebáceas distendidas, inflamadas, obstruídas ou com cicatrizes. A acne pode ser classificada em leve, moderada e grave (Figura 3). Na acne leve, observam-se comedões abertos ou fechados na face e poucas lesões inflamatórias. A moderada é caracterizada por um aumento nos números de pápulas e postulas inflamatórias não só no rosto como na região do tronco. Por fim, a acne é considerada grave quando há presença de nódulos e cistos (POCHI et al., 1991; DAWSON;

DELLAVALLE, 2013). A acne pode deixar sequelas que incluem manchas, cicatrizes atróficas e hipertróficas e queloide (KASSIR et al., 2020).

Figura 3. Classificação da acne a partir das lesões.

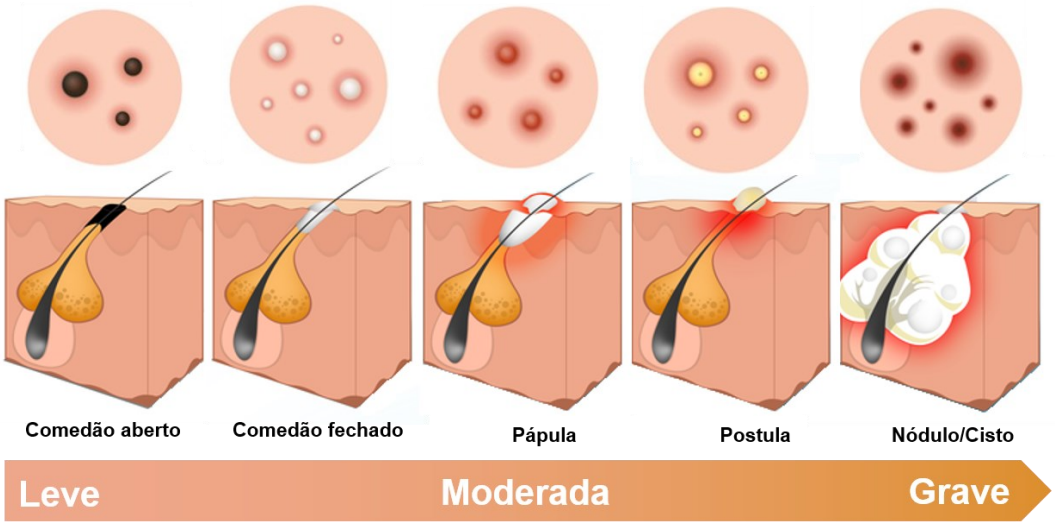

Fonte: Adaptado de Erickson (2016).

3.2.3 Tratamento

Atualmente, o mercado traz uma variedade de produtos para o manejo da acne. Nos últimos anos, estudos permitiram um maior entendimento da patogênese, permitindo que novas modalidades e combinações terapêuticas fossem desenvolvidas (MOHIUDDIN, 2019). Por se tratar de uma doença multifatorial, a combinação terapêutica parece ser a melhor alternativa na maioria dos casos. Dentre as alternativas, encontram-se *terapias sistêmicas* que incluem antibióticos, retinóides, contraceptivos e antiandrogênicos orais (KERI; SHIMAN, 2009) e os *agentes tópicos*, tais como peróxido de benzoíla, ácido salicílico, retinóides, ácido azeláico e antibióticos como clindamicina e eritromicina (ZAENGLEIN et al., 2016). Embora existam diferentes opções terapêuticas, o tratamento adequado para cada paciente deve estar baseado na classificação da acne. Os medicamentos tópicos são frequentemente utilizados em casos de acne leve a moderada enquanto que a combinação deles com os antibióticos orais são recomendados para a acne grave. Devido aos efeitos colaterais, estrogênios, antiandrogênios ou retinóides orais são reservados para os casos graves, particularmente nos casos em que não há resposta a antibióticos (WILLIAMS et al., 2012).

Devido a sua ação anti-inflamatória e antimicrobiana, a DAP se mostrou eficaz em pacientes com acne. Em 2005, a FDA aprovou o uso de gel de DAP a 5% para diversas indicações terapêuticas, incluindo a acne (PIETTE et al., 2008). Um estudo realizado por Draelos et al. (2007) avaliou a eficácia e a segurança de gel de DAP 5% em um ensaio clínico randomizado e duplo cego de fase III. O número de lesões da acne diminuíram significativamente em relação ao grupo controle após doze semanas de tratamento com duas aplicações diárias. As lesões inflamatórias e não inflamatórias da acne diminuíram cerca de 47,5 e 32%, respectivamente. Por se tratar de uma formulação tópica, resultaria em baixa absorção sistêmica da DAP e, desta forma, evitaria os efeitos adversos hematológicos das preparações orais (DRAELOS et al., 2007). Com o objetivo de aumentar a adesão dos pacientes ao tratamento, desenvolveu-se uma formulação com maior concentração de dapsona (7,5%), porém, aplicada uma vez ao dia (gel anterior necessitava de duas aplicações diárias). No estudo realizado por Thiboutot et. al (2016), avaliou-se a segurança, eficácia e a tolerabilidade dérmica do gel com 7,5% de DAP. Alcançou-se uma eficácia dentro de doze semanas, com um perfil de segurança semelhante ao gel de dapsona a 5% (THIBOUTOT et al., 2016).

3.4 Hanseníase

Por muitos anos, a hanseníase, também conhecida como lepra, foi considerada uma doença mutilante e incurável causando preconceito e discriminação de indivíduos que a portavam. Apesar da cura da doença já ser estabelecida, a hanseníase ainda é incompreendida e temida por vários indivíduos. A lepra é uma doença conhecida por seus sintomas dermatoneurológicos, isso porque o bacilo se instala nos nervos periféricos e na pele, ocasionado lesões com alterações de sensibilidade principalmente nas mãos, pés e olhos. A hanseníase é uma doença de progressão lenta, no entanto, se não tratada precocemente, pode provocar sérias sequelas, incapacitando fisicamente o doente e acarretando problemas psicológicos e diminuição na capacidade de trabalho (BRASIL, 2002). Em 2018, a OMS estimou cerca de 208.641 novos casos de hanseníase globalmente, sendo a maioria em países em desenvolvimento como Brasil, Índia e Indonésia. Mundialmente, estes países juntos representam cerca de 79,6% do total de novos casos, sendo que o Brasil contribuiu com 28.660 dos casos, ficando atrás somente da Índia (WHO, 2019). Apesar da redução do número de casos em grande parte do mundo, onde a prevalência é <1 caso/10.000 habitantes, a hanseníase continua sendo um importante problema de saúde no país (LAZO-PORRAS et al., 2020).

3.4.1 Etiologia e transmissão

A hanseníase é causada pelo *Mycobacterium leprae*, também conhecido como bacilo de Hansen. Trata-se de microrganismo intracelular obrigatório de crescimento lento, que infecta preferencialmente macrófagos presentes na pele e células de Schwann (células responsáveis pela produção da mielina que envolve os axônios dos neurônios do sistema nervoso periférico), caracterizando assim os sintomas dermatoneurológicos (UASKA SARTORI et al., 2020). As vias de transmissão deste agente etiológico não são totalmente conhecidas, mas há fortes evidências que o contato próximo com indivíduos portadores da hanseníase aumenta o risco de infecção, já que o bacilo é expelido através de aerossóis gerados durante a tosse ou espirro (ARAUJO et al., 2016). Por outro lado, apenas 5% dos indivíduos que entram em contato com o bacilo desenvolvem a doença, pois estima-se que a maior parte da população possua defesa natural contra este agente (BRASIL, 2017; MÁQUINA et al., 2020).

3.4.2 Sinais e sintomas

A manifestação clínica inicia após um período de incubação que pode variar entre 5 a 20 anos (BARBEITO-CASTIÑEIRAS et al., 2020). A evolução da doença vai ser determinada de acordo com a resposta imunológica do hospedeiro. Os principais sintomas se manifestam na pele e no sistema nervoso periférico, uma vez que o bacilo de Hansen tem preferência por essas áreas mais frias, já que seu crescimento requer uma temperatura de 30 ºC (MÁQUINA et al., 2020). Inicialmente, os sintomas clínicos se manifestam através de pápulas, tubérculos, nódulos, alterações da coloração e da espessura da pele em todo o corpo, mais frequentemente no rosto, orelhas, nádegas, costas, braços e pernas, podendo acometer também a mucosa nasal. Essas lesões sempre apresentam diminuição ou ausência da sensibilidade, se diferenciando das outras doenças dermatológicas. Com a evolução da doença, sintomas neurológicos periféricos começam a aparecer. Esses sintomas são decorrentes da neurite, ou seja, processo inflamatório nos nervos. A neurite se manifesta através de dor intensa, edema, perda da sensibilidade, formigamento, perda da força nos músculos, principalmente nas regiões dos olhos, mãos e pés. Com o passar do tempo, pode ocorrer comprometimento funcional evidenciado pela perda da capacidade de suar. Essas lesões são responsáveis pelas deformidades e incapacidades do portador da hanseníase (OMS, 2001).

3.4.3 Tratamento

Por muitos anos, a hanseníase foi considerada uma doença incurável levando ao isolamento de inúmeros portadores desta doença. Em 1854, no Ocidente, o uso do óleo de chaulmoogra no tratamento da lepra se tornou conhecido através dos relatos de um médico chamado Mouat (PARASCANDOLA, 2003). No entanto, muito antes disso, no Oriente, seu uso no tratamento de doenças de pele, especialmente na hanseníase, já era preconizado pelas Farmacopeias indiana e chinesa (NORTON, 1994). Em 1907, o laboratório Bayer desenvolveu o Antileprol®, o primeiro medicamento antileprótico industrializado a base de óleo de chaulmoogra (BARBOSA-FILHO et al., 2007). A partir deste momento, outras indústrias farmacêuticas desenvolveram vários produtos semelhantes, como o Alepol® e Moogrol® (ARAÚJO, 2005). O óleo de chaulmoogra é extraído por prensagem de sementes da árvore *Hydnocarpus kurzii,* seguido de saponificação com hidróxido de sódio (NORTON, 1994). É composto por três ácidos graxos principais: o ácido hidnocárpico, chaulmúgrico e górlico (Figura 4). Em menor quantidade, aparece o ácido mirístico, palmítico, oleico, linoleico e linolênico. Quanto ao mecanismo de ação, acredita-se que o óleo promova ativação das lipases do hospedeiro, desestruturando lipídeos da parede celular do microrganismo (NORTON, 1994; SAHOO et al., 2014).

Figura 4. Estrutura molecular dos três principais ácidos graxos presente no óleo de chaulmoogra.

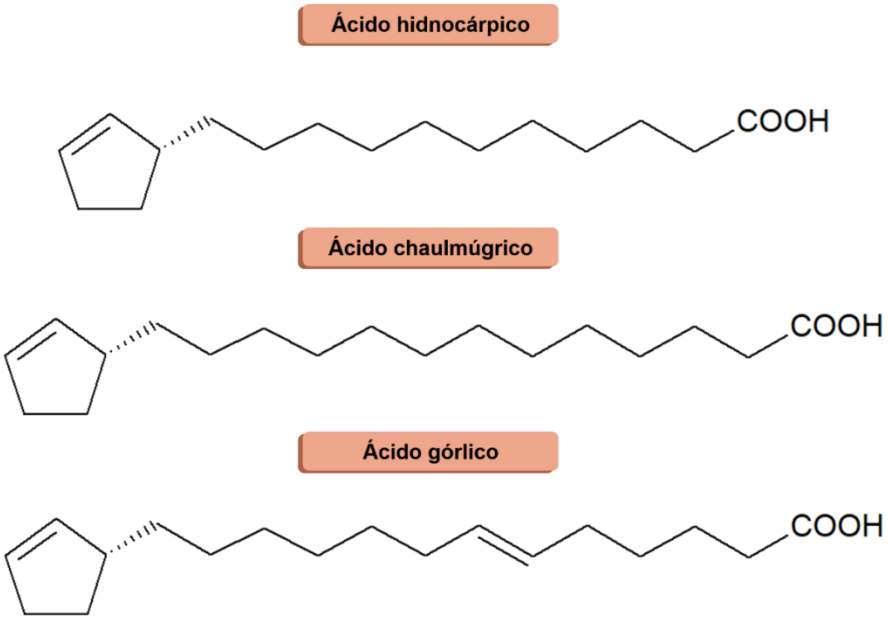

Com a descoberta das sulfonamidas, o tratamento da hanseníase foi modificado. Em 1946, americanos introduziram as sulfonas como opções terapêuticas ao tratamento da hanseníase resultado da experiência do médico norte-americano Guy Faget (KAR; GUPTA, 2015). Posteriormente, vários programas de controle da hanseníase foram atualizados em todo mundo, tendo a dapsona como âncora do tratamento. Com o aparecimento de cepas resistentes a DAP (DESIKAN, 2003), em 1981, a OMS incluiu a rifampicina e clofazimina no protocolo terapêutico. Apesar de ter passado por algumas mudanças em relação à sua duração, esta terapia é utilizada até hoje (LAZO-PORRAS et al., 2020; WHO, 2020).

3.4.3.1 Esquema terapêutico a para hanseníase

Para facilitar o tratamento e a classificação da doença em áreas endêmicas sem acesso a laboratórios, a OMS propôs o uso da poliquimioterapia conforme a classificação pauci- (PB) ou multibacilar (MB). A doença é classificada como "paucibacilar" quando se observam até cinco lesões cutâneas e "multibacilar" quando há mais de cinco lesões cutâneas ou quando há espessamento de nervos periféricos, perda de sensibilidade ou perda da força muscular mesmo sem apresentar mais de cinco lesões. Enquanto que a classificação criada pela OMS é baseada na quantidade de lesões, classificações como a de Ridley e Jopling tem como base os achados clínicos, histológicos e baciloscopias, exigindo equipamentos laboratoriais específicos para uma análise mais completa (MÁQUINA et al., 2020). Os pacientes PB ou MB recebem doses diárias de 100 mg de DAP e 50 mg de clofazimina, ambos autoadministrados, uma dose mensal de 600 mg de rifampicina (dois comprimidos de 300 mg) e 300 mg de clofazimina com administração supervisionada. A diferença do tratamento do PB e MB está na duração, que é de 6 meses e 12 meses, respectivamente. Cabe ressaltar que este esquema terapêutico é recomendado apenas para adultos. Para crianças entre 10 e 14 anos, utiliza-se uma dose mensal e supervisionada de rifampicina e clofazimina de 450 e 150 mg, respectivamente. As doses diárias de DAP e clofazimina são 50 mg. Para crianças menores de 10 anos ou com massa corpórea inferior a 40 kg, a dose mensal de rifampicina e clofazimina é de, respectivamente, 10 mg/kg e 100 mg; a dose diária de DAP é de 2 mg/kg e a de clofazimina continua sendo 50 mg. A duração do tratamento é similar àquela dos adultos (OMS, 2018).

3.5 Formulações tópicas

Formulações tópicas são projetadas para a entrega de moléculas em áreas superficiais como pele ou mucosas (SINGH MALIK et al., 2016). Diversas vantagens estão associadas a estas formulações, como evitar o metabolismo hepático de primeira passagem, reduzir os riscos

de irritação gastrointestinais, possibilitar a liberação controlada e de longo prazo, facilidade na administração e técnica indolor e não invasiva (PRAUSNITZ; LANGER, 2008; WONG, 2014). Por outro lado, o desenvolvimento de sistemas tópicos requer uma seleção criteriosa não só do fármaco, mas também dos excipientes, uma vez que as barreiras associadas a essas rotas podem limitar a disponibilidade do fármaco (TADWEE et al., 2011).

A pele é considerada o maior órgão do corpo e sua grande área superficial a torna uma via atrativa para a administração de fármacos. É composta por três camadas principais: epiderme, derme e hipoderme (Figura 5). A epiderme é um tecido dinâmico que está em constate renovação. É composta por uma camada basal ou germinativa, camada espinhosa, granulosa e córnea. Em regiões de atrito (palma dos pés e mãos), aparece a camada lúcida. São diferenciadas pela posição, morfologia e estado de diferenciação dos queratinócitos (BOUWSTRA et al., 2003). Ao deixar a camada basal, os queratinócitos se diferenciam durante a migração até as camadas mais sueperficiais. As últimas sequências de diferenciação dos queratinócitos estão associadas a profundas alterações em sua estrutura, que resultam em sua transformação em escamas cornificadas do estrato córneo quimicamente e fisicamente resistentes. Estas células são denominadas corneócitos e representam a principal barreira de permeação a moléculas (MENON, 2002; VENUGANTI et al., 2011). Abaixo da epiderme está localizada a derme. Esta camada é constituída por tecido conjuntivo contendo colágeno, fibras elásticas, células dendríticas e fibroblastos, além de vasos sanguíneos e linfáticos. Apêndices, como folículos capilares, glândulas sebáceas e sudoríparas também se originam na derme; podendo servir como uma via de permeação para algumas moléculas (ZAIDI; LANIGAN, 2010).

Figura 5. Anatomia da pele.

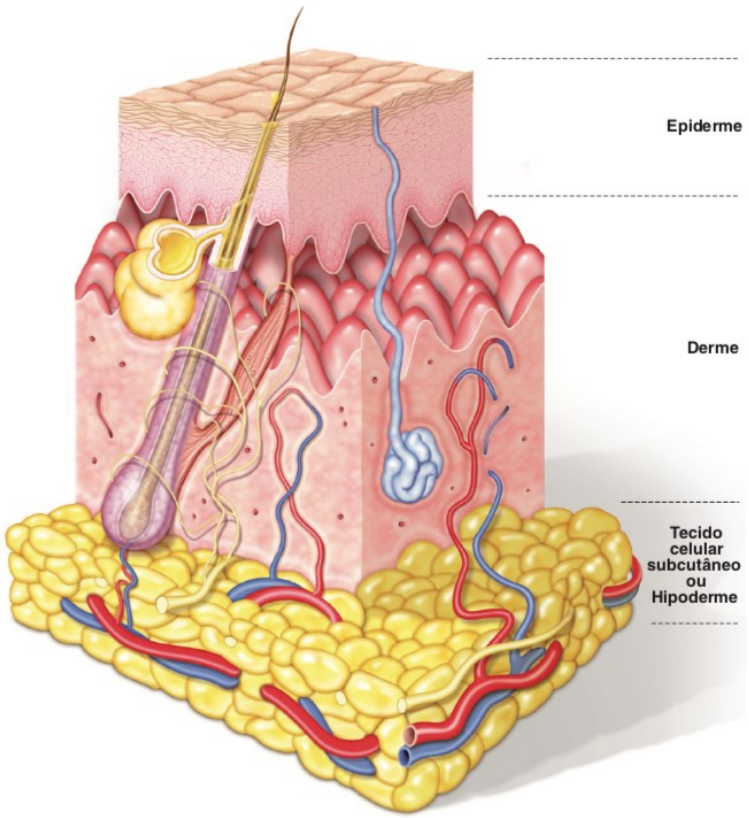

Fonte: Traduzido de Liciteloo (2016)

A absorção dérmica de fármacos é mediada a partir de três rotas principais (Figura 6): (1) *transcelular*, difusão do fármaco através dos corneócitos; (2) *intercelular*, difusão do fármaco entre os corneócitos, ou seja, pelas regiões extracelulares e (3) *apendágica*, difusão da molécula através de apêndices tais como folículos capilares, glândulas sebáceas e sudoríparas (BENSON, 2005; HERMAN; HERMAN, 2015).

Figura 6. Principais rotas do transporte de moléculas através da pele.

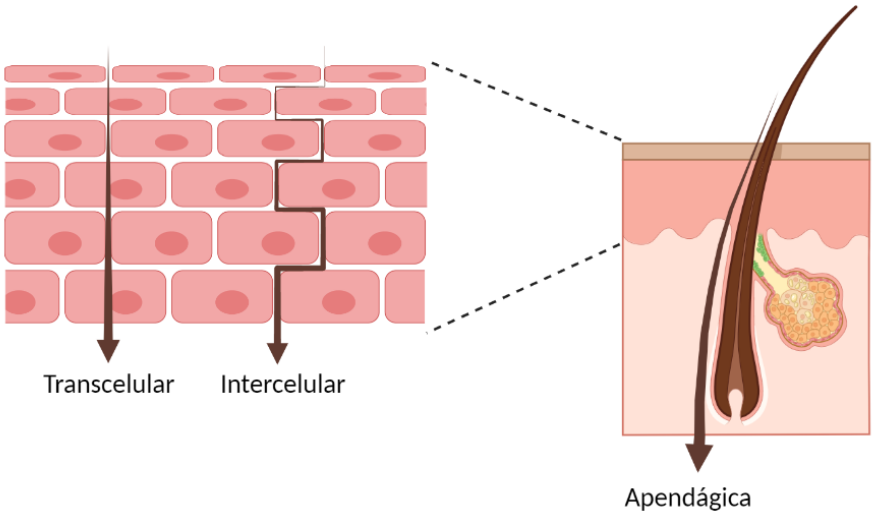

Fonte: Criada no Biorender (2021)

Devido as características morfológicas e fisiológicas da pele, alguns requisitos são necessários para fármacos que são candidatos à aplicação tópica, como baixo peso molecular (< 500 Da) e um valor de log P entre 1 e 3 (KOVÁČIK et al., 2020; NEUPANE et al., 2020). No entanto, muitos ativos não cumprem estes requisitos, exigindo estratégias químicas e físicas para melhorar a absorção destas moléculas. Ainda, sistemas micro e nanoparticulados podem ser considerados. Com a redução do tamanho de partícula, aumenta-se a área de superfície e dissolução do fármaco, elevando o gradiente de concentração que favorece a permeação através da pele. Além disso, as nanopartículas apresentam maior adesão às membranas biológicas em comparação com os fármacos dissolvidos, o que pode contribuir para a formação de reservatórios (ZHAI et al., 2014; PIREDDU et al., 2016; VIDLÁŘOVÁ et al., 2016; PELIKH et al., 2018).

3.5.1 Estratégias tecnológicas utilizadas em formulações tópicas contendo dapsona

3.5.1.1 Géis poliméricos

O Aczone®, gel aquoso de DAP, é disponibilizado comercialmente nas concentrações de 5 e 7,5 %, com implicações na periodicidade de aplicação (2 e 1x ao dia, respectivamente). Este produto apresenta uma fração de dapsona dissolvida e outra não dissolvida. A DAP dissolvida é responsável por atravessar o estrato córneo da epiderme para as camadas mais profundas da pele; alcançando o folículo de modo inespecífico (região de interesse na acne).

Por outro lado, a fração não dissolvida de DAP, que aparece na forma de microcristais, é direcionada ao folículo formando reservatórios para uma entrega sustentada (GARRET; COLLINS, 2011; OSBORNE, 1999, 2000, 2002).

O método para formular tal composição envolve a dissolução do carbômero em água separadamente à solubilização da DAP em etoxidiglicol. Ao final, ambas as fases aquosa e orgânica são combinadas, ocorrendo assim a cristalização de parte de fármaco adicionado. Este procedimento é conhecido como cristalização antissolvente. Além do etoxidiglicol, também conhecido como Transcutol® (DEGEE), as patentes relativas (GARRET; COLLINS, 2011; OSBORNE, 1999, 2000, 2002) ao preparo dos géis trazem polietilenoglicol (PEG) e 1-metil-2-pirrolidona (MPR) como agentes solubilizantes. A solubilidade da DAP nestes agentes é que determina a proporção de fármaco/solvente a ser utilizada. Um aspecto não explorado por estas patentes é o impacto da composição da formulação nas características do produto (ex.: alteração de viscosidade, espalhabilidade, etc.). Ainda, não há descrição do tipo de polimorfo presente na fase sólida e nem da proporção de DAP dissolvida e não dissolvida para cada solubilizante utilizado. Este trabalho de dissertação vai ao encontro desta lacuna (ver próximo capítulo).

3.5.1.2 Nano- e microcarreadores lipídicos

O uso de nanopartículas também tem sido considerado como estratégia para melhorar propriedades biofarmacêuticas da DAP (Figura 7). As nanopartículas lipídicas sólidas (NLS) são carreadores de fármacos compostos por lipídios sólidos a temperatura ambiente e foram desenvolvidas como um sistema de transporte alternativo a emulsões, lipossomas e nanopartículas poliméricas (MEHNERT; MADER, 2020). Podem melhorar a estabilidade e solubilidade de fármacos, além de promover um controle da liberação (FANG et al., 2008). Deshkar et al. (2018), por exemplo, prepararam NLS de DAP pelo método de microemulsão utilizando Precirol® ATO 5 (palmitoestearato de glicerila) e Gelucire® 50/13 (polioxilglicerídeo) como lipídeos sólidos. Gelucire® 50/13 resultou em maior eficiência de encapsulação, o que foi atribuído as imperfeições estruturais das NLS. Estruturas imperfeitas criam espaços para acomodar os compostos ativos de forma mais eficiente. A partir do delineamento de Box-Behnken, obteve-se uma formulação otimizada com alta eficiência de encapsulação (96%) e uma liberação de 61% de fármaco após 8 h (um perfil de liberação sustentado). Por fim, a NLS otimizada foi incorporada em um gel de carbômero 934P, que prolongou ainda mais a liberação do fármaco. A permeação do gel com a NLS foi duas vezes maior do que o gel convencional (DESHKAR et al., 2018).

Os carreadores lipídicos nanoestruturados (CLN) representam uma nova geração de NLS, que foram desenvolvidos com o objetivo de superar as limitações do sistema anterior. Durante o armazenamento das NLS, o fármaco encapsulado pode acabar sendo expulso do interior das partículas por conta da maior rigidez da estrutura da partícula como lipídeos sólidos são utilizados (MÜLLER et al., 2002). Os CLNs consistem em uma mistura de lipídeos sólidos e líquidos estabilizados por tensoativos que garantem uma acomodação mais efetiva do fármaco na estrutura da partícula (NASERI et al., 2015).

Elmowafy *et al.* (2019) desenvolveram CLNs variando a proporção de lipídios sólidos (palmitoestearato de glicerila), líquidos (triglicerídeos de ácido cáprico e caprílico) e agentes emulsificantes (polissorbato 80, etoxidiglicol ou brometo de cetiltrimetilamônio), selecionando o método de emulsificação seguido de sonicação para o preparo das nanopartículas. O polissorbato 80 foi o tensoativo que contribuiu para uma maior redução no tamanho. O aumento da quantidade de lipídeos líquidos nas formulações aumentou a eficiência de encapsulação além de facilitar a formação de partículas menores. O perfil de liberação obtido pelos CLNs mostrou uma fase inicial de liberação rápida seguida de uma fase de liberação constante, típica de sistemas bifásicos. Por apresentar alta afinidade pelos lipídeos, a liberação de 80% da DAP só foi alançada após 48 h (ELMOWAFY et al., 2019).

Nanoemulsões foram desenvolvidas com o interesse de encapsular, proteger e entregar componentes bioativos de forma sustentada. Esses sistemas são compostos de uma mistura de óleos, água e tensoativos, na qual é capaz de aumentar a biodisponibilidade de certos fármacos (MASON et al., 2006; MCCLEMENTS, 2012). Borges *et al*. (2013), por exemplo, desenvolveram nanoemulsões (NEs) tópicas de DAP com miristato de isopropila ou *N*-metil-pirrolidona como componente da fase oleosa. A *N*-metil-pirrolidona proporcionou um aumento na solubilização e liberação *in vitro* de DAP enquanto que o miristato de isopropila promoveu um aumento da permeação dérmica. Os autores concluíram que as NEs com *N*-metil-pirrolidona, por possuírem uma baixa permeação e alta liberação de fármaco, seriam mais eficazes para o tratamento de doenças superficiais de pele. Já aquelas com miristato de isopropila, por aumentarem o grau de permeação da DAP, seriam recomendadas para doenças cujo alvo de ação se situa nas camadas mais internas da pele (BORGES et al., 2013).

Microemulsões (MEs) também foram relatadas na literatura como uma estratégia para a entrega tópica de DAP. Mahore *et al.* (2017) desenvolveram MEs contendo monocaprilato de propilenoglicol e *N*-metil-2-pirrolidona a partir do método de emulsificação espontânea. Os sistemas otimizados foram veiculados em géis de Poloxamer® 407. Os autores avaliaram a liberação e permeação das MEs em relação a géis clássicos e observaram que as MEs

promovem maior taxa de liberação e permeação comparativamente a géis. Estes achados foram atribuídos a uma interação aumentada com os domínios lipídicos do estrato córneo e atuação dos surfactantes e co-surfactantes da formulação como promotores de absorção (MAHORE et al., 2017).

Figura 7. Tecnologias utilizadas em formulações tópicas para a liberação de DAP: (a) gel com DAP dissolvida e cristalizada; (b) nano/microemulsão; (c) nanopartículas lipídicas sólidas e (d) carreador lipídico nanoestruturado.

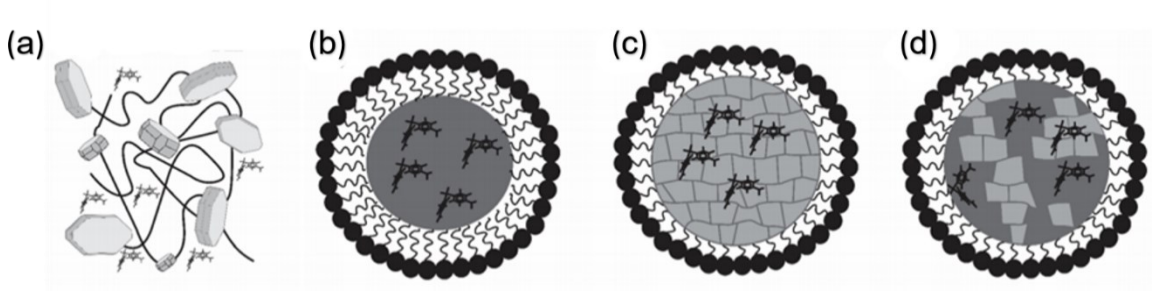

Fonte: Schneider-Rauber et al. (2020)

REFERÊNCIAS

AGUINAGA-INURRIAGA, A. *et al.* Dapsona (diaminodifenil-sulfona) en Dermatología: Conocimiento actual de un fármaco antiguo. **Dermatología Revista Mexicana**, v. 64, n. 3, p. 294–308, 2020.

AHMAD, R.; ROGERS, H. Pharmacokinetics and protein binding interactions of dapsone and pyrimethamine. **British Journal of Clinical Pharmacology**, v. 10, n. 5, p. 519–524, 1980.

AL-SALAMA, Z. T.; DEEKS, E. D. Dapsone 7.5% Gel: A Review in Acnes Vulgaris. **American Journal of Clinical Dermatology**, v. 18, n. 1, p. 139–145, 2017.

ALHALAWEH, A.; ALI, H. R. H.; VELAGA, S. P. Effects of polymer and surfactant on the dissolution and transformation profiles of cocrystals in aqueous media. **Crystal Growth and Design**, v. 14, n. 2, p. 643–648, 2014.

ANVISA. **Farmacopeia Brasileira**. 6º ed. Brasília, 2019a.

ANVISA. Farmacopeia Brasileira. 6ª ed. **Anvisa**, v. 1, p. 874, 2019b.

ANVISA. Consultas. Disponível em: <https://consultas.anvisa.gov.br/#/medicamentos/q/?substancia=3472>. Acesso em: 29/4/2021.

ARAÚJO, M. G. Evolution and current status of leprosy chemotherapy 1925 – 2005: Evolução e estado atual da quimioterapia da hanseníase. **Brazilian Dermatology Annals**, v. 80, n. 2, p. 199–202, 2005.

ARAUJO, S. *et al*. Molecular evidence for the aerial route of infection of *Mycobacterium leprae* and the role of asymptomatic carriers in the persistence of leprosy. **Clinical Infectious Diseases**, v. 63, n. 11, p. 1412–1420, 2016.

BARAN, W. *et al.* Effects of the presence of sulfonamides in the environment and their influence on human health. **Journal of Hazardous Materials**, v. 196, p. 1–15, 2011.

BARBEITO-CASTIÑEIRAS, G. *et al.* Leprosy in the twenty-first century: a microbiological, clinical, and epidemiological study in northwestern Spain. **European Journal of Clinical Microbiology and Infectious Diseases**, 2020.

BARBOSA-FILHO, J. *et al*. Natural products with antileprotic activity. **Brazilian Journal of Pharmacognosy**, v. 17, n. 1, p. 141–148, 2007.

BENSON, H. Transdermal Drug Delivery: Penetration Enhancement Techniques. **Current Drug Delivery**, v. 2, n. 1, p. 23–33, 2005.

BERNADES GOULART, I. M. *et al.* Efeitos adversos da poliquimioterapia em pacientes com hanseníase: Um levantamento de cinco anos em um Centro de Saúde da Universidade Federal de Uberlândia. **Revista da Sociedade Brasileira de Medicina Tropical**, v. 35, n. 5, p. 453–460, 2002.

BORGES, V. R. DE A. *et al.* Nanoemulsion containing dapsone for topical administration: A study of *in vitro* release and epidermal permeation. **International Journal of Nanomedicine**, v. 8, p. 535–544, 2013.

BOUWSTRA, J. A. *et al.* Structure of the skin barrier and its modulation by vesicular formulations. **Progress in Lipid Research**, v. 42, p. 1–36, 2003.

BRAGA, D.; GREPIONI, F. **Making crystals by design:** methods, techniques and applications. Weinheim: Wiley, 2007.

BRANDSTAETTER-KUHNERT, M. KOFLER, A.; HOFFMANN, R. Microscopic characterization and identification of pharmaceuticals. **Scientia. Pharmaceutica**, v. 31, p. 140–148, 1963.

BRASIL. **Guia para o controle da hanseníase**. Brasília, DF, 2002.

BRASIL. **Guia prático sobre a hanseníase**. Brasília, DF, 2017.

BRAUN, D. E.; GELBRICH, T.; GRIESSER, U. J. Experimental and computational approaches to produce and characterise isostructural solvates. **CrystEngComm**, v. 21, n. 36, p. 5533–5545, 2019.

BRAUN, D. E.; GRIESSER, U. J. Supramolecular Organization of Nonstoichiometric Drug Hydrates: Dapsone. **Frontiers in Chemistry**, v. 6, n. February, p. 1–17, 2018.

BRAUN, D. E. *et al.* Molecular level understanding of the reversible phase transformation between forms III and II of dapsone. **Crystal Growth and Design**, v. 17, n. 10, p. 5054–5060, 2017.

BRAUN, D. E.; VICKERS, M.; GRIESSER, U. J. Dapsone Form V: A Late Appearing Thermodynamic Polymorph of a Pharmaceutical. **Molecular Pharmaceutics**, v. 16, p. 3221−3236, 2019.

BROWN, M. B. *et al.* Dermal and transdermal drug delivery systems: Current and future prospects. **Journal of Delivery and Targeting of Therapeutic Agents**, v. 13, n. 3, p. 175–187, 2006.

BRUNO, I. J. *et al.* New software for searching the Cambridge Structural Database and visualizing crystal structures. **Acta Crystallographica Section B: Structural Science**, v. 58, n. 3 PART 1, p. 389–397, 2002.

BYRN, S. R.; PFEIFFER, R. R.; STOWELL, J. G. **Solid-state Chemistry of Drugs**. New York: Academic Press, New York., 1999.

CASPI, D. D. *et al.* Process development of ABT-450: A first generation NS3/4A protease inhibitor for HCV. **Tetrahedron**, v. 75, n. 32, p. 4271–4286, 2019.

CHAPPA, P. *et al.* Drug-Polymer Co-Crystals of Dapsone and Polyethylene Glycol: An Emerging Subset in Pharmaceutical Co-Crystals. **Crystal Growth and Design**, v. 18, n. 12, p. 7590–7598, 2018.

CINK, R. D. *et al.* Development of the Enabling Route for Glecaprevir via Ring-Closing Metathesis. **Organic Process Research & Development**, v. 24, n. 2, p. 183–200, 2020.

COELHO, A. A. TOPAS and TOPAS-Academic: An optimization program integrating computer algebra and crystallographic objects written in C^{++}: An. **Journal of Applied Crystallography**, v. 51, n. 1, p. 210–218, 2018.

CORDAIN, L. *et al.* Acne vulgaris. **Lancet**, v. 351, n. 9119, p. 1871–1876, 1998.

COSTA, A.; ALCHORNE, M. M. D. A.; GOLDSCHMIDT, M. C. B. Fatores etiopatogênicos da acne vulgar. **Anais Brasileiros de Dermatologia**, v. 83, n. 5, p. 451–459, 2008.

DAWSON, A. L.; DELLAVALLE, R. P. Acne vulgaris. **British Medical Journal**, v. 346, n. 7907, p. 1–7, 2013.

DEGITZ, K. *et al.* Pathophysiology of acne. **Journal of the German Society of Dermatology**, v. 5, n. 4, p. 316–323, 2007.

DESHKAR, S. S. *et al.* Formulation and Optimization of Topical Solid Lipid Nanoparticles based Gel of Dapsone Using Design of Experiment. **Pharmaceutical Nanotechnology**, v. 6, n. 4, p. 264–275, 2018.

DESIKAN, K. V. Multi-drug regimen in leprosy and its impact on prevalence of the disease. **Medical Journal Armed Forces India**, v. 59, n. 1, p. 2–4, 2003.

DESIRAJU, G. R.; VITTAL, J. J.; RAMANAN, A. **Crystal engineering: a textbook**. New Jersey: IISc Press, 2011.

DOLLASE, W. A. Correction of Intensities of Preferred Orientation in Powder Diffractometry: Application of the March Model. **Journal of Applied Crystallography**, v. 19, n. pt 4, p. 267–272, 1986.

DRAELOS, Z. D. *et al.* Two randomized studies demonstrate the efficacy and safety of dapsone gel, 5% for the treatment of acne vulgaris. **Journal of the American Academy of Dermatology**, v. 56, n. 3, p. 439.e1-439.e10, 2007.

ELMOWAFY, M. *et al.* Impact of nanostructured lipid carriers on dapsone delivery to the skin: *in vitro* and in *vivo* studies. **International Journal of Pharmaceutics**, v. 572, n. May, p. 118781, 2019.

ERICKSON, K. THE 101: Adult Acne. Disponível em: <http://www.jordanamattioli.com/blog//the-101-adult-acne>. Acesso em: 2/8/2021.

ETHIER, A. *et al.* The Role of Excipients in the Microstructure of Topical Semisolid Drug Products. In: Langley N., Michniak-Kohn B., Osborne D. (eds) The Role of Microstructure in Topical Drug Product Development. . **Springer**, v. 36, p 155-193, 2019.

EZHILARASAN, D. Dapsone-induced hepatic complications: it's time to think beyond methemoglobinemia. **Drug and Chemical Toxicology**, v. 44, n. 3, p. 330–333, 2021.

FANG, J. Y. *et al.* Lipid nanoparticles as vehicles for topical psoralen delivery: Solid lipid nanoparticles (SLN) versus nanostructured lipid carriers (NLC). **European Journal of Pharmaceutics and Biopharmaceutics**, v. 70, n. 2, p. 633–640, 2008.

Farmacopeia Brasileira. 5º ed. Brasília: ANVISA, 2010.

FDA. The Orange Book: Approved Drug Products with Therapeutic Equivalence evaluations. .

FRANÇA, M. T. *et al.* Could the small molecules such as amino acids improve aqueous solubility and stabilize amorphous systems containing Griseofulvin. **European Journal of Pharmaceutical Sciences**, v. 143, n. November 2019, p. 105178, 2020.

FRANÇA, M. T. *et al.* The role of glycyrrhizic acid in colloidal phenomena of supersaturation drug delivery systems containing the antifungal drug griseofulvin. **Journal of Molecular Liquids**, v. 301, 2020.

GARRET, J. S.; COLLINS, F. Topical treatment with dapsone in G6PD-deficient patients. US Pat n. 294,869A1, 2011.

GEORGE, J. Metabolism and interactions of antileprosy drugs. **Biochemical Pharmacology**, v. 177, n. April, p. 113993, 2020.

GHAOUI, N. *et al.* Update on the use of dapsone in dermatology. **International Journal of Dermatology**, p. 1–9, 2020.

HADGRAFT, J.; LANE, M. E. Drug crystallization: implications for topical and transdermal delivery Drug crystallization. **Expert Opinion on Drug Delivery**, v. 13, n. 6, p. 817–830, 2016.

HERMAN, A.; HERMAN, A. P. Essential oils and their constituents as skin penetration enhancer for transdermal drug delivery: A review. **Journal of Pharmacy and Pharmacology**, v. 67, n. 4, p. 473–485, 2015.

INDULKAR, A. S. *et al.* Impact of Monomeric versus Micellar Surfactant and Surfactant-Polymer Interactions on Nucleation-Induction Times of Atazanavir from Supersaturated Solutions. **Crystal Growth and Design**, v. 20, n. 1, p. 62–72, 2020.

IQBAL, B.; ALI, J.; BABOOTA, S. Recent advances and development in epidermal and dermal drug deposition enhancement technology. **International Journal of Dermatology**, v. 57, n. 6, p. 646–660, 2018.

KAR, H. K.; GUPTA, R. Treatment of leprosy. **Clinics in Dermatology**, v. 33, n. 1, p. 55–65, 2015.

KASSIR, M. *et al.* Selective RAR agonists for acne vulgaris: A narrative review. **Journal of Cosmetic Dermatology**, v. 19, n. 6, p. 1278–1283, 2020.

KERI, J.; SHIMAN, M. An update on the management of acne vulgaris. **Clinical, Cosmetic and Investigational Dermatology**, v. 2, p. 105–110, 2009.

KOVÁČIK, A.; KOPEČNÁ, M.; VÁVROVÁ, K. Permeation enhancers in transdermal drug delivery: benefits and limitations. **Expert Opinion on Drug Delivery**, v. 17, n. 2, p. 145–155, 2020.

KUHNERT-BRANDSTATTER, M.; MOSER, I. Polymorphism of Dapson and ethambutoldihydrochloride. **Microchimica Acta**, v. 71, n. 1, p. 125–136, 1979.

LADEMANN, J.; RICHTER, H.; SCHANZER, S.; et al. Penetration and storage of particles in human skin: Perspectives and safety aspects. **European Journal of Pharmaceutics and Biopharmaceutics**, v. 77, n. 3, p. 465–468, 2011. Elsevier B.V.

LAKSHMAN, D. *et al.* Investigation of drug-polymer miscibility, biorelevant dissolution, and bioavailability improvement of Dolutegravir-polyvinyl caprolactam-polyvinyl acetate-polyethylene glycol graft copolymer solid dispersions. **European Journal of Pharmaceutical Sciences**, v. 142, n. October 2019, p. 105137, 2020.

LAZO-PORRAS, M. *et al.* World Health Organization (WHO) antibiotic regimen against other regimens for the treatment of leprosy: A systematic review and meta-analysis. **BMC Infectious Diseases**, v. 20, n. 1, p. 1–14, 2020. BMC Infectious Diseases.

LEMMER, H. *et al.* World Solvatomorphism of the antibacterial dapsone: X-ray structures and thermal desolvation kinetics. **Crystal Growth and Design**, v. 12, n. 3, p. 1683–1692, 2012.

LINDENBERG, M.; KOPP, S.; DRESSMAN, J. B. Classification of orally administered drugs on the World Health Organization Model list of Essential Medicines according to the biopharmaceutics classification system. **European Journal of Pharmaceutics and Biopharmaceutics**, v. 58, n. 2, p. 265–278, 2004.

LOCKWOOD, D.; MARIOWE, S.; LAMBERT, S. **Antibiotic and Chemotherapy**. Londres: Saunders Elsevier, 2010

MACHADO, T. C. *et al.* The role of pH and dose/solubility ratio on cocrystal dissolution, drug supersaturation and precipitation. **European Journal of Pharmaceutical Sciences**, v. 152, p. 105422, 2020.

MACRAE, C. F.; BRUNO, I. J.; CHISHOLM, J. A.; et al. Mercury CSD 2.0 - New features for the visualization and investigation of crystal structures. **Journal of Applied Crystallography**, v. 41, n. 2, p. 466–470, 2008.

MACRAE, C. F.; EDGINGTON, P. R.; MCCABE, P.; et al. Mercury: Visualization and analysis of crystal structures. **Journal of Applied Crystallography**, v. 39, n. 3, p. 453–457, 2006.

MACRAE, C. F.; SOVAGO, I.; COTTRELL, S. J.; et al. Mercury 4.0: From visualization to analysis, design and prediction. **Journal of Applied Crystallography**, v. 53, p. 226–235, 2020.

MAHORE, J. G.; SURYAWANSHI, S. D.; SHIROLKAR, S. V.; DESHKAR, S. S. Enhancement of percutaneous delivery of dapsone by microemulsion gel. **Journal of Young Pharmacists**, v. 9, n. 4, p. 507–512, 2017.

MAKULA, A.; MADDELA, R.; PILLI, N. R.; et al. A novel and Rapid LC–MS/MS assay for the Determination of Mycophenolate and Mycophenolic Acid in Human Plasma. **Journal of Young Pharmacists**, v. 9, n. 1, p. 107–114, 2017.

MÁQUINA, A. *et al.* Lepra: Da Antiguidade aos Nossos Tempos. **Journal of the Portuguese Society of Dermatology and Venereology**, v. 77, n. 4, p. 323–338, 2020.

MARWAH, H. *et al.* Permeation enhancer strategies in transdermal drug delivery. **Drug Delivery**, v. 23, n. 2, p. 564–578, 2016.

MASON, T. G. *et al.*. Nanoemulsions: Formation, structure, and physical properties. **Journal of Physics Condensed Matter**, v. 18, n. 41, 2006.

MCCLEMENTS, D. J. Nanoemulsions versus microemulsions: Terminology, differences, and similarities. **Soft Matter**, v. 8, n. 6, p. 1719–1729, 2012.

MEHNERT, W.; MADER, K. Advances in the Cognitive Neuroscience of Neurodevelopmental Disorders: Views from Child Psychiatry and Medical Genetics. **Neurodevelopmental Disorders**, v. 47, p. 165–196, 2020.

MENON, G. K. New insights into skin structure: Scratching the surface. **Advanced Drug Delivery Reviews**, v. 54, n. SUPPL., p. S3, 2002.

MOHIUDDIN, A. A Comprehensive Review of Acne Vulgaris. **Clinical Research in Dermatology,** v. 6, n. 2, p. 1–34, 2019.

MOLINELLI, E. *et al.* Metabolic, pharmacokinetic, and toxicological issues surrounding dapsone. **Expert Opinion on Drug Metabolism & Toxicology**, v. 15, n. 5, p. 367–379, 2019.

MONTEIRO, L. *et al.* Development and characterization of a new oral dapsone nanoemulsion system: Permeability and *in silico* bioavailability studies. **International Journal of Nanomedicine**, v. 7, p. 5175–5182, 2012.

MULLER, R. H.; MADER, K.; SVEN, G. Solid lipid nanoparticles (SLN) for controlled drug delivery - a review of the state of the art. , v. 50, n. 2314, p. 1–63, 2000.

MÜLLER, R. H.; RADTKE, M.; WISSING, S. A. Solid lipid nanoparticles (SLN) and nanostructured lipid carriers (NLC) in cosmetic and dermatological preparations. **Advanced Drug Delivery Reviews**, v. 54, n. SUPPL., p. 131–155, 2002.

NASERI, N.; VALIZADEH, H.; PZAKERI-MILANI, P. Solid Lipid Nanoparticles and Nanostructured Lipid Carriers: Structure, Preparation and Application. **Advanced Pharmaceutical**

Bulletin, v. 5, n. 3, p. 305–313, 2015.

NEUPANE, R.; BODDU, S. H. S.; RENUKUNTLA, J.; BABU, R. J.; TIWARI, A. K. Alternatives to biological skin in permeation studies: Current trends and possibilities. **Pharmaceutics**, v. 12, n. 2, 2020.

NORTON, S. A. Useful plants of dermatology. I. Hydnocarpus and chaulmoogra. **Journal of the American Academy of Dermatology**, v. 31, n. 4, p. 683–686, 1994.

OLIVEIRA, F. R. *et al.* Clinical applications and methemoglobinemia induced by dapsone. **Journal of the Brazilian Chemical Society**, v. 25, n. 10, p. 1770–1779, 2014.

OOMMEN S.T., RAO M., RAJU C.V.N. Effect of oil of hydnocarpus on wound healing. **Internacional Journal. Leprosy Other Mycobacterial Diseases**, n. 67, p. 154–158, 1999.

S OOMMEN S.T. The effect of oil of hydnocarpus on excision wounds [4], **Internacional Journal. Leprosy Other Mycobacterial Diseases,** n. 68, p. 69–70, 2000.

OMS. Controle da Hanseníase na Atenção Básica: Guia Prático Para Profissionais Da Equipe De Saúde Da Família. **Ministerio da Saude do Brasil**, n. 111, p. 1–86, 2001.

OMS. Guidelines for the Diagnosis, Treatment and Prevention of Leprosy. **World Health Organization,** 2018.

OSBORNE, D. W. Compositions and methods for topical applications of theraputic agents. US Pat n. 5,863,560, 1999.

OSBORNE, D. W. Compositions and methods for topical application of theraputic agentes. US Pat n. 6,060,085, 2000.

OSBORNE, D. W. Topical dapsone for the treatment of acne. Depositante: Allergan IN. US. Procurador: Gowling Lafleur Henderson LLP. CA n. 2,776,702, 2002.

PAIK, J. Topical Minocycline Foam 4%: A Review in Acne Vulgaris. **American Journal of Clinical Dermatology**, v. 21, n. 3, p. 449–456, 2020.

PARASCANDOLA, J. Chaulmoogra oil and the treatment of leprosy. **Pharmacy in history**, 2003.

PATZELT, A. *et al.* Selective follicular targeting by modification of the particle sizes. **Journal of Controlled Release**, v. 150, n. 1, p. 45–48, 2011.

PELIKH, O. *et al.* Hair follicle targeting with curcumin nanocrystals: Influence of the formulation properties on the penetration efficacy. **Journal of Controlled Release**, , n. August, p. 1–16, 2020.

PELIKH, O.; KECK, C. M. Hair follicle targeting and dermal drug delivery with curcumin drug nanocrystals—essential influence of excipients. **Nanomaterials**, v. 10, n. 11, p. 1–25, 2020.

PELIKH, O. *et al.* Nanocrystals for improved dermal drug delivery. **European Journal of Pharmaceutics and Biopharmaceutics**, v. 128, n. April, p. 170–178, 2018.

PIETERS, F.; ZUIDEMA, J. The pharmacokinetics of dapsone after oral administration to healthy volunteers. **British Journal of Clinical Pharmacology**, v. 22, n. 4, p. 491–494, 1986.

PIETTE, W. W. *et al.* Hematologic safety of dapsone gel, 5%, for topical treatment of acne vulgaris. **Archives of Dermatology**, v. 144, n. 12, p. 1564–1570, 2008.

PIREDDU, R. *et al*. Diclofenac acid nanocrystals as an effective strategy to reduce *in vivo* skin inflammation by improving dermal drug bioavailability. **Colloids and Surfaces B: Biointerfaces**, v. 143, p. 64–70, 2016.

POCHI, P. E. *et al* Report of the consensus conference on acne classification: Washington, D.C., March 24 and 25, 1990. **Journal of the American Academy of Dermatology**, v. 24, n. 3, p. 495–500, 1991.

PRAUSNITZ, M. R.; LANGER, R. Transdermal drug delivery. **Nature Biotechnology**, v. 26, n. 11, p. 1261–1268, 2008.

RIBEIRO, B. DE M. *et al* Etiopathogeny of acne vulgaris: a practical review for day-to-day dermatologic practice. **Surgical & Cosmetic Dermatology**, v. 7, n. 3, p. 20–26, 2015.

RODRIGUEZ, R.; ALVAREZ-LORENZO, C.; CONCHEIRO, A. Rheological evaluation of the interactions between cationic celluloses and Carbopol 974P in water. **Biomacromolecules**, v. 2, n. 3, p. 886–893, 2001.

RYTTING, E. *et al* Aqueous and cosolvent solubility data for drug-like organic compounds. **AAPS Journal**, v. 7, n. 1, 2005.

SAHOO, M. R. *et al* Hydnocarpus: An ethnopharmacological, phytochemical and pharmacological review. **Journal of Ethnopharmacology**, v. 154, n. 1, p. 17–25, 2014.

SAMUELS, D. V. *et al* Acne vulgaris and risk of depression and anxiety: A meta-analytic review. **Journal of the American Academy of Dermatology**, v. 83, n. 2, p. 532–541, 2020.

SANTOS, G. S. S. *et al.* Desenvolvimento e caracterização de nanopartículas lipídicas destinadas à aplicação tópica de dapsona. **Quimica Nova**, v. 35, n. 7, p. 1388–1394, 2012.

SARDANA, K. *et al.* Antibiotic resistance to *Propionobacterium acnes:* Worldwide scenario, diagnosis and management. **Expert Review of Anti-Infective Therapy**, v. 13, n. 7, p. 883–896, 2015.

SCHNEIDER-RAUBER, G. *et al.* Polymorphism and surface diversity arising from stress-induced transformations – the case of multicomponent forms of carbamazepine. **Acta Crystallographica Section B**, v. B77, 2021.

SCHNEIDER-RAUBER, G. *et al.* Effect of Solution Composition on the Crystallization of Multicomponent Forms of Carbamazepine beyond Crystal Form and Shape: Surface as a Source of Diversity in the Solid-Form Landscape. **Crystal Growth & Design**, 2020.

SCHOLZ, P.; ARNTJEN, A.; MÜLLER, R. H.; KECK, C. M. ARTcrystal® process for industrial nanocrystal production - Optimization of the ART MICCRA pre-milling step. **International Journal of Pharmaceutics**, v. 465, n. 1–2, p. 388–395, 2014.

SINGH MALIK, D.; MITAL, N.; KAUR, G. Topical drug delivery systems: A patent review. **Expert Opinion on Therapeutic Patents**, v. 26, n. 2, p. 213–228, 2016.

STOTLAND, M.; SHALITA, A. R.; KISSLING, R. F. Dapsone 5% Gel. **American Journal of Clinical Dermatology**, v. 10, p. 221–227, 2009.

TADWEE, I. K.; GORE, S.; GIRADKAR, P. Advances in Topical Drug Delivery System : A Review Abstract : Novel Topical Drug Delivery Systems : **Pharmaceutical Research**, v. 1, p. 14–23, 2011.

TAYLOR, R.; MACRAE, C. F. Rules governing the crystal packing of mono-and dialcohols. **Acta Crystallographica Section B: Structural Science**, v. 57, n. 6, p. 815–827, 2001.

THIBOUTOT, D. M. *et al.* Efficacy, Safety, and Dermal Tolerability of Dapsone Gel, 7.5% in Patients with Moderate Acne Vulgaris: A Pooled Analysis of Two Phase 3 Trials. **journal of clinical and aesthetic dermatology**, v. 9, n. 10, p. 18–27, 2016.

THIBOUTOT, D. M. *et al.* Pharmacokinetics of Dapsone Gel , 5 % for the Treatment of Acne Vulgaris. **Clinical Pharmacokinectis**, v. 46, n. 8, p. 697–712, 2007.

UASKA SARTORI, P. V. *et al.* Human Genetic Susceptibility of Leprosy Recurrence. **Scientific Reports**, v. 10, n. 1, p. 1–5, 2020.

UEDA, K. *et al.* Molecular Mobility Suppression of Ibuprofen-Rich Amorphous Nanodroplets by HPMC Revealed by NMR Relaxometry and Its Significance with Respect to Crystallization Inhibition. **Molecular Pharmaceutics**, v. 16, n. 12, p. 4968–4977, 2019.

VENUGANTI, V. *et al.* Structure-skin permeability relationship of dendrimers. **Pharmaceutical Research**, v. 28, n. 9, p. 2246–2260, 2011.

VIDLÁŘOVÁ, L. *et al.* Nanocrystals for dermal penetration enhancement - Effect of concentration and underlying mechanisms using curcumin as model. **European Journal of Pharmaceutics and Biopharmaceutics**, v. 104, p. 216–225, 2016.

WHO. Global leprosy update, 2018: moving towards a leprosy- free world. **Weekly Epidemiological Record**, v. 94, n. August 2019, p. 389–412, 2019.

WHO. Leprosy elimination. Disponível em: <https://www.who.int/news-room/fact-sheets/detail/leprosy>. .

WILLIAMS, H. C.; DELLAVALLE, R. P.; GARNER, S. Acne vulgaris. **The Lancet**, v. 379, n. 9813, p. 361–372, 2012.

WOLF, R.; TUZUN, B.; TUZUN, Y. Dapsone: Unapproved uses or indications. **Clinics in Dermatology**, v. 18, n. 1, p. 37–53, 2000.

WONG, T. W. Electrical, magnetic, photomechanical and cavitational waves to overcome skin barrier for transdermal drug delivery. **Journal of Controlled Release**, v. 193, p. 257–269, 2014.

WOZEL, G.; BLASUM, C. Dapsone in dermatology and beyond. **Archives of Dermatological Research**, v. 306, n. 2, p. 103–124, 2014.

WOZEL, V. E. G. The Story of Sulfones in Tropical Medicine and Dermatology. **International Journal of Dermatology**, v. 28, n. 1, p. 17–22, 1989.

WOZEL, V. E. G. Innovative use of dapsone. **Dermatologic Clinics**, v. 28, n. 3, p. 599–610, 2010.

YANG, H. *et al.* A novel method for determining the viscosity of polymer solution. **Polymer Testing**, v. 23, n. 8, p. 897–901, 2004.

YATHIRAJAN, H. S. *et al.* Experimental Crystal Structure Determination. **CSD communication,** 2004.

ZAENGLEIN, A. L. *et al.* Guidelines of care for the management of acne vulgaris. **Journal of the American Academy of Dermatology**, v. 74, n. 5, p. 945- 973.e33, 2016.

ZAIDI, Z.; LANIGAN, S. W. **Dermatology in Clinical Practice**. London: Springer, 2010.

ZHAI, X. *et al.* Dermal nanocrystals from medium soluble actives - Physical stability and stability

affecting parameters. **European Journal of Pharmaceutics and Biopharmaceutics**, v. 88, n. 1, p. 85–91, 2014.

ZHANG, J. *et al.* Impact of Polymer Enrichment at the Crystal-Liquid Interface on Crystallization Kinetics of Amorphous Solid Dispersions. **Molecular Pharmaceutics**, v. 16, n. 3, p. 1385–1396, 2019.

ZHU, Y. I.; STILLER, M. J. Dapsone and sulfones in dermatology: Overview and update. **Journal of the American Academy of Dermatology**, v. 45, n. 3, p. 420–434, 2001.

ZUIDEMA, J.; HILBERS-MODDERMAN, E. S. M.; MERKUS, F. W. H. M. Clinical Pharmacokinetics of Dapsone. **Clinical Pharmakokinetics**, v. 11, p. 299–315, 1986.

4 CAPÍTULO II – CARACTERIZAÇÃO DE CRISTAIS EM GÉIS COMERCIAIS DE DAPSONA

Este capítulo trata da caracterização de formas sólidas presentes em géis comerciais de DAP frente as substituições do solvente orgânico (agente solubilizante). As formulações foram reproduzidas conforme patentes do gel comercial (OSBORNE, 1999, 2000, 2002). A forma sólida presente em cada gel foi analisada por difração de raios X e microscopia. A quantidade de DAP dissolvida foi quantificada por espectrofotometria UV-vis. A distribuição dos géis em pele humana também foi avaliada com auxílio de um estereoscópio. O produto deste capítulo é um artigo científico, que foi publicado na revista *Molecular Pharmaceutics* em julho de 2022. Além da descoberta de nova forma sólida, a qual foi depositada em banco específico, este estudo demonstrou que é preciso ter cuidado durante a substituição do agente solubilizante em géis tópicos, particularmente quando há fármaco na forma sólida, já que isto pode afetar na quantidade de cristais, forma cristalina do fármaco; com impacto direto no desempenho do produto.

PORT, B. C. B. *et al* .Effect of vehicle composition on the preparation of different types of dapsone crystals for topical drug delivery. **Molecular Pharmaceutics**, v. *19* (7), p. 2164-2174, 2021.

Link para consulta:
https://pubs.acs.org/doi/10.1021/acs.molpharmaceut.2c00031

4.1 ARTIGO

THE EFFECT OF VEHICLE COMPOSITION ON THE PREPARATION OF DIFFERENT TYPES OF DAPSONE CRYSTALS FOR TOPICAL DRUG DELIVERY

Bianca da Costa Bernardo Port,[a] Gabriela Schneider-Rauber,[a] Debora Fretes Argenta,[a] Mihails Arhangelskis,[b] Carlos Eduardo Maduro de Campos,[c] Adailton João Bortoluzzi,[d] Thiago Caon[a]**

[a] Postgraduate Program in Pharmacy (PGFAR); [b] Faculty of Chemistry, University of Warsaw, 1 Pasteura Street, Warsaw, 02-093, Poland; [c] Department of Chemistry; Federal University of Santa Catarina, Trindade, Florianopolis, 88040-900, Brazil

*Corresponding authors: gabisrauber@gmail.com; caon.thiago@ufsc.br

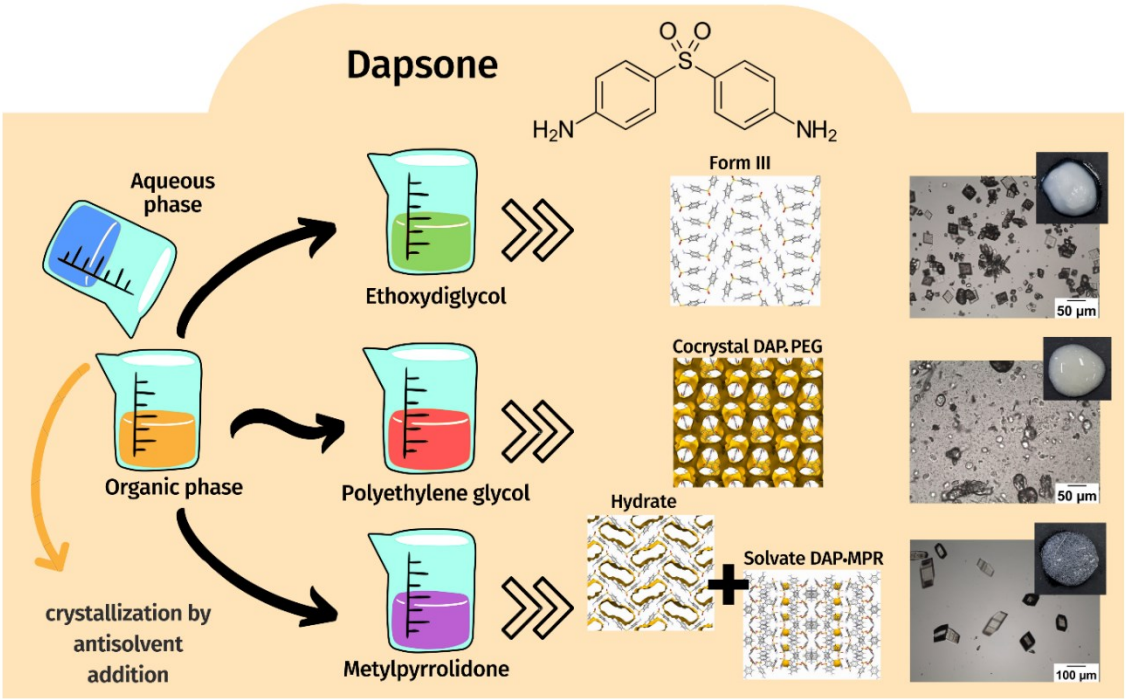

ABSTRACT

Topical formulations composed of API-pure crystals have been increasingly studied, especially in regard to the impact of particle size in penetration efficiency. Less attention, however, has been devoted to the solid-state properties of drugs delivered to the skin. In this study we address the effect of formulation composition on the crystal form existing in topical products. Dapsone (DAP) gel formulations were prepared by mixing an organic solution containing DAP with an aqueous solution containing polymers and preservatives. The organic solvent was chosen between ethoxydiglycol (DEGEE), polyethyleneglycol (PEG) and 1-methyl-2-pirrolidone (MPR) to assess the impact of composition on DAP crystal form. Such solvent variations resulted in different particulate matter. In terms of crystalline nature, the presence of DEGEE in formulations induced the crystallization of DAP hydrate, while PEG cocrystal and a mixture of hydrate and MPR solvate crystallized from same amounts of PEG and MPR, respectively. Microscopic analysis of the gels showed heterogeneous particles with different characteristics. The behavior of gels after application to the skin was also tested. Interestingly, the different formulations seemed to accumulate in different regions of the skin. This could be the result of the effect of vehicle composition/excipients on the characteristics of the skin, such as hydration. The site-specific accumulation, however, was more pronounced in crystal-loaded gels as opposed to blank formulations. These results indicate that future studies should consider the effect of formulation composition on the API crystal form landscape as part of the strategies used to successfully target drug delivery to the skin.

Keywords: *Dapsone; Crystal engineering; Crystal form; Formulation; Gel; Topical drug delivery; Skin.*

1 INTRODUCTION

The solid characteristics (i.e., crystal form, disorder and amorphous content, morphology, particle size, and surface identity) of a drug candidate are widely recognized as critical to control manufacturing processes and modulate the performance of pharmaceuticals.[1–7] For instance, Caspi et al.[8] and Cink et al.[9] have used crystallization to purify and to improve the filterability of the active pharmaceutical ingredient (API) glecaprevir in the steps of synthesis and formulation preparation for early clinical trials. Also, in terms of overcoming solubility and dissolution problems, recent studies highlight that selecting the appropriate combination of API solid form and formulation composition are key to generate and maintain supersaturation for appropriate physiologically based pharmacokinetics (PBPK) properties.[10–17] The literature, as illustrated above, has been predominantly devoted to deepening the understanding of solid dosage forms targeting oral route. When it comes to the selection of crystals for interaction with skin, however, the works are sparse and frequently focus on crystallization as a problem to be avoided.[18–21] An open question, therefore, is how the state-of-the-art of solid-state chemistry and crystal engineering translates into topical and transdermal formulations containing crystals.

Drug delivery systems to and through the skin have been considered as alternatives to reduce side effects, avoid first-pass metabolism in the liver, and modulate drug delivery. Various technological strategies have been reported to either enhance the permeation of drugs through the stratum corneum aiming at systemic exposure or to target the treatment of specific sites of the skin.[22–25] It has been shown, for instance, that drugs in particulate form (e.g., crystals and carrier-based systems) tend to penetrate the hair follicle more efficiently and form depots for sustained local release.[26,27] Indeed, topical formulations composed of nanosized API-pure crystals have been increasingly studied.[26,28–31] Their higher surface area improves dissolution rate and results in higher concentration gradient, which drives tissue penetration. In addition, nanocrystals have greater adhesion to biological membranes in comparison to the dissolved drug, a characteristic that may contribute to the formation of reservoirs.[28,30–33]

With respect to the formulation of topical products containing crystals, the main focus of the previous studies has been the impact of particle size on penetration depth and efficiency.[34–36] Only recently has the effect of vehicle and formulation composition been evaluated as for crystals applied to the skin. Pelikh and co-workers,[26,29] for example, found that the vehicle's viscosity and lipophilic nature had a minor effect on the penetration of curcumin

nanocrystals. The presence of humectants such as glycerol and urea, in turn, was remarkable at promoting passive diffusion, although the hydration of the stratum corneum was disadvantageous to the follicular route. This illustrates that selecting the appropriate combination of formulation composition and particulate matter is key to successfully target drug delivery to the skin. To the best of our knowledge, however, no study has focused on the effect that formulation composition may have on the properties of the solid API, such as crystal form and habit, and how both aspects may impact topical product performance. In the present work, we selected dapsone (4,4-diaminodiphenylsulphone, DAP) as a model to fill this gap and add to the existing literature.

DAP (Figure 1) belongs to the class of sulfones. Its most known pharmacological activity is related to the antimicrobial action of inhibiting the enzymes dihydrofolate synthase and dihydrofolate reductase, responsible for the synthesis of folate in bacteria.[37] The drug also has anti-inflammatory properties, although the mechanisms are still not well understood. Due to its double activity as antimicrobial and anti-inflammatory, DAP is currently used in several treatments of dermatological disorders such as herpetiform dermatitis, leprosy, and acne vulgaris. Topical formulations containing particulate DAP appear as localized treatment to such diseases, counteracting the known systemic side effects of the drug (i.e., hemolytic anemia, methemoglobinaemia, and hemolysis), especially in patients with G6PD deficiency.[38−41]

Topical preparations of DAP have only been marketed in the USA as aqueous gels for acne containing 5 or 7.5% of the drug for twice and once a day application, respectively.[44] In these products, it is claimed that one fraction of DAP is dissolved and accounts for crossing the stratum corneum of the epidermis. The other fraction of undissolved drug, that is, microparticulate DAP, is said to target the follicle and form reservoirs for sustained delivery. The preparation of such formulations may be described as the mixture of an organic solution of DAP with an aqueous solution containing polymer and preservative excipients, as well as the well-known procedure of crystallization by antisolvent addition. Patents mention the use of varied water/organic solvent proportions as well as the use of different organic solvents to solubilize DAP in topical formulations, namely, diethylene glycol monoethyl ether (DEGEE, also known as ethoxydiglycol and transcutol), polyethylene glycol (PEG), and 1-methyl-2-pirrolidone (MPR) (Figure 1).[42,43]

Our investigation focuses on whether varying the composition of the vehicle of such formulations impact crystal form, particle size and morphology. The initial hypothesis was that, indeed, the nature and the concentration of excipients is critical, not only because DAP has numerous crystal forms reported in the literature (i.e., five polymorphs (I−V), one hydrate,[45]

and many solvates and cocrystals,[46] including one multicomponent crystal form with PEG)[47] but also because the characteristics of the gels can affect crystal growth.[31] For example, Foster et al. have used gels as crystallization substrates to selectively target the growth of different crystal forms.[7] In our study we used phase diagram studies to evaluate the nature of the solid form in equilibrium with different solution compositions (DEGEE, PEG, MPR, and mixtures thereof with water). Such studies were the basis for the interpretation of the characteristics of three gel formulations containing DAP. The physicochemical characterization of the formulations is also discussed in combination to their behavior when applied to the skin. We close the study with structural analyses of DAP crystal forms that are relevant to the formulations and elaborate on concepts of crystal engineering applied to topical and transdermal drug delivery.

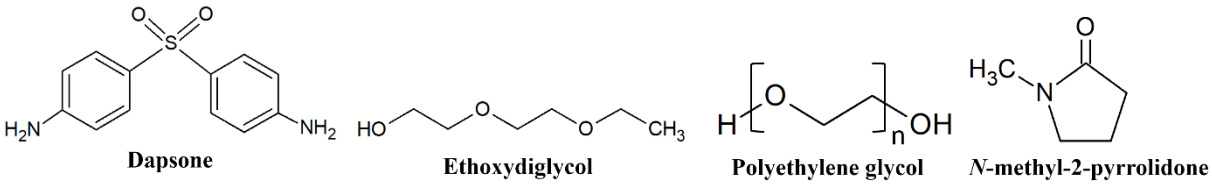

Figure 1. Chemical structures of studied compounds. Although 1-methyl-2-pyrrolidone has been used as a solubilizing and permeation enhancer agent in the past, it is important to warn that there is currently a restriction on its use in pharmaceutical and cosmetic formulations. According to the harmonized classification and labelling (ATP09) approved by the European Union, this substance may damage the unborn child, cause serious eye irritation, skin irritation, and respiratory irritation.

2 EXPERIMENTAL SECTIONS

2.1 Materials

All chemicals were used as received, without further purification (DAP was identified as polymorph III; see **Figures S1−S4** for raw material characterization). DAP 97% and MPR 99% were obtained from Sigma-Aldrich Products (São Paulo, São Paulo, Brazil). PEG was kindly donated by Croda (Campinas, São Paulo, Brazil). DEGEE andethanol PA were supplied by Chemo-union (Sorocaba, São Paulo, Brazil) and Neon (Suzano, São Paulo, Brazil) respectively. The gelling agent for the preparation gel, the carbomer 980, was kindly donated by Ashland (São Paulo, São Paulo, Brazil). The ultrapure water used in the assays was obtained through the Milli-Q system (Millipore, Bedford, MA).

2.2 Phase diagram studies

To compose the phase diagram study, the solubility of DAP in different systems was evaluated. An excess amount of DAP was added to 2 mL of solutions containing water and the respective organic solvent (namely DEGEE, PEG 600 and MPR) in different mass proportions. Duplicate samples were prepared for each data point. The vials were sealed and stirred in a magnetic stirrer (Multistirrer 15, Velp Scientifica, Italy) for 72 h at room temperature. By the end of the experiments, samples from each vial were centrifuged at 6,200 rpm for 10 min. The concentration of DAP in the filtrates was determined using UV spectrometry (see **Section 2.4**) while the precipitates were analyzed by X-ray powder diffraction (see **Section 2.5**).

2.3 Formulation preparation

The gels were prepared according to methods described elsewhere.[48−50] Unless specified, the proportions of the constituents are shown as mass percents. The aqueous phase was prepared by adding 0.85% carbomer 980 in 66.95% previously weighed water. The mixture was subjected to stirring at 300 rpm until complete solubilization of the gelling agent was achieved. Separately, the organic phase was prepared using 25% organic solvent (DEGEE, PEG, or MPR), 0.2% methylparaben, and 5% DAP under stirring at 300 rpm. With the aid of a graduated pipet, the aqueous phase was then poured into the organic phase at approximately 0.85 g·s−1, which was kept under stirring for 5 min. By the end of the addition of the aqueous phase, precipitation was clearly observed. Finally, 2% of sodium hydroxide solution (10%) was added to change the pH and gel the formulation. Each resulting formulation was also prepared

without the gelation step. The aim of such procedure was to (i) allow the quantification of DAP in solution (see **section 2.4**), (ii) facilitate the diffraction analyses (see **section 2.5**), and (iii) test for phase and particle modifications as a function of gelation. All formulations were prepared in duplicates and were characterized on the day of preparation and after 7 days of storage at room conditions to account for aging issues (i.e., crystallization and phase and particle transformations).

2.4 Quantification of DAP in solution

The fraction of DAP in solutions coming from either the solubility studies or the formulations were quantified from the supernatant obtained after centrifugation at 6200 rpm for 10 min. An aliquot of the centrifugate was adequately diluted in ethanol PA.[51] The analyses were carried out in duplicates. The resulting solutions were analyzed using UV spectrophotometry (Cary 60, Agilent, Santa Clara, CA) at 295 nm. A calibration curve was used in the quantification step ($y = 0.1192x - 0.0028$; $r2 = 0.9991$).

2.5 Powder X-ray diffraction (PXRD)

X-ray diffraction patterns were obtained from an Xpert Pro Multi-Purpose diffractometer (PANAnalytical). The diffractometer operating with Cu Kα radiation ($\lambda = 1.5418$ Å), current of 40 mA and voltage of 45 kV, was equipped with a position-sensitive linear detector Xcelerator. The powder/gel were mounted into the small cavities of Si zero-background sample holders. The measurements were carried out at room temperature spinning the sample about 2 s/rev, by scanning 2θ in the range of 3− 60°, covering an angular interval of 0.017° every 51 s.

2.6 Crystal structure search and analysis

ConQuest (2020.2.0)[52] and the literature were searched for known crystal structures of DAP. The reference crystallographic information files used in our study are as follows: Form III (DAPSUO13),[53] Form V,[54] hydrate (ANSFON02),[55] and a multicomponent crystal form with PEG (YIPMIW)[44] (crystal data information are shown in **Table S1**). Mercury[52,56–59] was used for general structural analysis and comparison of different crystallographic information files. The calculated diffraction patterns of known structures retrieved from the literature were used to characterize the experimental diffractograms (**Figure S6**).

2.7 Rietveld refinement and quantitative phase analysis

Rietveld refinement was used to verify the identity of the crystalline phases and quantify the compositions of phase mixtures (**Figure 3**). The refinement was carried out in TOPAS Academic 6,[60] using the structures identified in **section 2.6** to model the diffraction profiles of experimental PXRD patterns. The diffraction line profile was modeled with a pseudo-Voigt function combined with simple axial divergence model, while the background was described with a Chebyshev polynomial function. Other refinable parameters included zero shift and March−Dollase[61] preferred orientation correction. Finally, the unit cell parameters were refined in order to account for the differences between the low-temperature crystal structures found in CSD and room-temperature PXRD data collection.

2.8 Microscopy analysis

Crystal habit, particle size, and agglomeration state were evaluated using an Olympus BX40 (Olympus Cooperation, Tokyo, Japan) transmission optical microscope equipped with a Micrometrics 318CU 3.2MP CMOS digital camera (Micromeritics Instrument Corporation, São Paulo, Brazil). The samples were prepared on a glass slide covered by a glass lid and analyzed at magnifications of 100× and 200×. The images were obtained at room temperature. The characterization of the solids is detailed in **Supporting Information section 6 and Figures S11−S15.**

2.9 Formulation's behavior on human skin

An Olympus SZX16 stereo microscope system (Olympus, Japan) skin. The experiments were carried out on abdominal human skin model, which was obtained from abdominoplasty surgeries. The study was approved by the Research Ethics Committee of the University (CAE number: 87349418.7.0000.0121). Skin samples were collected in Krebs buffer shortly after surgery, and then the adipose tissue was removed. They were stored in aluminum foil at −20 °C until use. Intact skin areas of 2 × 2 cm^2 without visible wounds and scratches were selected. The skin was analyzed right after the application and 2 h after incubation at 37 °C. This assay was adapted based on methodologies used in other studies targeting the follicle.[29,26]

3 RESULTS AND DISCUSSION

3.1 Phase diagram studies

Solubility studies were used not only to identify the most stable crystal form of DAP in the solvent composition of formulations but also to evaluate the risk of phase modifications and to screen novel crystal forms. The phase diagrams were expected to show a threshold of solvent activity, beyond which the crystal form invariably changes when the system is thermodynamically controlled, yet the studies of DAP in DEGEE/water (**Figure 2a**) were rather inconsistent as the presence of hydrate and anhydrous Form III was stochastic. The literature shows that kinetics plays an important role in the crystallization of anhydrous DAP in aqueous solutions. Until 2018, for instance, only four anhydrous forms of DAP were known (i.e., forms I−IV), and Form III was considered the most stable polymorph at room temperature.[62] During studies of DAP hydrate,[45] however, a new polymorph was found and named Form V. In-depth studies[54] expanded the characterization of Form V and the solubility experiments in different organic solvents, all of which consistently indicated that Form V is thermodynamically more stable than Form III, and they are both monotropically related.[54] The authors concluded that Form V was possibly discovered late because of its low rate of crystal nucleation and growth (i.e., it is a slow crystallizer) compared to the high rates for Form III (i.e., it is a fast crystallizer).[54] It is possible that our experimental findings in DEGEE/water may also be explained by differences in the kinetics of nucleation and growth between DAP hydrate and Form III. This hypothesis is supported by the fact that solubility studies of DAP hydrate previously shown in the literature had to be equilibrated for remarkable 21 days.[45]

In the case of the PEG/water and MPR/water (**Figure 2b,c**), in turn, two regions were clearly identified in the phase diagrams: one region showing the hydrate as the stable form in high water proportions, and another region of lower water activities in which other multicomponent crystal forms were identified. The diagrams show that above 10% PEG or MPR in water, DAP tends to crystallize with PEG or MPR, respectively. The higher the organic solvent proportion in water, the lower the risk of hydrate crystallization. Importantly, the existence of a solvate of DAP with MPR had not been reported in the literature before. The new phase was first isolated in our phase diagram studies, which were also the basis for growing crystals used in structure solution and characterization analyses (see the **Supporting Information section 5, Figures S6−S10, and Table S2**).

Both PEG and MPR may be promising alternatives for controlling the crystallization of DAP because the kinetic component does not seem to be predominant in the equilibrium of

DAP hydrate and DAP solvate crystals. The equilibrium between hydrate and anhydrous form of DAP (as when DAP is crystallized from DEGEE:water), in turn, seems to be highly affected by kinetics. In terms of formulation development, this means a higher risk of batch-to-batch and storage variations.

In addition to the identification of crystal form, the phase diagrams were also used to estimate the fraction of drug dissolved and crystallized in DAP formulations. Although the amount of dissolved DAP is much higher in high proportions of DEGEE in comparison to PEG and MPR, the solubilities are similar in the range between 10 and 25% of all three solvent compositions with water (which are the same compositions used in DAP gels). In the formulations, however, the presence of other excipients may result in additional intermolecular interactions and different characteristics of solubility and supersaturation, as discussed in the next section.

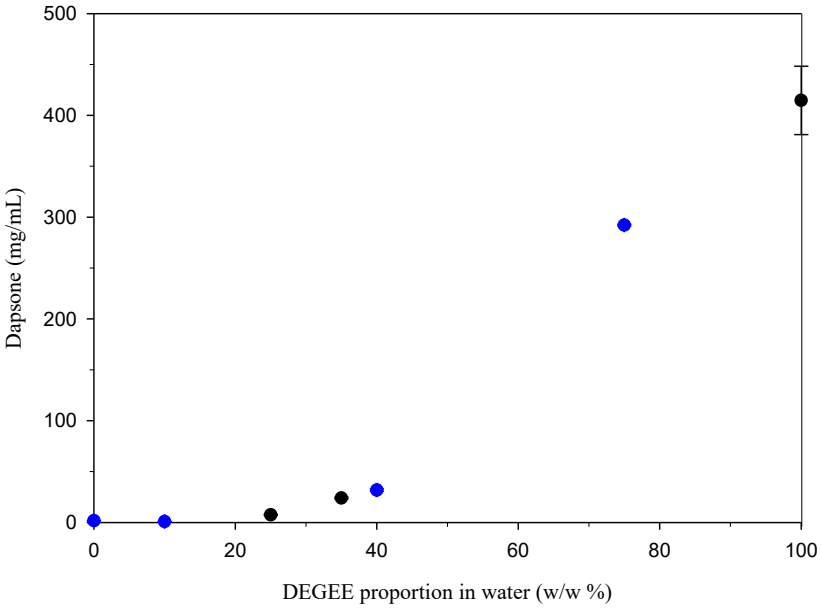
Dapsone (mg/mL)
0
100
200
300
400
500
0
20
40
60
80
100
DEGEE proportion in water (w/w %)

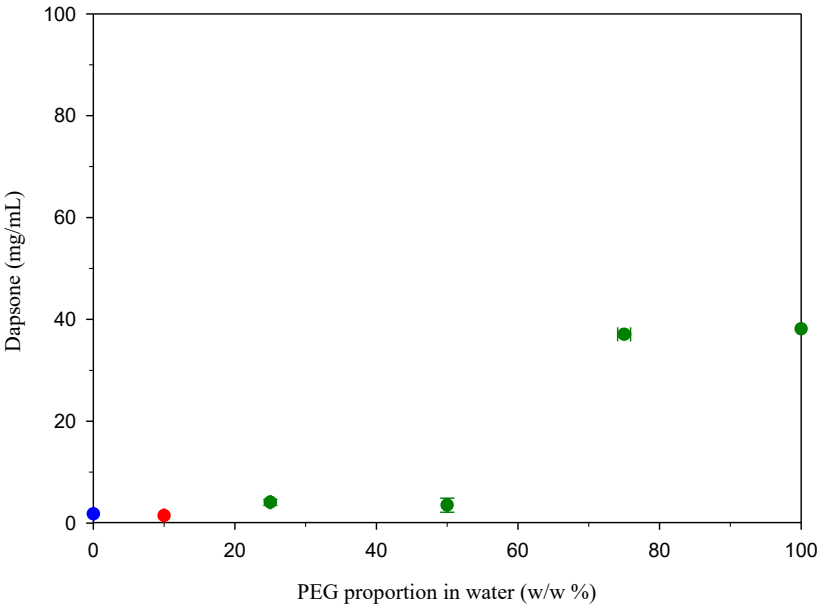
Dapsone (mg/mL)
0
20
40
60
80
100
0
20
40
60
80
100
PEG proportion in water (w/w %)

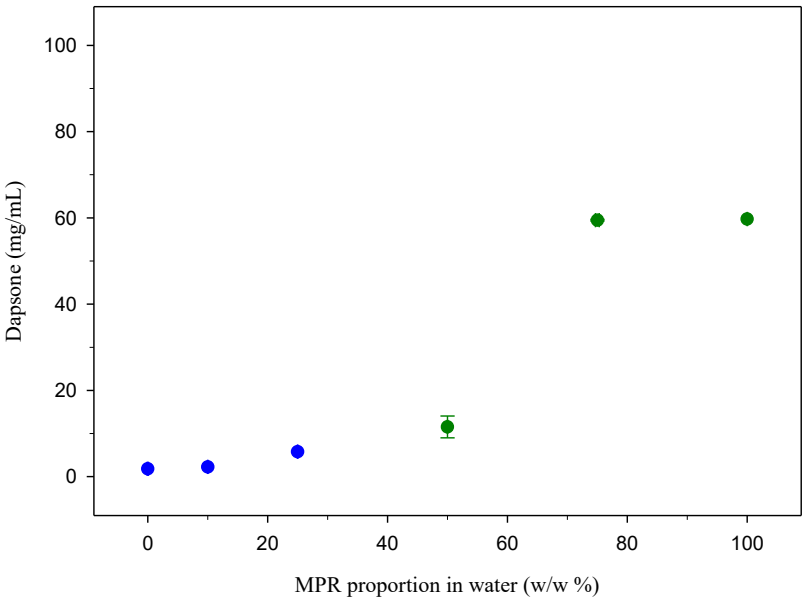
Dapsone (mg/mL)
0
20
40
60
80
100
0
20
40
60
80
100
MPR proportion in water (w/w %)

Figure 2. Phase diagrams of dapsone (DAP) in DEGEE/water (a), PEG600/water (b), and 1-methyl-2-pyrrolidone/water (c). The graphs are a combination of different experiments, namely, the quantification of DAP in solution (solubility) and identification of the solid phase. Plots relate the amount of DAP in solution (mg mL^{-1}) versus the mass-to-mass ratio of solvent in water. The colors of the symbols show the identity of the solid phases in equilibrium with solution. Black circles, DAP Form III; green circles, the respective DAP solvate or cocrystal; and blue circles, DAP hydrate. Regions characterized as mixtures of Form III and multicomponent phases are shown in red.

3.2 Formulation studies

The gel formulations of DAP were prepared by a method that is very similar to what is known as antisolvent addition in the crystallization literature. This method involves API solubilization in a suitable organic solvent to obtain a highly concentrated solution. Separately, a miscible antisolvent system in which the API has low solubility is prepared and then added to the organic solution. As a result, drug crystallization is observed. Several parameters can change the outcome of this process of crystallization (e.g., the rate of antisolvent addition, the agitation speed, the concentration of API in the organic solvent, the solvent constitution, the temperature, and the addition of crystalline seeds). In our experiments, three different gel formulations were prepared simply by replacing the organic solvent. The composition and all the other process parameters were kept the same. The organic solvent proportion of 25% in water was selected based on the literature.[48−50] According to the phase diagram studies, the amount of DAP dissolved in these solvent compositions is similar regardless of the differences in crystal form.

Table 1. Fraction of dapsone (DAP) dissolved in the formulation immediately after preparation and after 7 days.

Formulation	Solubility ($mg.mL^{-1}$)[a]	Form crystalline[a]	DAP dissolved ($mg.mL^{-1}$)	DAP dissolved ($mg.mL^{-1}$)	DAP precipitated ($mg.mL^{-1}$)	Form crystalline
FDE	7.53 ± 0.54	Form III	8.06 ± 1.35	7.59 ± 0.12	418.30 ± 14.63	Hydrate
FPE	4.06 ± 0.40	PEG cocrystal	8.40 ± 1.70	7.61 ± 0.42	411.21 ± 14.65	PEG cocrystal
FMP	5.76 ± 0.04	MPR solvate	33.28 ± 3.75	29.06 ± 2.32	167.77 ± 46.11	MPR solvate and hydrate

[a] Values extracted from the phase diagram studies (see **section 3.1** for details).

The amount of precipitated drug in the gels was indirectly determined from the quantification of DAP in solution (**Table 1**). The results demonstrate that DEGEE and PEG formulations (namely, FDE and FPE, respectively) show a higher amount of precipitated DAP

than the MPR formulation (namely, FMP). For instance, while FDE and FPE contain about 418 and 411 mg·mL−1 solid DAP, respectively, FMP shows less than half of it (∼167 mg·mL−1). Consequently, FMP shows 4 times more DAP in solution than FDE and FPE.

The solution concentrations of FPE and FMP, however, vary from the solubility shown in the phase diagram studies. The formulations containing PEG and MPR show a 2- and 6-fold increase in the amount of dissolved DAP at the proportion of 25% organic solvent in comparison to the solubility. It indicates that both formulations are in a supersaturated state, particularly FMP. This characteristic did not vary significantly after 7 days of storage.

The association of PXRD analyses with microscopy also shows that none of the crystals of DAP in the formulations change with the gelation process (**Figures S16−S18**) and short-term storage (**Figures S20−S22**). In terms of the crystalline nature, the analyses have shown that formulations contain different DAP particles (**Figure 3**). The diffractograms collected from FDE showed a pattern of reflections that agree with DAP hydrate. This is shown in the Rietveld analyses by the comparison of experimental and calculated patterns (**Figure 3a**). In contrast, from the phase diagram studies, DAP Form III was expected in 25% DEGEE. The existence of a different phase in FDE confirms that the equilibrium between Form III/hydrate may be strongly affected by kinetics and is difficult to control.

In the cases of PEG/water and MPR/water, systems containing 25% of organic solvent in water were expected to result in PEG cocrystal and hydrate, respectively. This result was indeed observed in gels prepared with PEG (**Figure 3b**), yet a mixture of hydrate and MPR solvate is obtained in formulations prepared with 25% MPR (**Figure 3c**), which may also explain the high amount of dissolved DAP in FMP (**Table 1**).

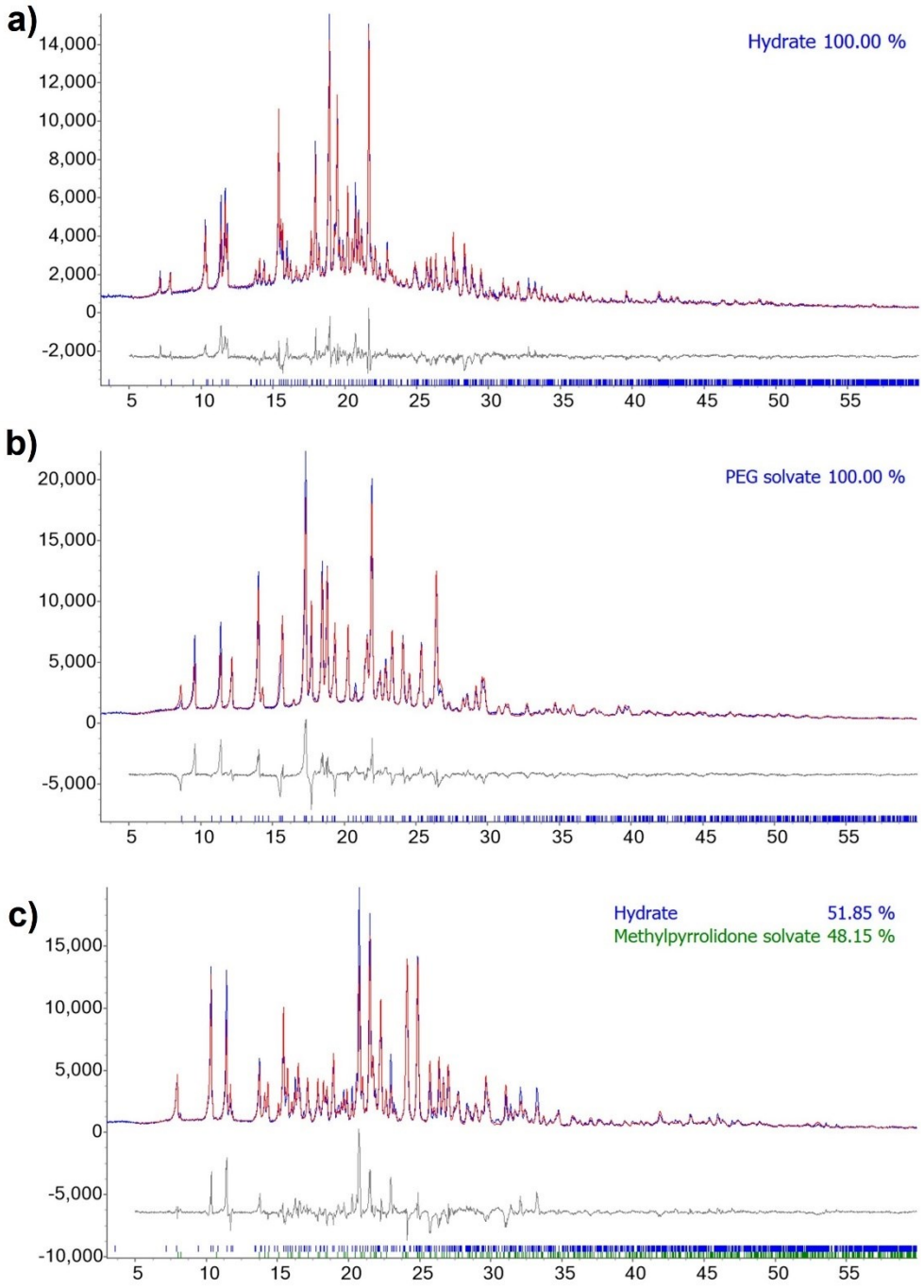

Figure 3. Crystal phase analysis of dapsone (DAP) in formulations by Rietveld method. (a) FDE formulation comparing diffraction patterns of sample with hydrate. (b) FPE formulation comparing the diffraction patterns of sample with PEG cocrystal. (c) FMP formulation comparing diffraction patterns of sample with DAP hydrate and 1-methyl-2-pyrrolidone solvate. Rietveld refinement fit of the experimental pattern (red) and the calculated one (blue). Gray traces are the corresponding residuals of the differences between them; vertical ticks mark the allowed Bragg reflections.

The microscopic analysis shows heterogeneous particles in terms of size and morphology (**Figure 4**). Different particles within the same formulation could either indicate that one solid may crystallize in various shapes/surface characteristics, or the crystallized material is composed of a mixture of phases that show different morphology characteristics. The diffraction pattern in **Figure 3c** indicates a mixture of DAP crystal forms in FMP, while microscopy shows a mixture of prismatic crystals with different shapes (**Figure 4**). Isolated and agglomerated prismatic crystals presenting different contrast characteristics are shown in formulations prepared in DEGEE/water. Agglomerated small particles and a few thin needles are seen in the formulations with PEG/water. Differences in the processes of nucleation and growth that are driven, for example, by supersaturation and viscosity may explain these microscopic variations in FPE. Although Rietveld analyses are not suggestive of mixtures, their presence in FDE and FPE, however, is not excluded because crystalline phases may not be detected in concentrations below 5%, particularly when preferred orientation is present.

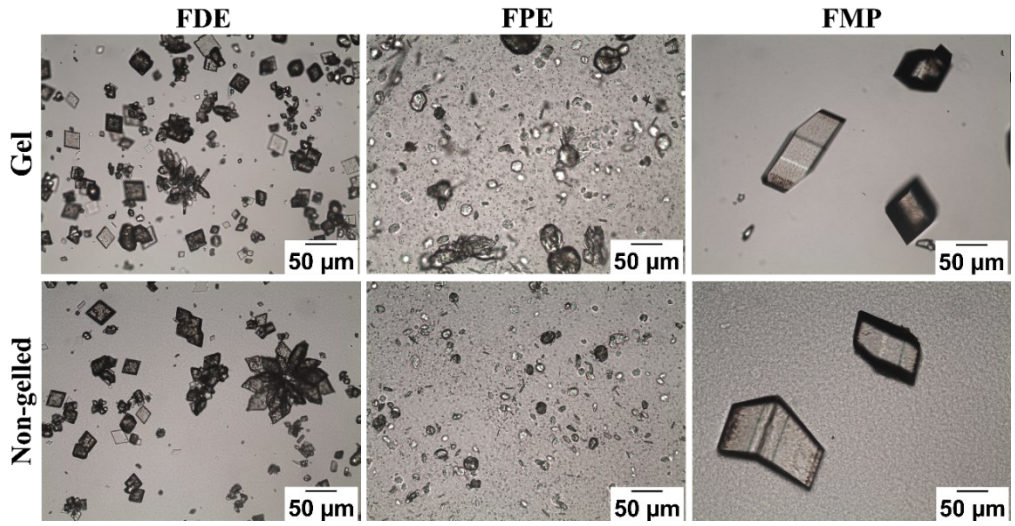

Figure 4. Microscopic images of the formulations (FDE, DEGEE/water; FPE, PEG600/water; FMP, 1-methyl-2-pyrrolidone/water).

All the formulations also showed markedly different macroscopic characteristics (**Figure 5**). The gel containing DEGEE had characteristics of an emulgel. The formulation was white, viscous, and homogeneous. The gel composed of MPR showed a similar viscosity, but precipitate agglomeration was visually noticed. The formulation with PEG600, in turn, was yellow and presented lower viscosity and a greater amount of precipitate agglomerated in the gel. The viscosity of gels is known to change with the presence of particles and salts, the type of polymer used, the solvent nature, and composition. [62–65] In our study, gels with and without DAP did not show significant changes in viscosity, except for PEG-based formulations. In this

case, the presence of crystals seems to negatively affect viscosity. Preliminary analyses have also tested the behavior of DAP-loaded and unloaded gels after application to the skin.

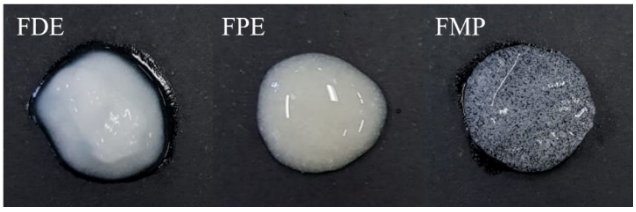

Figure 5. Macroscopic analysis of formulations (FDE, DEGEE:water; FPE, PEG 600:water; FMP, 1-methyl-2-pyrrolidone:water).

Figure 6 shows the results in two stages, immediately after the application and after incubating the skin with formulation at 37 °C for 2 h. Interestingly, the different formulations appeared to accumulate in different regions of the skin. The formulation composed of PEG, for instance, was more homogeneously distributed on the skin while the gel containing DEGEE showed a tendency to concentrate around the hair, particularly after incubation (**Figure 6a**). The gel containing MPR seemed to accumulate in cavities of the skin surface like the interface of corneocytes, again, mainly after incubation. These experimental findings may result from a combination of different characteristics found in the formulations, such as differences in the viscosity and the physicochemical characteristics of the organic solvents (e.g., lipophilicity and vapor pressure). The vehicles used may also interact with the stratum corneum and change its properties.[66] Pelikh and co-workers,[26,29] for example, found that the presence of humectants such as glycerol and urea promoted the passive diffusion of curcumin from nanocrystals, while it decreased its appendageal transport. Patel et al.[67] have also shown that excipients permeate the skin to different degrees, and this characteristic can be used to estimate the drug overall permeation and build IVIV correlations. Therefore, the effect of different vehicles on the skin may have also contributed to the behavior of the formulations containing DAP. The sitespecific accumulation of the formulations, however, seemed to be more pronounced in the presence of DAP crystals, (i.e., DAP-loaded gels). This fact was particularly observed in the formulation with DEGEE (**Figure 6b**). Hence, our results show that the amount of dissolved/precipitated DAP, particle size, and crystalline nature should be as carefully controlled as the hydrating effect of the vehicle onto the skin, for example. To the best of our knowledge, this phenomenon has never been reported before. The combined effect of appropriate particulate matter and solvent/vehicle, therefore, should be added to the strategies used to form site-specific depots

for targeted skin release and permeation profiles. Such strategies may also benefit from follicle-plugging experiments, in situ microscopy, synchrotron, and probe-based analyses.[19–21,66]

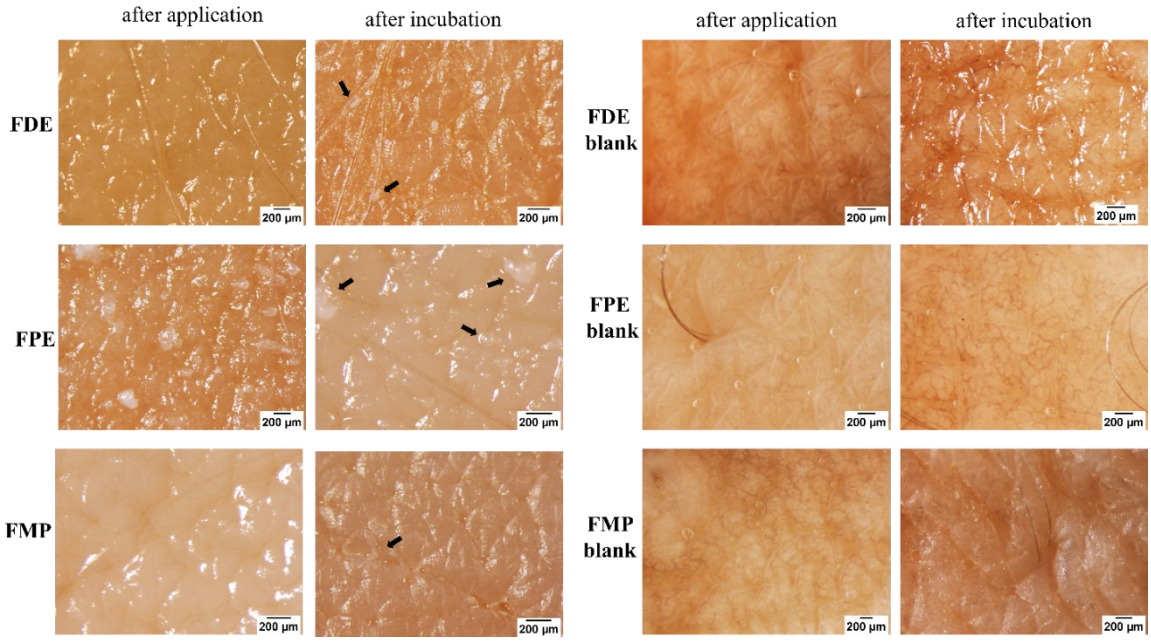

Figure 6. Micrographs showing the behavior of formulations with (a) and without (b) DAP on human skin (FDE, DEGEE/water; FPE, PEG600/water; FMP, 1-methyl-2-pyrrolidone/water). The arrows highlight the predominant location of the gels on the skin, e.g., around the hair (for FDE), evenly distributed agglomerates of product (for FPE), and accumulated on cavities of the skin surface (for FMP).

3.3 Crystal structure-to-function analyses

DAP is an example of polymorphic API that often crystallizes with molecules of different nature. For this reason, in our studies, phase diagrams in DEGEE/water, PEG/water, and MPR/ water, and formulation analyses were considered together. They become important in screening, understanding, and controlling the nature of crystals produced in different solvent proportions. In DEGEE/water, for instance, the equilibrium between anhydrous DAP and its hydrate was investigated as a function of solution composition. In PEG/water and MPR/ water, in turn, anhydrous DAP, hydrate, and the PEG cocrystal or MPR solvate, respectively, may compete to crystallize depending on solvent activity.

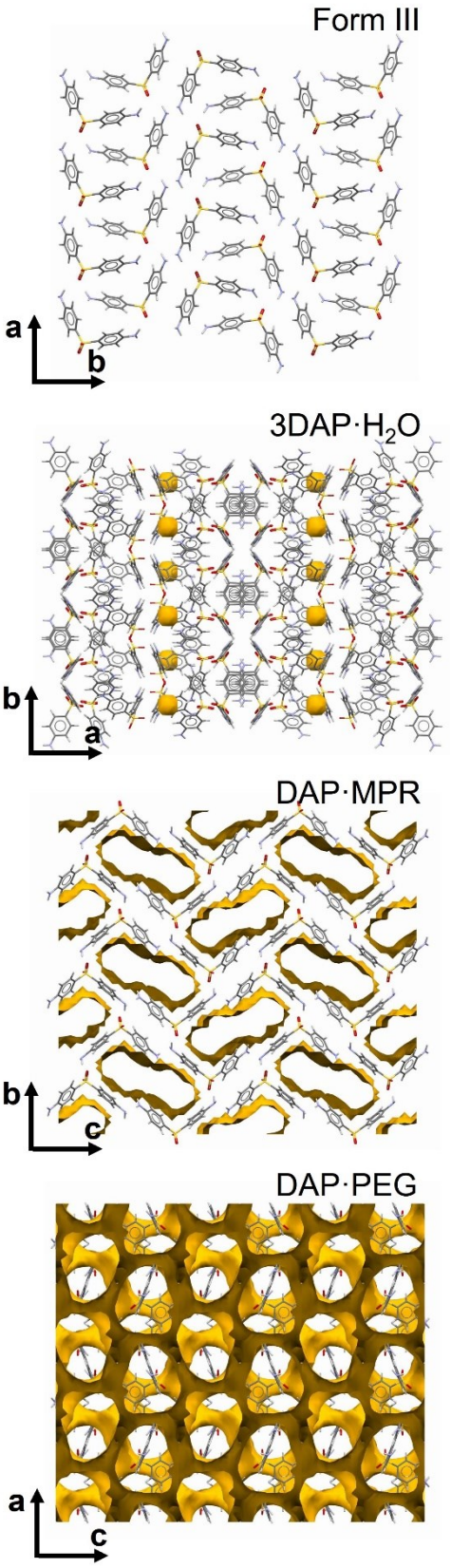

Figure 7. Structural comparison of the studied dapsone materials. Guest molecules in multicomponent crystal forms are removed for clarity. Yellow contours represent the void space occupied by coformers.

These DAP crystals vary considerably in their structural characteristics (**Table S1**). **Figure 7** illustrates the packing differences of Form III, hydrate, and solvates. The variation in the arrangement of molecules of water, 1-methyl-2-pirrolidone, and polyethyleneglycol-600 (PEG600) in the crystals is noticeable (i.e., pocket, channel, and intersecting channels, respectively). **Table 2** also shows that the volume occupied by coformers in the structures of the hydrate and solvates varies from 0.4% to about 50%. Such substantial differences in packing are held stable by equally diverse intermolecular interactions. While only one amine hydrogen and one sulfone oxygen are hydrogen bound per DAP molecule in Form III, extra hydrogen bonds are available in multicomponent crystal forms (**Table 2**).

Differences in structural anisotropy and the strength of intermolecular interactions in the lattice of DAP crystals are also translated into variations of morphology and surface characteristics. As a summary, the crystallographic information on the particles of DAP found in the formulations shows them as considerably different materials in terms of structural model, composition, drug load, and shape.

The impact of these particle variations was visible in the aspect of the gels and their behavior after application onto the skin. While the presence of particles, solvent nature, and composition are known to affect gel properties, specific crystal structure-to-function relationships may also challenge the performance of topical products containing crystals and their delivery to the skin. The combination of packing characteristics and strength of intermolecular interactions, for example, modify the mechanical behavior of organic solids. In the case of gels containing particulate matter, particle deformation and breakage may contribute to spreadability. Additionally, the acceptable appearance of skin after product application is affected by crystal shape and size, as well as by the dissolution that results from the conformer release from the lattice (i.e., dehydration and desolvation). Properties related to the interaction of crystals with their environment (e.g., dissolution, phase transformations, adhesion to biological tissues compatibility with formulations excipients, flow, agglomeration, and segregation) are surface-specific or strongly affected by surface chemistry. This is to say that the type of functional groups exposed on crystal surfaces allow for different intermolecular interactions among particles, the gel, and, ultimately, the skin. Using multicomponent crystal forms to formulate increases the diversity of interactions available; therefore, the chances for selecting crystal forms with desired properties and targeted action. Importantly, these characteristics can be modified “simply” by changing the type of cosolvent selected to formulate. To the best of our knowledge, the landscape of solid form and surface has not been explored as a technological strategy to deliver crystals to the skin yet.

Table 2. Comparison of main intermolecular interactions in DAP crystal forms. The hydrogen-bond (HB) geometry refers to normalized H-atom positions. In multicomponent crystal forms, the volume occupied by the coformer molecules is calculated in Mercury [128,130,133] with probe radius of 1.2 Å and grid spacing of 0.7 Å.

Crystal	**HB**				**Coformer**			**Morphology**		**CSD Refcode**
	Type	D(Å)	d(Å)	< (°)	Arrangement	V (%)	Release (T_{peak}, °C)	Calculated	Experimental	
Form III	$_{DAP}$N-H···O=S_{DAP}	2.962	2.012	154.8	-	-	-	Plate	Plate	DAPSUO13
Hydrate	$_{DAP}$N-H···O=S_{DAP}	2.936	2.155	132.3	Pocket	0.4	40-90[a]	Plate	Prism	ANSFON02
		3.023	2.055	158.6						
		3.006	2.013	165.4						
	$_{DAP}$N-H···O_{H2O}	3.026	2.026	163.3						
	$_{H2O}$O-H···O=S_{DAP}	2.778	1.801	167.1						
1-methyl-2-pyrrolidone solvate	$_{DAP}$N-H···O=S_{DAP}	3.019	2.010	171.8	Channel	32.6	96	Needle	Needle	This work
		3.068	2.225	139.4						
	$_{DAP}$N-H···O_{MPR}	2.845	1.845	167.9						
PEG 600 solvate[c]	$_{DAP}$N-H···O=S_{DAP}	2.987	1.981	170.8	Intersecting channels	52.2	101[b]	Prism	Plate	YIPMIW
		2.995	2.005	164.4						
	$_{DAP}$N-H···O-C_{PEG}	2.835	1.940	145.4						
		3.380	2.622	131.3						

4 CONCLUSION

Our study focuses on the effect that the composition of topical formulations has on the characteristics of solid active pharmaceutical ingredients. We used DAP as a model and showed that the selection of different organic phase components resulted in formulations containing DAP particles with differences in size, crystal form and morphology. The findings epitomize the need for careful screening and characterization studies when formulating crystals in equilibrium with a liquid medium. For example, a new DAP solvate with methylpyrrolidone was found during the studies. The heterogeneity of the particles within the samples is also to be highlighted. Microscopic analyses showed heterogeneous crystals in all three formulations. The morphology heterogeneity was associated with a mixture of phases in gels containing MPR, while DEGEE- and PEG-based gels had pure crystalline forms. Also, the equilibrium between DAP Form III / hydrate proved to be difficult to control and strongly affected by kinetics. These results indicate the importance of deepening the knowledge of the impact that solid form landscape may have on topical formulations. The goal is to control and/or mitigate the risk of formulating crystals in contact with complex solutions, especially those containing excipients that may form multicomponent crystals with the API. As for the behavior of the gel formulations on the skin, our studies suggest that the surface characteristics of the crystals may be critical when used in the topical delivery pathway. To the best of our knowledge, this phenomenon has never been proposed before. The site-specific accumulation of API particles on the skin may be a balance of the effect of the vehicle composition on both the preparation of different types of crystals and – as previously shown in the literature – the skin hydration. Further studies should be carried out to assess the relationship between solid-state characteristics and the performance of API crystals deliberately used in topical formulations.

ASSOCIATED CONTENT

Supporting Information

The following Supporting Information is available free of charge at the ACS website.

DSC thermograms of DAP (raw material and 1-methyl-2-pyrrolidone.solvate); TGA thermograms of DAP solid forms and point of the phase diagram; PXRD patterns of formulation, point of the phase diagram and dap solid forms; Infrared spectrum of DAP (raw material and 1-methyl-2-pyrrolidone.solvate) ; crystallographic data of dapsone

crystal forms; ORTEP diagram of the crystal structure of dapsone·1-methyl-2-pyrrolidone; and micrographs of formulations.

AUTHOR INFORMATION

Corresponding Authors

Gabriela Schneider-Rauber - *Postgraduate Program in Pharmacy (PGFAR), Federal University of Santa Catarina, Trindade, Florianopolis, 88040-900, Brazil;* orcid.org/0000 -0002-9267-0196; E-mail: gabisrauber@gmail.com

Thiago Caon - *Postgraduate Program in Pharmacy (PGFAR), Federal University of Santa Catarina, Trindade, Florianopolis, 88040-900, Brazil;* orcid.org/0000-0003-3030-6310;

E-mail: caon.thiago@ufsc.br

Authors

Bianca da Costa Bernardo Port - *Postgraduate Program in Pharmacy (PGFAR), Federal University of Santa Catarina, Trindade, Florianopolis, 88040-900, Brazil* orcid.org/0000-0001-6567-1102

Debora Fretes Argenta - *Postgraduate Program in Pharmacy (PGFAR), Federal University of Santa Catarina, Trindade, Florianopolis, 88040-900, Brazil* orcid.org/0000-0002-0623-4567

Mihails Arhangelskis - *Faculty of Chemistry, University of Warsaw, 1 Pasteura Street, Warsaw, 02-093, Poland* orcid.org/0000-0003-1150-3108

Carlos Eduardo Maduro de Campos - *Department of Physics, Federal University of Santa Catarina, Trindade, Florianopolis, 88040-900, Brazil* orcid.org/0000-0001-5475-5116

Adailton João Bortoluzzi - *Department of Chemistry, Federal University of Santa Catarina, Trindade, Florianopolis, 88040-900, Brazil* orcid.org/0000-0002-9493-5987

Present Addresses note

Gabriela Schneider-Rauber - *Department of Applied Science and Technology (DISAT), Politecnico di Torino. Corso Duca degli Abruzzi 24, 10129, Torino, Italy.*

Notes

The authors declare no conflict of interest.

ACKNOWLEDGEMENTS

Authors thank the Brazilian governmental agencies CNPq/MCTI (Universal 01/2016 - Grant number: 408229/2016-0) for the financial support. GSR also would like to thank the Coordination for the Improvement of Higher Education Personnel – CAPES/Brazil for her fellowship (PDEE PRINT-CAPES/UFSC call 06/PGFAR/2019). The authors

would like to thank the Protozoology Laboratory/UFSC, LAMEB/UFSC and the Department of Physics/UFSC for the use of microscope, stereomicroscope, and hot stage unit, respectively. X-Ray Powder Diffraction measurements were carried out at Multi-User facility (LDRX) at the Department of Physics/UFSC. We also thank FURP and CRODA for the donation of DAP and PEG600, respectively.

ABBREVIATIONS:

API, active pharmaceutical ingredient; DAP, dapsone; DEGEE, diethylene glycol monoethyl ether, FDE, formulation with diethylene glycol monoethyl ether; FPE, formulation with polyethyleneglycol; FMP, formulation with 1-methyl-2-pirrolidone; G6PD, glucose-6-phosphate dehydrogenase; MPR, 1-methyl-2-pirrolidone; PBPK, physiologically based pharmacokinetics; PEG, polyethyleneglycol; PXRD, powder X-ray diffraction**.**

REFERENCES AND NOTES

*Although 1-methyl-2-pyrrolidone has been used as a solubilizing and permeation enhancer agent in the past, it is important to warn that there is currently a restriction on its use in pharmaceutical and cosmetic formulations. According to the harmonized classification and labelling (ATP09) approved by the European Union, this substance may damage the unborn child, cause serious eye irritation, skin irritation and respiratory irritation.

References

(1) Braga, D.; Grepioni, F. Making Crystals by Design: Methods, Techniques and Applications; Wiley: Weinheim, 2007.

(2) Byrn, S. R.; Pfeiffer, R. R.; Stowell, J. G. Solid-State Chemistry of Drugs; Academic Press: New York, 1999.

(3) Schneider-Rauber, G.; Arhangelskis, M.; Bond, A. D.; Ho, R.; Nere, N. K.; Bordawekar, S.; Sheikh, A. Y.; Jones, W. Polymorphism and surface diversity arising from stress-induced transformations − the case of multicomponent forms of carbamazepine. Acta Crystallogr., Sect. B: Struct. Sci., Cryst. Eng. Mater. 2021, 77, 54−67.

(4) Desiraju, G.R.; Vittal, J.J.; Ramanan, A. Crystal Engineering: A Textbook; IISc Press, 2011.

(5) Schneider-Rauber, G.; Bond, A. D.; Ho, R.; Nere, N.; Bordawekar, S.; Sheikh, A. Y.; Jones, W. Effect of Solution Composition on the Crystallization of Multicomponent Forms of Carbamazepine beyond Crystal Form and Shape: Surface as a Source of Diversity in the Solid-Form Landscape. Cryst. Growth Des. 2021, 21, 52−64.

(6) Taylor, L. S.; Braun, D. E.; Steed, J. W. Crystals and Crystallization in Drug Delivery Design. Cryst. Growth Des. 2021, 21, 1375−1377.

(7) Foster, J. A.; Damodaran, K. K; Maurin, A.; Day, G. M.; Thompson, H. P. G.; Cameron, G. J.; Bernal, J. C.; Steed, J. W. Pharmaceutical polymorph control in a drug-mimetic supramolecular gel. Chem. Sci. 2017, 8, 78−84.

(8) Caspi, D. D.; Cink, R. D.; Clyne, D.; Diwan, M.; Engstrom, K.M.; Napolitano, G.; Grieme, T.; Mei, J.; Miller, R. W.; Mitchell, C. Process development of ABT-450 - A first generation NS3/4A protease inhibitor for HCV. Tetrahedron 2019, 75, 4271−4286.

(9) Cink, R. D.; Lukin, K. A.; Bishop, R. D.; Zhao, G.; Pelc, M. J.; Towne, T. B.; Gates, B. D.; Ravn, M. M.; Hill, D. R.; Ding, C. Development of the Enabling Route for Glecaprevir via Ring-Closing Metathesis. Org. Process Res. Dev. 2020, 24, 183−200.

(10) Machado, T. C.; Kuminek, G.; Cardoso, S. G.; RodríguezHornedo, N. The role of pH and dose/solubility ratio on cocrystal dissolution, drug supersaturation and precipitation. Eur. J. Pharm. Sci. 2020, 15, 2105422.

(11) Zhang, J.; Shi, Q.; Tao, J.; Peng, Y.; Cai, T. Impact of Polymer Enrichment at the Crystal-Liquid Interface on Crystallization Kinetics of Amorphous Solid Dispersions. Mol. Pharmaceutics 2019, 16, 1385− 1396.

(12) Indulkar, A.S.; Gao, Y.; Raina, S.A.; Zhang, G. G. Z.; Taylor, L.S. Impact of Monomeric versus Micellar Surfactant and SurfactantPolymer Interactions on Nucleation-Induction Times of Atazanavir from Supersaturated Solutions. Cryst. Growth Des. 2020, 20, 62−72.

(13) Ueda, K.; Yamamoto, N.; Higashi, K.; Moribe, K. Molecular Mobility Suppression of Ibuprofen-Rich Amorphous Nanodroplets by HPMC Revealed by NMR Relaxometry and Its Significance with Respect to Crystallization Inhibition. Mol. Pharmaceutics 2019, 16, 4968−4977.

(14) Alhalaweh, A.; Ali, H. R. H.; Velaga, S.P. Effects of polymer and surfactant on the dissolution and transformation profiles of cocrystals in aqueous media. Cryst. Growth Des. 2014, 14, 643−648.

(15) Lakshman, D.; Chegireddy, M.; Hanegave, G.K.; Sree, K.N.; Kumar, N.; Lewis, S.A.; Dengale, S.J. Investigation of drug-polymer miscibility, biorelevant dissolution, and bioavailability improvement of Dolutegravir-polyvinyl caprolactam-polyvinyl acetate-polyethylene glycol graft copolymer solid dispersions. Eur. J. Pharm. Sci. 2020, 14, 2105137.

(16) Franca, M. T.; Martins Marcos, T.; A. Costa, P. F.; P. Gerola, A.; Stulzer, H. K. The role of glycyrrhizic acid in colloidal phenomena of supersaturation drug delivery systems containing the antifungal drug griseofulvin. J. Mol. Liq. 2020, 301, 112336.

(17) Franca, M. T.; Marcos, T.M.; Pereira, R.N.; Stulzer, H.K. Could ¸the small molecules such as amino acids improve aqueous solubility and stabilize amorphous systems containing Griseofulvin? Eur. J. Pharm. Sci. 2020, 14, 3105178.

(18) Hadgraft, J.; Lane, M.E. Drug crystallization − implications for topical and transdermal delivery Drug crystallization − implications for topical and transdermal delivery. Expert Opin. Drug Deliv 2016, 13, 817−830.

(19) Goh, C.F.; O'Flynn, D.; Speller, R.; Lane, M.E. Spatial resolution of drug crystallisation in the skin by X-ray micro-computed tomography. Micron 2021, 14, 5103045.

(20) Goh, C.F.; Boyd, B.J.; Craig, D. Q. M.; Lane, M.E. Profiling of drug crystallization in the skin. Expert Opin. Drug Deliv. 2020, 17, 1321−1334.

(21) Goh, C.F.; Moffat, J.G.; Craig, D. Q. M.; Hadgraft, J.; Lane, M.E. Monitoring Drug Crystallization in Percutaneous Penetration Using Localized Nanothermal Analysis and Photothermal Microspectroscopy. Mol. Pharmaceutics 2019, 16, 359−370.

(22) Brown, M.B.; Martin, G.P.; Jones, S.A.; Akomeah, F.K. Dermal and transdermal drug delivery systems: Current and future prospects. Drug Deliv. 2006, 13, 175−187.

(23) Marwah, H.; Garg, T.; Goyal, A.K.; Rath, G. Permeation enhancer strategies in transdermal drug delivery. Drug Deliv. 2016, 23, 564−578.

(24) Iqbal, B.; Ali, J.; Baboota, S. Recent advances and development in epidermal and dermal drug deposition enhancement technology. Int. J. Dermatol 2018, 57, 646−660.

(25) Benson, H. Transdermal Drug Delivery: Penetration Enhancement Techniques. Curr. Drug Deliv 2005, 2, 23−33.

(26) Pelikh, O.; Keck, C. M. Hair follicle targeting and dermal drug delivery with curcumin drug nanocrystals□essential influence of excipients. Nanomaterials 2020, 10, 2323.

(27) Lademann, J.; Richter, H.; Schanzer, S.; Knorr, F.; Meinke, M.; Sterry, W.; Patzelt, A. Penetration and storage of particles in human skin: Perspectives and safety aspects. Eur. J. Pharm. Biopharm 2011, 77, 465−468.

(28) Pelikh, O.; Stahr, P. L.; Huang, J.; Gerst, M.; Scholz, P.; Dietrich, H.; Geisel, N.; Keck, C. M. Nanocrystals for improved dermal drug delivery. Eur. J. Pharm. Biopharm 2018, 128, 170−178.

(29) Pelikh, O.; Eckert, R. W.; Pinnapireddy, S. R.; Keck, C. M. Hair follicle targeting with curcumin nanocrystals: Influence of the formulation properties on the penetration efficacy. J. Controlled Release 2020, 329, 598−613.

(30) Vidlárová, L.; Romero, G. B.; Hanusˇ, J.; Sˇtepánek, F.; Muˇller, R. H. Nanocrystals for dermal penetration enhancement - Effect of concentration and underlying mechanisms using curcumin as model. Eur. J. Pharm. Biopharm 2016, 104, 216−225.

(31) Ruiz-Palomero, C.; Kennedy, S. R.; Soriano, M. L.; Jones, C. D.; Valcárcel, M.; Steed, J. W. Pharmaceutical crystallization with nanocellulose organogels. Chem. Commun. 2016, 52, 7782−7785.

(32) Pireddu, R.; Caddeo, C.; Valenti, D.; Marongiu, F.; Scano, A.; Ennas, G.; Lai, F.; Fadda, A. M.; Sinico, C. Diclofenac acid nanocrystals as an effective strategy to reduce in vivo skin inflammation by improving dermal drug bioavailability. Colloids Surf., B 2016, 143, 64−70.

(33) Zhai, X.; Lademann, J.; Keck, C. M.; Müller, R. H. Dermal nanocrystals from medium soluble actives - Physical stability and stability affecting parameters. Eur. J. Pharm. Biopharm 2014, 88, 85− 91.

(34) Scholz, P.; Arntjen, A.; Müller, R. H.; Keck, C. M. ARTcrystal® process for industrial nanocrystal production - Optimization of the ART MICCRA pre-milling step. Int. J. Pharm. 2014, 465, 388−395.

(35) Patzelt, A.; Richter, H.; Knorr, F.; Schäfer, U.; Lehr, C. M.; Dähne, L.; Sterry, W.; Lademann, J. Selective follicular targeting by modification of the particle sizes. J. Controlled Release 2011, 150, 45− 48.

(36) Breuckmann, P.; Meinke, M. C.; Jaenicke, Th.; Krutmann, J.; Rasulev, U.; Keck, C. M.; Müller, R. H.; Klein, A. L.; Lademann, J.; Patzelt, A. Influence of nanocrystal size on the in vivo absorption kinetics of caffeine after topical application. Eur. J. Pharm. Biopharm. 2021, 167, 57−64.

(37) Molinelli, E.; Paolinelli, M.; Campanati, A.; Brisigotti, V.; Offidani, A. Metabolic, pharmacokinetic, and toxicological issues surrounding dapsone, Expert Opin. Drug Metab. Toxicol 2019, 15, 367−379.

(38) Zuidema, J.; Hilbers-Modderman, E. S. M.; Merkus, F. W. H. M. Clinical Pharmacokinetics of Dapsone. Clin. Pharmakokinet 1986, 11, 299−315.

(39) Goulart, I. M. B.; Arbex, G. L.; Carneiro, M. H.; Rodrigues, M. S.; Gadia, R. Efeitos adversos da poliquimioterapia em pacientes com hanseni´ ase: Um levantamento de cinco anos em um Centro de Saudé da Universidade Federal de Uberlandia.ˆRev. Soc. Bras. Med. Trop. 2002, 35, 453−460.

(40) Oliveira, F. R.; Pessoa, M. C.; Albuquerque, R. F. V.; Schalcher, T. R.; Monteiro, M. C. Clinical applications and methemoglobinemia induced by dapsone. J. Braz. Chem. Soc. 2014, 25, 1770−1779.

(41) Zhu, Y. I.; Stiller, M. J. Dapsone and sulfones in dermatology: Overview and update. J. Am. Acad. Dermatol 2001, 45, 420−434.

(42) Al-Salama, Z. T.; Deeks, E. D. Dapsone 7.5% Gel: A Review in Acnes Vulgaris. Am. J. Clin. Dermatol 2017, 18, 139−145.

(43) Stotland, M.; Shalita, A. R.; Kissling, R. F. Dapsone 5% Gel. Am. J. Clin. Dermatol 2009, 10, 221−227.

(44) The Orange Book: Approved Drug Products with Therapeutic Equivalence evaluations; U.S. Food Drug Administration, 2020.

(45) Braun, D. E.; Griesser, U. J. Supramolecular Organization of Nonstoichiometric Drug Hydrates: Dapsone. Front. Chem. 2018, 6, 00031.

(46) Braun, D. E.; Gelbrich, T.; Griesser, U. J. Experimental and computational approaches to produce and characterise isostructural solvates. CrystEngComm 2019, 21, 5533−5545.

(47) Chappa, P.; Maruthapillai, A.; Voguri, R.; Dey, A.; Ghosal, S.; Basha, M. A. Drug-Polymer Co-Crystals of Dapsone and Polyethylene Glycol: An Emerging Subset in Pharmaceutical Co-Crystals. Cryst. Growth Des 2018, 18, 7590−7598.

(48) Osborne, D.W. Compositions and methods for topical applications of theraputic agents. U.S. Patent 5,863,560, 1999.

(49) Osborne, D.W. Compositions and methods for topical application of theraputic agentes. U.S. Patent 6,060,085, 2000.

(50) Osborne, D.W. Topical dapsone for the treatment of acne. CA Patent 2,776,702, 2002.

(51) Farmacopeia Brasileira, 5th ed.; ANVISA: Brasi´ lia, 2010.

(52) Bruno, I. J.; Cole, J. C.; Edgington, P. R.; Kessler, M.; Macrae, C. F.; McCabe, P.; Pearson, J.; Taylor, R. New software for searching the Cambridge Structural Database and visualizing crystal structures. Acta Crystallogr. Sect. B Struct. Sci. 2002, 58, 389−397.

(53) Braun, D. E.; Krüger, H.; Kahlenberg, V.; Griesser, U. J. Molecular level understanding of the reversible phase transformation between forms III and II of dapsone. Cryst. Growth Des 2017, 17, 5054−5060.

(54) Braun, D. E.; Vickers, M.; Griesser, U. J. Dapsone Form V: A Late Appearing Thermodynamic Polymorph of a Pharmaceutical. Mol. Pharmaceutics 2019, 16, 3221−3236.

(55) Yathirajan, H. S.; Nagaraja, P.; Nagaraj, B.; Bhaskar, B. L.; Lynch, D. E. ANSFON02 : 4,4'-Diaminodiphenylsulfone hydrate. CSD Commun. 2004. DOI: 10.5517/cc8l7bd.

(56) Taylor, R.; Macrae, C. F. Rules governing the crystal packing of mono-and dialcohols. Acta Crystallogr. Sect. B Struct. Sci. 2001, 57, 815−827.

(57) Macrae, C. F.; Edgington, P. R.; McCabe, P.; Pidcock, E.; Shields, G. P.; Taylor, R.; Towler, M.; van de Streek, J. Mercury: Visualization and analysis of crystal structures. J. Appl. Crystallogr. 2006, 39, 453−457.

(58) Macrae, C. F.; Bruno, I. J.; Chisholm, J. A.; Edgington, P. R.; McCabe, P.; Pidcock, E.; Rodriguez-Monge, L.; Taylor, R.; Van De Streek, J.; Wood, P. A. Mercury CSD 2.0 - New features for the visualization and investigation of crystal structures. J. Appl. Crystallogr. 2008, 41, 466−470.

(59) MacRae, C. F.; Sovago, I.; Cottrell, S. J.; Galek, P. T. A.; McCabe, P.; Pidcock, E.; Platings, M.; Shields, G. P.; Stevens, J. S.; Towler, M.; Wood, P. A. Mercury 4.0: From visualization to analysis, design and prediction. J. Appl. Crystallogr. 2020, 53, 226−235.

(60) Coelho, A. A. TOPAS and TOPAS-Academic: An optimization program integrating computer algebra and crystallographic objects written in C++: An. J. Appl. Crystallogr. 2018, 51, 210−218.

(61) Dollase, W. A. Correction of Intensities of Preferred Orientation in Powder Diffractometry: Application of the March Model. J. Appl. Crystallogr. 1986, 19, 267−272.

(62) Kuhnert-Brandstatter, M.; Moser, I. Polymorphism of Dapson and ethambutoldihydrochloride. Microchim. Acta 1979, 71, 125−136.

(63) Ethier, A.; Bansal, P.; Baxter, J.; Langley, N.; Richardson, N.; Patel, A. M. The Role of Excipients in the Microstructure of Topical Semisolid Drug Products. AAPS Adv. Pharm. Sci. Ser. 2019, 36, 155− 193.

(64) Yang, H.; Li, H.; Zhu, P.; Yan, Y.; Zhu, Q.; Chenggao, F. A novel method for determining the viscosity of polymer solution. Polym. Test 2004, 23, 897−901.

(65) Rodriguez, R.; Alvarez-Lorenzo, C.; Concheiro, A. Rheological evaluation of the interactions between cationic celluloses and Carbopol 974P in water. Biomacromolecules 2001, 2, 886−893.

(66) Kovácik, A.; Kopecˇ ná, M. K.; Vávrová, K. Vaˇ vrova´ , Permeation´ enhancers in transdermal drug delivery: benefits and limitations. Expert Opin. Drug Deliv. 2020, 17, 145−155.

(67) Patel, A.; Iliopoulos, F.; Caspers, P. J.; Puppels, G. W.; Lane, M. E. In vitro-in vivo correlation in dermal delivery: the role of excipients. Pharmaceutics 2021, 13, 542.

5 CAPÍTULO III – DESENVOLVIMENTO DE NANOCARREADORES COM ÓLEO DE CHAULMOOGRA E INVESTIGAÇÃO DO EFEITO CICATRIZANTE

Este capítulo trata do desenvolvimento e caracterização de nanoemulsões de DAP associada ao óleo de chaulmoogra para aplicação tópica. As nanoemulsões foram preparadas pela técnica de emulsificação espontânea e então caracterizadas quanto ao tamanho, carga de superfície, índice de polidispersão (PDI), teor, eficiência de encapsulação. Após a otimização das formulações, realizaram-se ensaios de estabilidade de longa duração (60 dias), estabilidade térmica e física, liberação *in vitro* bem como estudos de permeação cutânea. Por fim, avaliou-se o efeito cicatrizante do carreador sem a DAP e do óleo puro através do ensaio de "scratch". O papel do óleo de chaulmoogra tanto em atividades biológicas secundárias que tem relação com a hanseníase quanto a possibilidade de melhoria da estabilidade física e térmica de nanoemulsões representaram as principias contribuições deste estudo, encorajando ainda mais estudos com este óleo vegetal. O produto deste capítulo é um artigo científico, que será submetido para apreciação na revista *Colloids and Surfaces B: Biointerfaces*.

Chaulmoogra oil-based nanoemulsions for leprosy treatment: a case study with the dapsone

Bianca da Costa Bernardo Port[a], Débora Fretes Argenta[a], Douglas Santos Porto[a], Isabella Dai Prá Zuchi[b], Izabella Thaís Silva[b] and Thiago Caon[a]*

[a] Department of Pharmaceutical Sciences, Federal University of Santa Catarina, Florianópolis - SC, 88040-900

[b] Department of Microbiology, Immunology, and Parasitology, Federal University of Santa Catarina, Florianópolis - SC, 88040-900

*Corresponding author: thiagocaon@gmail.com

Abstract

Drugs used to treat leprosy such as dapsone (DAP) can result in various adverse effects when administered orally. The disease-causing pathogen has a preferential distribution in peripheral regions of the body and symptoms are manifested primarily in the skin and peripheral nerves. This aspect motivated the development of topical formulations in this study. Nanoemulsions (NEs) were selected as drug carriers to enhance permeation and sustain the drug release. Chaulmoogra oil (CH) was included in the oil phase of NEs considering its history of use in leprosy. Its effect on formulation characteristics (size, PDI, surface load and stability) and epithelial cell migration was evaluated. DAP was considered as a model drug. NEs prepared with CH showed to be more monodisperse and the particle diameter increased with the oil content. Hot-stage analyses and accelerated stability studies revealed that the CH improve both physical and thermal stability. NEs with higher CH content presented greater interaction with the human skin in spectroscopic analyses, which was also confirmed in permeation studies. Another positive effect is that free and nanoencapsulated CH improved the cell migration, which would be useful to treat skin lesions that commonly appear in patients with leprosy. In summary, the presence of CH is able to improve the anti-leprosy formulation characteristics and provide different benefits to patients.

Keywords: nanoemulsions; chaulmoogra oil; dapsone; leprosy.

1. INTRODUCTION

Hansen's disease (HD), also known as leprosy, is a chronic infection caused by the slow growing bacteria *Mycobacterium leprae*. Although the incubation period is close to 5 years, symptoms can occur within 1 year [1]. Even though this disease has been eradicated in many parts of the world, HD remains an important health problem in countries as India and Brazil. According to the World Health Organization, HD is considered a neglected tropical disease. Approximately 202,256 new cases were reported in the world in 2019 [2]. The wide spectrum of clinical manifestations varies according to the host's immune response [3,4]. In general, the symptoms are manifested in the skin and peripheral nerves through lesions and loss of sensitivity, edema, muscle paralysis caused by neuritis, but also can affect the upper respiratory tract mucosa and eyes [5]. Given that *M. leprae* growing occurs in temperatures close to 30°C, the symptoms of HD are manifested preferentially in body peripheral regions [3].

Chaulmoogra oil (CH) was used for the leprosy treatment through topical, oral or even parenteral administration until the 1940s [6]. This oil is extracted by pressing the seeds of trees of the genus *Hydnocarpus* [7]. Its composition is based on three main fatty acids: hydnocarpic (HA), chaulmugric (CA) and gorlic acid (GA) (Fig. 1). Other acids may be found in smaller amounts such as oleic, palmitic and linoleic acid [8]. A secondary immunizing action has been suggested for this oil. According to this theory, fatty acids, in particular HA and CA, would stimulate the production of lipases in the host, disrupting lipids from the cell wall of the microorganism [9,10]. Another proposed mechanism is the direct antimicrobial action of HA, which has a chemical structure analogous to biotin. Jacobsen and Levy [9] showed the antagonist effect of this fatty acid in metabolic reactions of microorganisms that need biotin as a coenzyme. Thus, HA would play a role as a mycobacteria multiplication inhibitor agent.

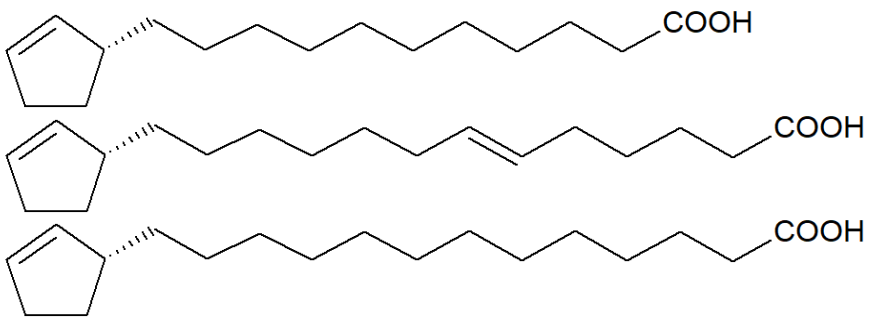

Figure 1. Chemical structure of the main fatty acids of CH. (a) hydnocarpic, (b) chaulmugric and (c) gorlic acid.

Despite several clinical benefits reported in literature, some physicians and researchers believe that CH and its derivatives cause a palliative effect, which motivated the investigation of new therapeutic alternatives [11]. In this context, dapsone (Fig. 2) emerged as an effective drug for HD. Few years ago, rifampicin and clofazimine were also incorporated in standardized treatment protocols to avoid or reduce microbial resistance problems that started to appear [12]. These drugs are administered orally over a period of 6 to 12 months depending on the disease classification [13–15]. In long-term therapies, the use of DAP has been associated with adverse gastrointestinal effects and even serious hematological effects such as hemolytic anemia, methemoglobinemia and agranulocytosis [16,17]. These symptoms are mainly caused by hydroxylamine, a metabolite generated from acetylation and hydroxylation reactions of DAP [18]. In the elderly, children and in patients with glucose-6-phosphatase dehydrogenase (G6PD) enzyme deficiency, more complications are often observed [19].

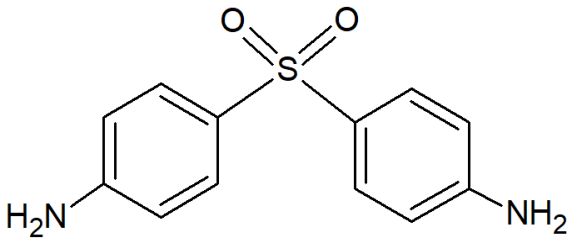

Figure 2. Chemical structure of DAP.

The topical administration of DAP can reduce or even avoid these adverse effects and improve patient adherence to treatment regimens. In the leprosy, the local application is advantageous because both the pathogen and the disease lesions are found on the skin. The incorporation of DAP in nanostructures has shown to be a promising formulation approach as they are able of providing a sustained drug release and enhance both drug absorption [3,20].

In this study, DAP and CH were incorporated in a same nanostructure aiming to avoid microbial resistance problems and increase efficacy. As the oil and DAP are characterized by a low aqueous solubility, they were incorporated into a lipid formulation (nanoemulsions-NE) to obtain a high encapsulation efficiency. In addition to high biocompatibility, these systems interact more easily with the skin when compared to other nanoparticle types [21,22]. A marketed emulsifying agent containing phosphatidylcholine dissolved in safflower seed oil known as Phosal 50+® (PHO) was tested during NE preparation. After NE optimization, physicochemical characterization and stability assays were considered. The effect of CH on the release of DAP from nanoemulsions was evaluated through dialysis method. The distribution

of DAP in human skin was monitored by *ex vivo* permeation studies. Finally, *in vitro* scratch assays were performed to investigate the effect of CH as healing agent after nanoencapsulation considering that ulcerative skin lesions are common in HD patients.

2. MATERIALS AND METHODS

2.1. *Materials*

DAP, polysorbate 80 and phosphoric acid were purchased from Sigma-Aldrich (St Louis, MO, USA). CH was obtained from Avi Naturals (Delhi, India). Phosal 50 SA+ was donated by Lipoid (Ludwigshafen, Germany). Phosphate buffered (PBS) saline was prepared with 10.1 mM Na_2HPO_4, 1.8 mM KH_2PO_4, 136.9 mM NaCl, 2.7 mM KCl and adjusted to pH 7.4 with 1 M HCl. Krebs-Ringer bicarbonate buffer was prepared with 119 mM NaCl, 4.7 mM KCl, 1.2 mM KH_2PO_4, 25 mM $NaHCO_3$, 2.5 mM $CaCl_2$.2H2O, 1.0 mM $MgCl_2.6H_2O$, 5.5 mM glucose and adjusted to pH 7.4 with 1 M HCl. Ethanol and acetone were supplied by Vetec Química Fina Ltda. (Duque de Caxias, Brazil) and methanol HPLC grade by Merck KGaA (Darmstadt, Germany). Ultrapure water was obtained from a Milli-Q® purification system (Millipore, Milford, MA, USA).

2.2. *Nanoemulsion preparation*

Oil-in-water (O/W) NEs were prepared by spontaneous emulsification procedure following a method previously described [23]. Briefly, oil phase was obtained by dissolving PHO and DAP in ethanol. For NEs containing CH, a mixture of ethanol and acetone (50:50) was considered for constituent solubilization. The aqueous phase of all NEs was composed of polysorbate 80 and water. NEs were prepared by adding the organic phase to the aqueous phase and the resulting systems were kept under continuous stirring for 15 min. Finally, formulations were concentrated by evaporation under reduced pressure at 60 °C until 2.5 mg mL^{-1} of DAP. The final composition of the formulations is presented in Table 1.

2.3. *Physicochemical characterization*

2.3.1. Particle size, polydispersity index, surface charge and pH

Aliquots of the NEs were diluted in ultrapure water (1:10) to determine the mean droplet size and polydispersity index (PDI) by photon correlation spectroscopy. Analyses were performed at 25 °C selecting 90° as the angle of the laser beam. Potential zeta (ZP) values were

obtained from electrophoretic mobility measurements. All analyses were carried out in triplicate using a Malvern Zetasizer Nano-ZS 90 (Malvern Instruments, Malvern, UK). pH was determined by immersing the electrode directly into the sample using a MSTecnopon model mPA-210 (São Paulo, Brazil) at room temperature.

2.3.2. Encapsulation efficiency

The encapsulation efficiency (EE) was evaluated through the ultracentrifugation technique (Ultracel®-30K units, Millipore). Briefly, 1 mL of the formulation was added to ultrafiltration units and then centrifuged at 6,200 rpm for 10 min at 25 ºC. The amount of free DAP in the supernatant was determined by HPLC (section 2.9). The EE (%) of DAP was calculated by using the Equation 1.

Equation 1.

$$EE\% = \frac{(Total\ amount\ of\ DAP - amount\ of\ free\ DAP)}{Total\ amount\ of\ DAP}\ x\ 100$$

2.3.3. FT-IR spectral analysis

The formulations NE2-DAP, NE3-DPA and NE4-DAP as well as their components were analyzed by Fourier transform infrared (FTIR) spectroscopy (IRPrestige-21, Shimadzu, Kyoto, Japan). KBr was used for sample preparation and the scanning range was fixed at 500-4,000 cm^{-1} at room temperature, with the collection of 20 scans at a resolution of 4 cm^{-1}. KBr crystals were initially ground, mixed with the samples and then pelletized.

2.4. *Stability studies*

2.4.1. Storage stability

The formulations NE2-DAP, NE3-DPA and NE4-DAP showed high zeta potential values and low polydispersity (or PDI) in the initial formulation screening assays and thus they were selected for stability studies or next steps. The mean droplet size, PDI, ZP and pH was monitored immediately after preparation and 15, 30 and 60 days after storage at 25 ± 2°C. All analyses were performed in triplicate.

2.4.2. Accelerated stability evaluation

The physical stability based on phase separation behavior was evaluated by using the LUMISizer® equipment (LUM. GmbH, Berlin, Germany), which uses centrifugal force to accelerate the occurrence of instability phenomena such as sedimentation, flocculation and creaming. The technique measures the intensity of transmitted light as a function of time and position over the entire sample length in a cuvette during centrifugation. For this analysis, NEs were placed in rectangular polycarbonate cuvettes (optical path of 2.0 mm) and centrifuged at 4,000 rpm (2,226 xg) at 25 °C to capture 300 transmission profiles at an interval of 250 s (total time = 20.8 h). The instability index, a factor calculated by the equipment software SEPView®, was used to compare the stability of NEs. The value "0" indicates no separation or change in light transmission whereas "1" represents a complete segregation of phases.

2.4.3. Thermal stability

An Olympus BX50 microscope (Tokyo, Japan) equipped with a Mettler Toledo FP-82 hot-stage system (Ohio, US) was used to evaluate the thermal stability of NEs. Approximately 20 μL of each formulation was added on a glass slide and then covered with a cover glass. Images were obtained before and after heating (10 °C min^{-1}) in an optical microscope.

2.4.4. Apparent solubility assays

Excess amounts of DAP were added to 3 mL of different solutions: 1) water/ethanol 50:50; 2) water/ethanol 75:25; 3) PBS with 2% polysorbate 80 and 4) PBS pH 7.4. The flasks were sealed and then stirred (Multistirrer 15, Velp Scientifica, Italy) for 24 h at 37°C. For drug quantification, samples from each vial were centrifuged at 6,200 rpm for 15 min. The concentration of DAP in the supernatant was determined spectrophotometrically (Cary 60, Agilent, EUA) at 295 nm.

2.5. *In vitro release studies*

In vitro release studies of DAP from NEs (NE2-DAP, NE3-DPA and NE4-DAP) were performed through the dialysis bag method. For the release assays, dialysis tubing cellulose membranes (Sigma-Aldrich®, USA) were filled with 1 mL of each formulation and placed inside a beaker containing 50 mL of the dissolution media under agitation. Aliquots of dissolution media (1 mL) were taken at 0.5, 1, 2, 3, 4, 5, 6 h and diluted with ethanol for

quantification. An equal volume of the fresh medium was replaced. DAP saturation in the release medium was previously evaluated (section 2.4.4.) to ensure the maintenance of sink condition. The resulting solutions were analyzed in a spectrophotometer at 295 nm.

2.6. *Ex vivo skin permeation studies*

The cutaneous permeation/retention assays of NE2-DAP, NE3-DPA and NE4-DAP were performed in Franz-type diffusion cells presenting a diffusion area of 1.77 cm^2. Abdominal human skin model was selected for the assays. The skin was obtained from abdominoplasty surgeries and the study was approved by the Research Ethics Committee of the University (CAE number: 87349418.7.0000.0121). Subcutaneous fat was removed using a scalpel and the tissue of interest was washed with Krebs-Ringer buffer (pH 7.4) before storage at -20 °C. Before permeation assays, the frozen skin was equilibrated with PBS pH 7.4 for 30 min to maintain the tissue hydration level given that this variable may affect the permeation of drugs. The skin was mounted at the interface of the donor and receptor chamber with the stratum corneum facing upwards. The receptor chamber was filled with 10 mL of phosphate buffer containing 2% polysorbate 80. After addition of 1.5 mL of each formulation in the donor chamber, the system was kept at 37 °C and under continuous stirring at 310 rpm. After 8 h, aliquots of 400 μL were withdrawn from the receptor chamber and analyzed by HPLC (see section 2.9).

At the end of the permeation assay, the amount of DAP retained in the skin was also analyzed. The excess of formulation on the skin was removed and the epidermis was separated from the dermis using a scalpel. DAP was extracted from the tissues with 3 mL of acetonitrile, followed by overnight storage to increase the extraction efficiency. In the next day, the tissues were vortexed for 10 min, sonicated for 30 min, centrifuged for 30 min at 6,200 rpm and finally the supernatant was filtered and analyzed by HPLC.

2.6.1. FT-IR analysis of stratum corneum

The SC was carefully separated from other underlying skin layers and divided into sections of approximately 20 mg with a scalpel. SC samples were submerged in the formulations (NE2-DAP, NE3-DPA and NE4-DAP) or PBS (control) for the same period of permeation assay. FT-IR spectra were recorded in a frequency range from 600 to 4,000 cm^{-1} on a Perkin-Elmer Frontier equipment (Waltham, USA) with the collection of 16 scans at a resolution of 4 cm^{-1}. Data were shown as the mean spectrum of three different samples for each treatment.

2.7. *In vitro cytotoxicity assay*

The cytotoxicity of NEs containing higher surfactant concentration (8 and 6% m/m) were determined by using the sulforhodamine B assay [24], which evaluates the cellular protein content. Stem cells from human exfoliated deciduous teeth (SHED, Curitiba Biotech ™) were seeded into 96-well microplates (2.5×10^5 cells mL^{-1}) and the incubated for 24 h at 37 °C in a 5% CO_2 atmosphere. After cellular confluence, cells were treated with different concentrations of NEs and pure CH maintaining the concentration of CH in the range of 0.0098 to 10 mg mL^{-1}. After 24 h of incubation, cells were stained with sulforhodamine B and absorbance was measured in a microplate spectrophotometer (Spectra MD2, Molecular Devices, Sunnyvale, CA, USA) at 510 nm. The percentages of viable cells were plotted against each sample concentration, and the CC_{50} values (concentrations that reduced cell viability by 50% when compared to untreated controls) were determined based on concentration-response curves using GraphPad Prism 8.0 (GraphPad software, La Jolla, CA).

2.8. *Scratch assay*

Scratch assay was performed to investigate the potential of free and nanoencapsulated CH on the cell migration and proliferation. In this study, SHED cells were initially seeded in 96-well cell culture plates (1.0×10^5 cells mL^{-1}) and then incubated for 24 h at 37 ◦C under culture conditions for cell confluence. Then, a linear artificial wound was generated on the cell monolayer with a sterile micropipette tip. Cell debris were removed by washing the plates with PBS (pH 7.4). NE2 and NE3 (25 µg mL^{-1} of CH) as well as pure CH (25 µg mL^{-1}) were then added to the cells and incubated at 37◦C and 5% of CO_2. Representative images from each well of the streaked areas under each condition were photographed at time 0 and after 24 h to estimate relative cell migration. Data were analyzed using the ImageJ software. All assays were performed in triplicate. The wound closure percentage after 24 h was calculated according to the following equation:

Equation 2.

$$Wound\ closure\ (\%) = 100 - \left(\frac{cell\ free\ gap\ area\ t\ =\ 24}{cell\ free\ gap\ area\ t\ =\ 0}\right) x\ 100$$

2.9. *Drug quantification*

Quantification of DAP from the formulations and permeation studies was performed by high-performance liquid chromatography (HPLC). The samples were analyzed using a Perkin-Elmer Series 200 HPLC system (Waltham, MA, USA) equipped with a UV detector, pump, autoinjector and online degasser. A C8 column (250 × 4.6 mm, 5 μm particle size; Perkin Elmer, Shelton, USA) linked to a guard column of the same packing material (KJ0-4282, Phenomenex, Torrance, CA, USA) was considered as a stationary phase. The mobile phase was composed of water acidified with phosphoric acid (pH 5.5) and methanol in a ratio of 65:35 (v/v), respectively. Elution was performed isocratically at a flow rate of 1.0 mL min^{-1} with a sample injection volume of 20 μL and a total sample acquisition time of 8 min. The wavelength of the detector was set to 295 nm. The method showed to be linear in the range 1 to 100 μg mL^{-1} ($y = 103203x + 34706$; $R^2 = 0.999$); precise (intraday and interday relative standard deviations lower than 2.5 and 3%, respectively), accurate (recovery values higher than 98%) and specific.

2.10. *Statistical analysis*

Results were analyzed by using GraphPad Prism version 8.0. One-way ANOVA with post-hoc Tukey was considered for multiple comparisons. *p*-values of less than 0.05 were considered statistically significant.

3. RESULTS

3.1. *Characterization of formulations*

3.1.1. Droplet size, PDI, surface charge, encapsulation efficiency and pH

The impact of different CH concentrations (0, 2.0, 4.0 and 6.0%) on the particle size, PDI and surface charge was investigated prior to DAP incorporation (Table 1). NEs containing CH exhibited significantly higher droplet size (189-298 nm) when compared with NEs without the oil (127-156 nm). An increase in droplet size was observed with the amount of CH or PHO. When the concentration of PHO was increased from 5 to 8%, the droplet size changed from 128 to 156 nm. PDI values were higher than 0.3 for NE without CH (0.37 ± 0.05) while NEs containing different concentrations of CH showed PDI values ≤ 0.26, suggesting a role of CH in particle stabilization. ZP was negative for all NEs and a reduction of this parameter with increasing concentrations of CH was found. The lowest ZP value (-13.6± 0.7 nm) was observed in the NE containing the highest CH concentration.

After this initial screening with blank formulations, DAP was incorporated into NE2, NE3 and NE4 (Table 2). NE1 and NE5 formulations were not considered due to the high PDI and low ZP values, respectively. The incorporation of DAP to these systems did not affect the droplet size, PDI and ZP. As already observed in blank NEs, the higher oil content resulted in an increased droplet size. PDI values ranged from 0.19 to 0.25 and ZP was higher than 24 mV. EE values higher than 99% were found for all NEs. The colloidal suspensions also showed acidic pH values (4.4-4.6), which is compatible with a topical application.

Table 1. Composition (%, w/w) and characterization of blank nanoemulsions (mean ± SD; n = 3).

	NE1	NE2	NE3	NE4	NE5
PHO	5.0	8.0	6.0	4.0	2.0
CH	-	-	2.0	4.0	6.0
Polysorbate 80	2.0	2.0	2.0	2.0	2.0
Droplet size (nm)	127.9 ± 4.4	155.6 ± 2.0	189.7 ± 1.5	227.0 ± 1.74	298.0 ± 6.44
PDI	0.37 ± 0.05^{a}	0.26 ± 0.01^{b}	0.18 ± 0.01^{c}	0.21 ± 0.01^{bc}	0.24 ± 0.01^{bc}
Potential zeta (mV)	- 29.2 ± 1.3^{a}	- 29.1 ± 4.9^{a}	-27.7 ± 1.1^{a}	-26.5 ± 2.7^{a}	-13.6 ± 0.7^{b}

ANOVA/Tukey was considered for multiple comparisons. Each parameter (droplet size, PDI and ZP) was individually analyzed. Different letters indicate statistically significant differences (p<0.05).

Table 2. Characterization of formulations loaded with DAP (mean ± SD; n = 3).

	NE2-DAP	NE3-DAP	NE4-DAP
Droplet size (nm)	163.4 ± 4.5^{a}	193.0 ± 3.1^{b}	234.8 ± 12.0^{c}
PDI	0.25 ± 0.01^{a}	0.19 ± 0.02^{b}	0.24 ± 0.03^{a}
Potential zeta (mV)	-30.0 ± 1.8^{a}	-29.1 ± 2.6^{a}	-24.8 ± 1.8^{a}
pH	4.4 ± 0.2^{a}	4.4 ± 0.2^{a}	4.6 ± 0.1^{a}
EE (%)	>99^{a}	>99^{a}	>99^{a}

ANOVA/Tukey was considered for multiple comparisons. Each parameter (droplet size, PDI and ZP) was individually analyzed. Different letters indicate statistically significant differences (p<0.05).

3.1.2. FT-IR analyses

Infrared spectroscopy is a very useful technique for studying intermolecular interactions in formulations. Band shifts or changes in their intensities can suggest specific interactions [25]. In the FT-IR spectrum of DAP, wider bands between 3,300 and 3,400 cm^{-1} were found, which correspond to amino groups. The bands at 1,592 and 1,281 cm^{-1} are attributed to bending

vibrations of -NH_2 and C-N aromatic groups, respectively. Symmetric and asymmetric vibrations of the sulfone group are found at 1,143 and 1,110 cm^{-1}, respectively. Finally, the band at 828 cm^{-1} is related to the vibration of *p*-disubstituted aromatic ring [26,27].

In FT-IR spectrum analysis of CH, the small band at 3,382 cm^{-1} is attributed to the stretching vibration of hydroxyl (OH) group. C=O and C-O stretching vibrations are detected at 1,748 and 1,163 cm^{-1}, respectively. These last IR bands are attributed to fatty acids present in the oil. Once the fatty acids present a cyclopentene in their structures, the band at 1,464 cm^{-1} is related to the CH_2 bending vibration of cyclic bonds [28].

The FT-IR spectrum of PHO showed bands suggestive of phosphatidylcholine, which is the major constituent of this market product. The bands at 1,092 and 970 cm^{-1} are attributed to the PO_4 group and C-N bond, respectively. Bands at 1,744 and 1,237 cm^{-1} correspond to the stretching vibration of C=O and C-O, respectively.

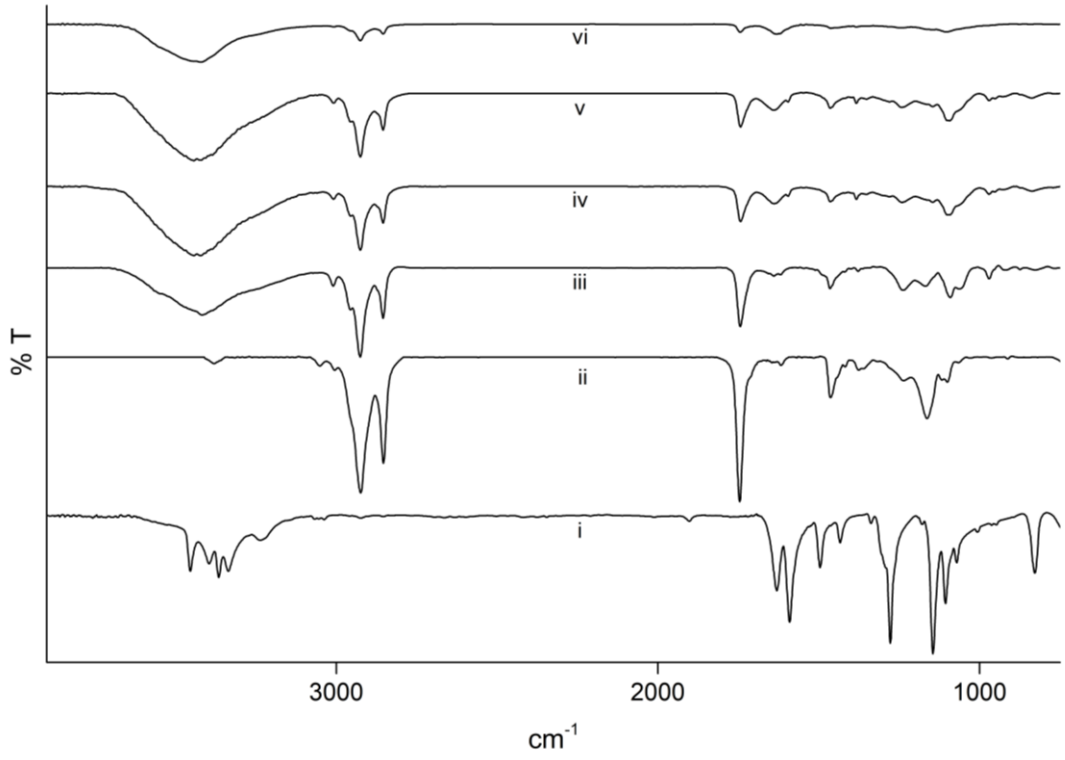

Figure 3. FT-IR spectra of DAP (i), CH (ii), PHO (iii); NE2-DAP (iv); NE3-DAP (v) and NE4-DAP (vi).

Spectral analyses of the formulations showed characteristic bands of the PHO spectrum, which may be attributed to high content of this agent and a surface distribution of this agent in the oil droplets. A reduction in the intensity of these bands was clearly observed with the decrease of the PHO concentration in NEs. Characteristics bands of DAP were not observed in

the FT-IR spectra of NEs, suggesting that the drug is not located on the particle surface. Significant spectral differences were revealed for NE4-DAP compared to NE2-DAP and NE3-DAP. NE4-DAP showed a greater reduction in band intensities, suggesting a greater interaction among their constituents.

3.2. *Stability studies*

Storage stability of formulations was carried out at room temperature because CH solidifies at lower temperatures, resulting in phase separation. Its solidification point is below 16 °C [29]. Particle size, PDI, surface charge, pH and macroscopic aspects of all formulations with DAP were monitored after 15, 30 and 60 days of storage. No significant differences were observed for all analyzed parameters (p>0.05) (Fig. 4). A slight reduction of pH was found, which may be attributed to the release of acids from the oil.

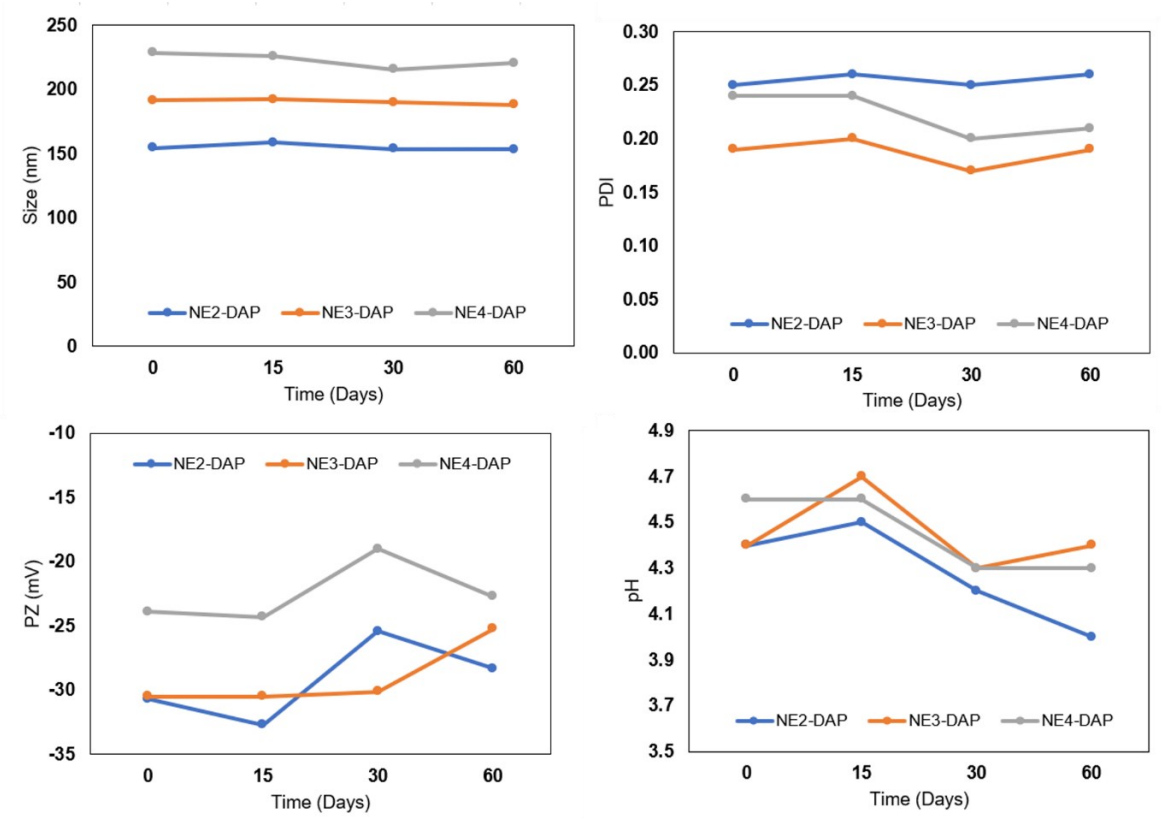

Figure 4. Droplet size, PDI, surface charge, pH of NEs immediately after preparation and 15, 30 and 60 days of storage at 25ºC (n=3).

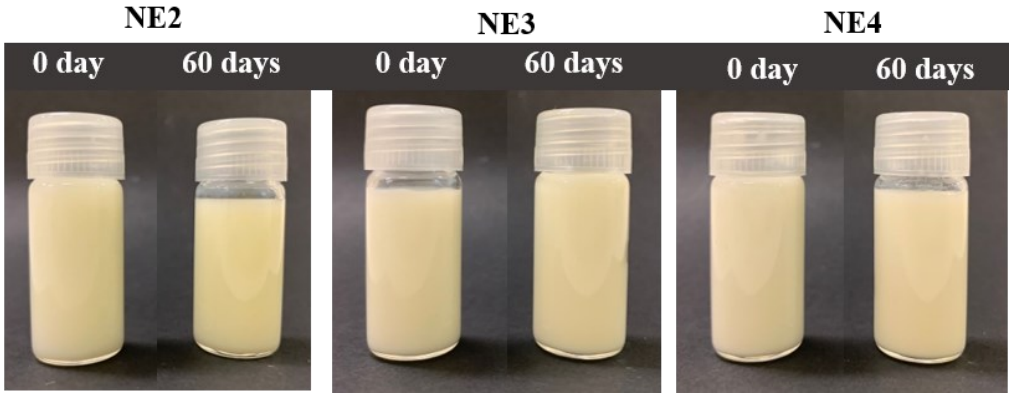

Figure 5. Macroscopic characteristics of NEs after a storage of 60 days at room temperature.

After NE preparation, the appearance of the formulations was milky (Fig. 5). Although the appearance has remained milky after a storage of 60 days at 25 ºC, a slightly yellowish color was observed for the formulations, particularly for NE2-DAP. Signs of microbial contamination were also not found in the analyzed period.

3.3. *Accelerated stability study*

In this study, the transmittance of each colloidal suspension was monitored over time after a centrifugation process in a LUMISizer® equipment (Fig. 6). The kinetics of the droplet separation phenomena is characterized by shape and progression of light transmission profiles measured as a function of time and position over the entire sample length. High transmission values indicate low concentration of particles whereas lower values indicate high concentration of particles [30]. Initially, all samples showed a light transmission of 5%. After a centrifugation period of 20.8 h, the transmittance values were greater than 55, 15 and 20% for NE2-DAP, NE3-DAP and NE4-DAP, respectively. Instability index of these formulations was also calculated. NE2-DAP was more unstable (IS = 0.454), followed by NE3-DAP (IS = 0.170) and NE4-DAP (IS = 0.177). NEs presenting higher oil content were more stable, suggesting that CH positively affect the stability.

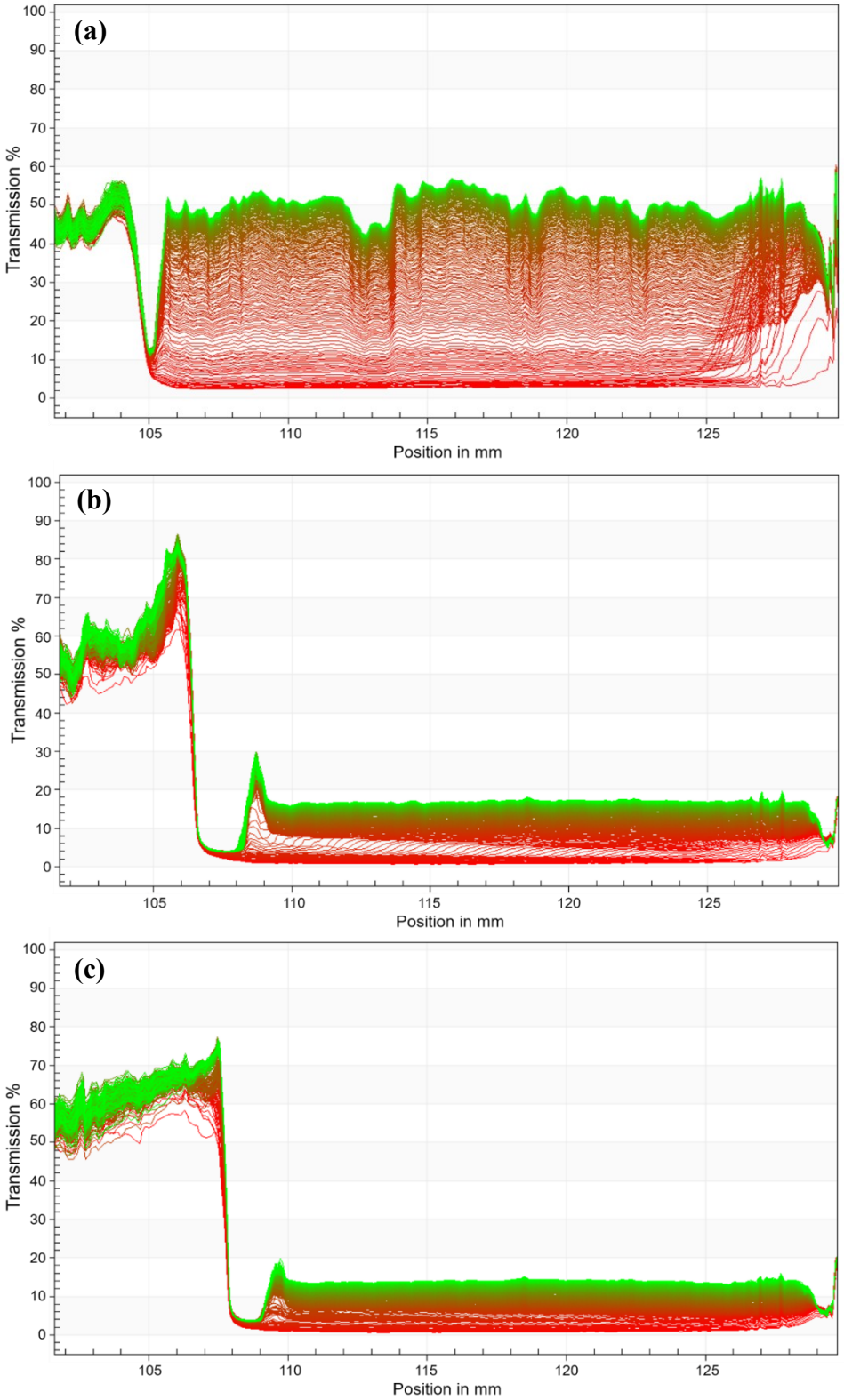

Figure 6. Transmission profiles obtained for NE2-DAP (a), NE3-DAP (b) and NE4-DAP (c) after analytical centrifugation in the LUMiSizer® equipment. The first and the last registered profiles are shown in red and in green, respectively (*n=3*).

3.3.1. Thermal stability

The thermal stability of nanodroplets was evaluated by hot-stage microscopy. The images showed stable NEs up to approximately the water boiling temperature (Fig. 7). Some bubbles were generated from a specific temperature (95.4, 99.5 and 99.9 ºC for NE-2-DAP, NE3-DAP and NE4-DAP, respectively), suggesting that the water present in the NEs was evaporated. All formulations showed to be thermically stable up to 95 ºC. Interestingly, formulations prepared with a higher content of CH showed to be more stable.

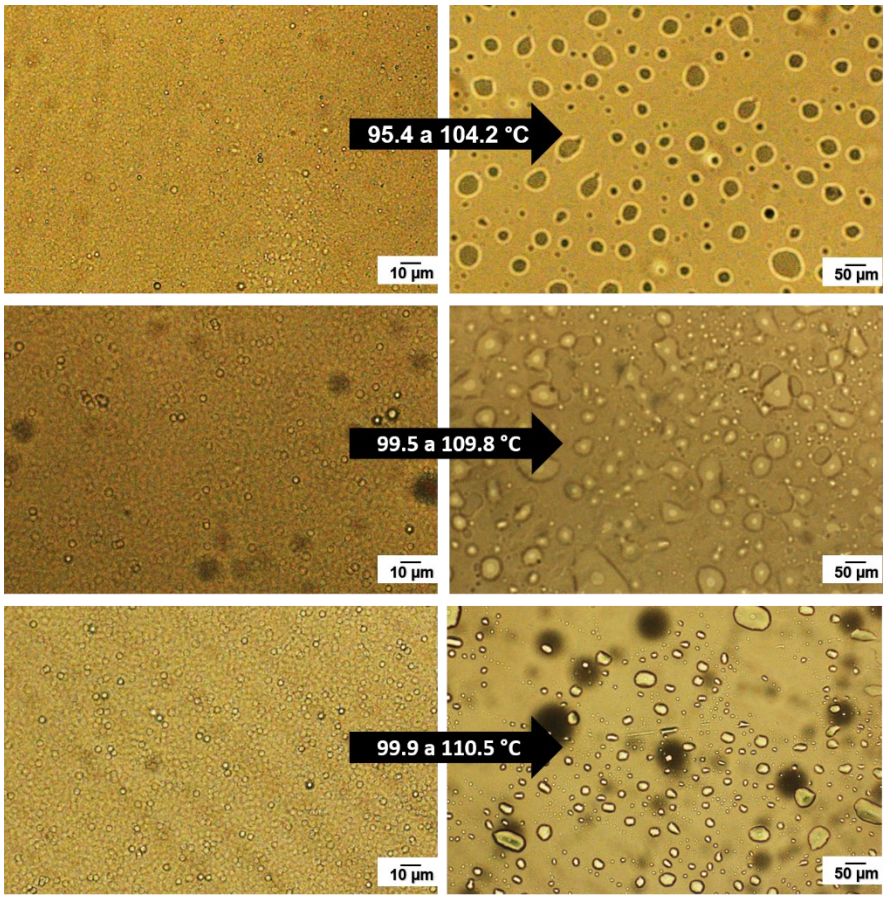

Figure 7. Optical micrographs of the NE2-DAP (a), NE3-DAP (b) and NE4-DAP (c) at two different temperatures (heating rate of 10 °C.min^{-1}).

3.4. *Apparent solubility assays*

Prior to *in vitro* release and *ex vivo* permeation assays, the solubility of DAP in different solutions was tested (Fig. 8). After an equilibrium period of 24 h, the apparent solubility of DAP was 64-times higher in the mixture of water and ethanol (50/50, V/V) than in PBS. Although the DAP is ten times less soluble in aqueous solutions with ethanol at 25% (V/V) compared to the previous condition, this ethanol concentration is enough for a complete drug

solubilization of DAP loaded in formulation (sink condition). Moreover, low concentrations of organic solvents are desirable for this assay type. Once the dialysis bag is permeable to solvents, a lower proportion of ethanol would result in less unspecific disorganization of the nanoemulsified system. For *ex vivo* permeation assays, PBS containing 2% (w/v) of polysorbate 80 was selected for the composition of the receptor fluid. Lower diffusion of polysorbate 80 than ethanol from the receptor chamber to donor compartment is expected. Thus, less impact of the receptor fluid on drug release would be observed.

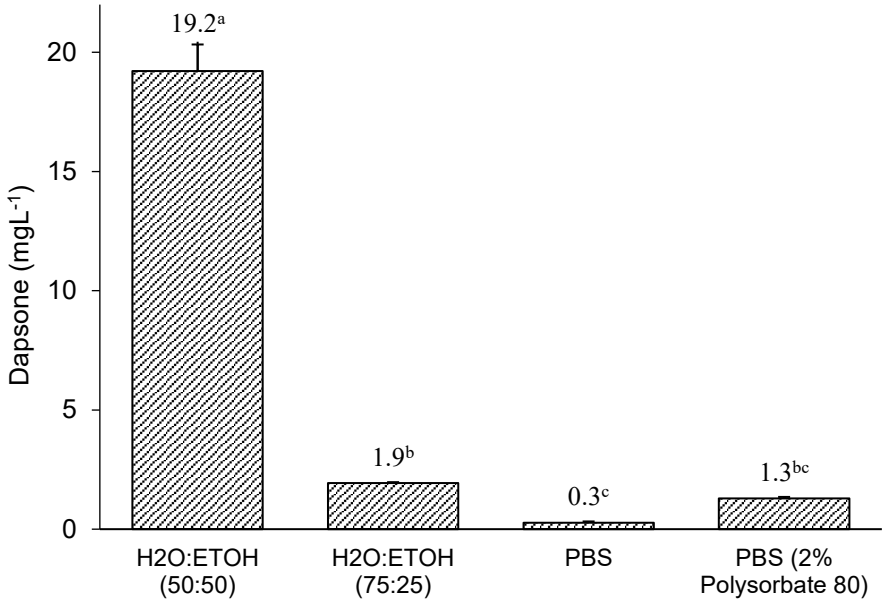

Figure 8. Solubility of DAP in 50% (V/V) of ethanol in water, 25% (V/V) of ethanol in water, PBS (pH 7.4) and 2% (w/v) polysorbate 80 in PBS. (*n=3*). ANOVA/Tukey was considered to compare all groups. Different letters indicate statistically significant differences ($p<0.05$).

3.5. *In vitro drug release assays*

After 6 h, the amount of DAP released from NE2-DAP, NE3-DAP and NE4-DAP was 88.4, 86.9 and 100%, respectively (Fig. 9). The drug release profiles showed a biphasic release behavior with an initial burst followed by slow sustained drug release. The NE with the highest content of oil (NE4-DAP) showed a higher release rate of DAP, which can be attributed to the lower solubility of the drug in the CH compared to the release medium (1.4 $mg.mL^{-1}$ and 1.9 $mg.mL^{-1}$, respectively). Different release kinetic models were considered to study the release mechanism of DAP from formulations (Table 3). Korsmeyer-Peppas was the most suitable kinetic model as it resulted in the highest R^2 value. Diffusional exponents (n) were calculated from the slope of the curve of the log cumulative percentage drug release *versus* log time. For

all formulations, the value of "n" was below 0.5, indicating that the DAP release cannot be described as a simple Fickian diffusion.

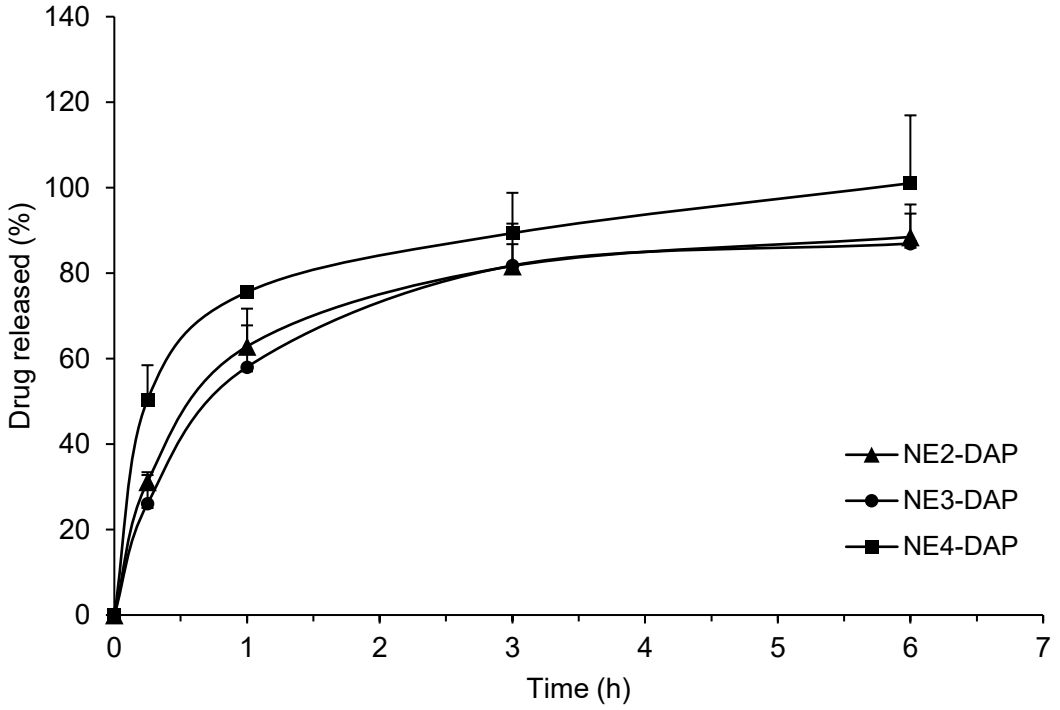

Figure 9. *In vitro* release profiles of DAP from NE2-DAP, NE3-DAP and NE4-DAP. (*n=2*).

Table 3. Mathematical modeling of release kinetics of dapsone from different nanoemulsions.

	Zero order	**First order**	**Higuchi**	**Korsmeyer-Peppas**	
	R^2	**R^2**	**R^2**	**R^2**	**n**
NE2-DAP	0.7815	0.8081	0.911	0.9594	0.3725
NE3-DAP	0.7363	0.7639	0.8783	0.9357	0.3866
NE4-DAP	0.8279	0.9199	0.9316	0.9735	0.214

3.6. *Ex vivo permeation studies in human skin*

The impact of different concentrations of CH and PHO as well as nanostructures on the permeation and retention of DAP through the human skin was also evaluated. The assays were performed in a receptor fluid composed of PBS (pH 7.4) with 2% polysorbate® 80 to

maintain the sink condition. Ethanol was not considered for the composition of this fluid because if it affected the quantification of DAP by developed HPLC method.

After 8 h, DAP was not found in the receptor compartment for the control, NE2-DAP and NE3-DAP (method quantitation limit = 0.44 μg mL^{-1}). Only the NE4-DAP resulted in a quantified amount of DAP in the receptor fluid after this period, which was 5.0 μg cm^{-2}. The amount of DAP retained in epidermis was 1.11, 3.05, 2.01 and 3.40 μg cm^{-2} for control, NE2-DAP, NE3-DAP and NE4-DAP, respectively (Fig. 10). In dermis, these values 0.81, 1.27, 1.06 and 1.60 μg cm^{-2}, respectively. The DAP presented a greater retention in the epidermis compared to the dermis, which may be attributed to its more lipophilic nature (log P = 0.97) [31]. Pereira (2016) also showed a preferential distribution of DAP in epidermis after treatment with DAP loaded nanocapsules [32]. All nanoemulsions showed to be more effective in increasing the distribution of the drug in the skin than the control. The formulation NE4-DAP was the most effective, which may be explained by the higher oil content. CH content appears to have a more significant impact on skin permeation than PHO.

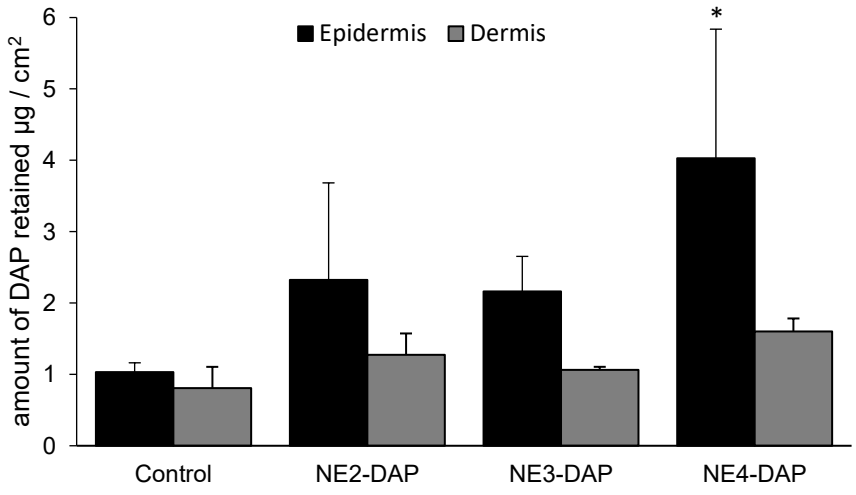

Figure 10. Amount of DAP retained in human epidermis and dermis after 8h (*n*=4).
*indicate statistically significant differences from the control (p<0.05)

3.6.1. FT-IR analysis of human stratum corneum

Spectroscopic studies were considered to evaluate the effect of the NEs on the biophysical properties of the stratum corneum (SC; Fig. 11). FT-IR spectrum of untreated SC showed various bands related to the molecular vibration of proteins and lipids. The absorption bands from 3,000 to 2,800 cm^{-1} observed in untreated SC are associated with C-H stretching of the alkyl groups present in lipids. Bands at 2,920 and 2,850 cm^{-1} are associated with CH_2

whereas CH_3 vibrations appear at 2,955 and 2,870 cm^{-1}, both asymmetric and symmetrical, respectively. In fact, long alkyl chains of ceramides, cholesterol, and fatty acids are found in SC [33]. The reduction in intensity or significant changes in these bands suggest disorder of the hydrocarbon chains or lipid domains [34]. Strong bands related to the amide I and amide II stretch vibrations of SC proteins, in turn, are observed at 1,650 and 1,550 cm^{-1}, respectively. These bands represent various secondary structures of keratin [35]. The amide I band results from the C=O stretching vibration and the amide II bands from the C-N bending vibration. Both absorption bands are sensitive to hydrogen-bonding interactions [36].

More significant changes were observed in lipid than protein domains. Formulations with higher content of CH and lower content of PH resulted in more significant changes in SC, corroborating permeation data. Tissue samples treated with NE4-DAP showed broader and lower-intensity absorption bands at 2,960, 2,920, 2,873 and 2,853 cm^{-1}. This event indicates an increased translational movement or mobility of lipid acyl chains [37]. The sample NE2-DAP (without CH in its composition) demonstrated similar lipid bands to the control, indicating that the presence of oil in the nanostructure is the main determinant of the interaction with the skin. Bands at 1,632 and 1,540 cm^{-1} (amide region) also showed broader and lower intensity after treatment with NE4-DAP when compared to the control (untreated tissue). The changes found in these bands suggest disorder in the protein domains. No changes in this region were detected for NE2-DAP and NE3-DAP.

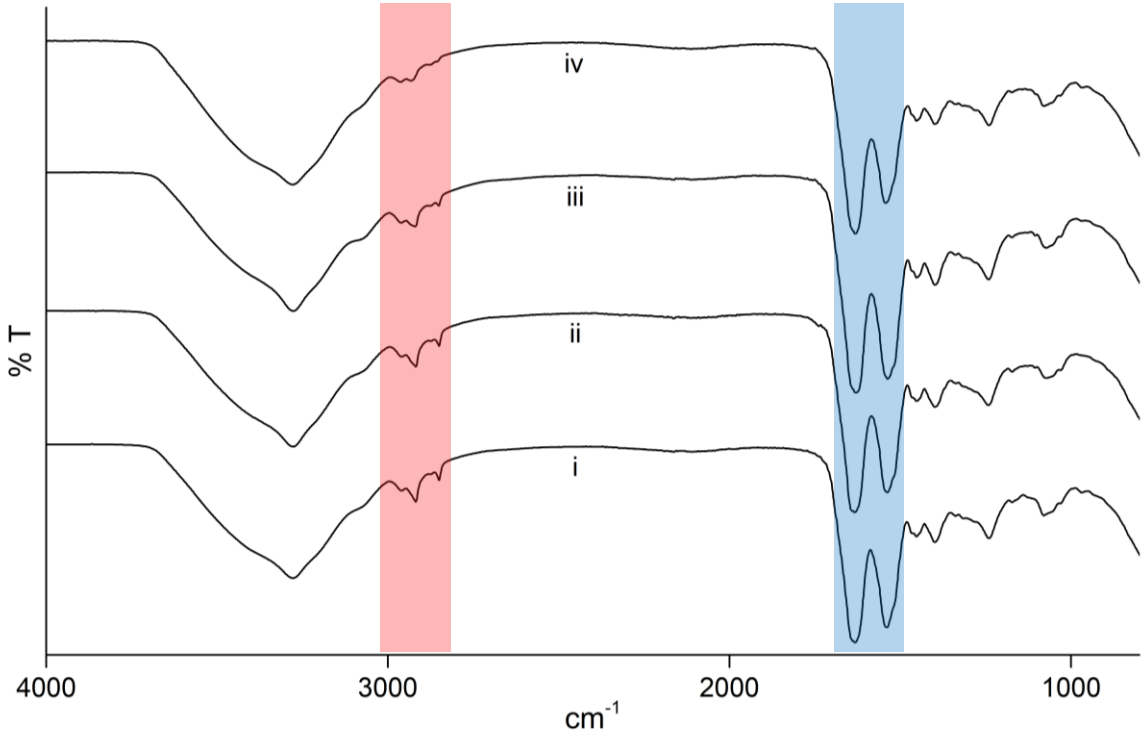

Figure 11. FT-IR analyses (*n*=2) of untreated SC (i) and tissue treated with NE2-DAP (ii), NE3-DAP (iii) and NE4-DAP (iv). Bands highlighted in red correspond to CH_2 and CH_3 of lipids. Bands highlighted in blue are associated with amide I and II for proteins.

3.7. *In vitro citotoxicity assays*

Cytotoxicity assays were performed prior to the strach assay to avoid false-negative results. Once the cytotoxicity of DAP is already known, only blank formulations were considered in this assay. Pure CH showed a very low cytotoxicity (Fig. 12) in relation to the formulations. Its IC_{50} was 7.861 mg mL^{-1}, a value 40 and 30 times higher than NE2 and NE3, respectively. The IC_{50} value for the NE containing CH (0.274 mg mL^{-1}) showed a slight reduction in relation to the formulation without the oil (0.189 mg mL^{-1}), suggesting that formulation has more impact on cytotoxicity than its composition.

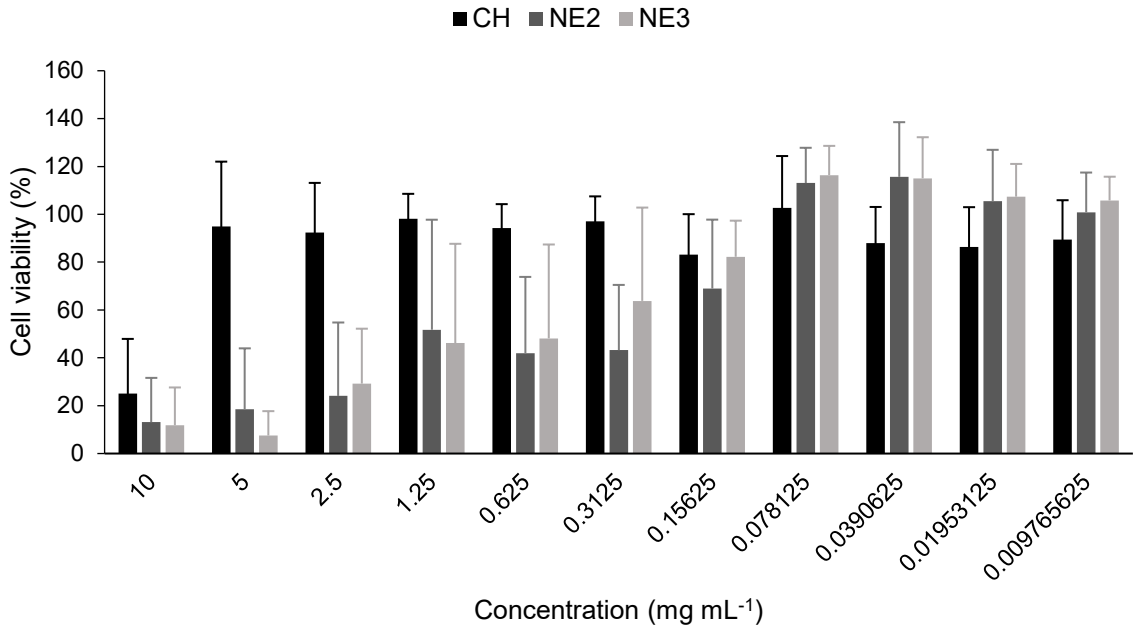

Figure 12. *In vitro* cytotoxicity of CH, NE2 e NE3 in SHED cells (*n*=4).

3.8. *Scratch assay*

The wound re-epithelialization effect of the pure CH and NE was studied by considering the scratch assay. After treatment with the same samples of cytotoxicity assay, cell migration was monitored up to 24 h. Both free CH and NEs containing CH significantly increased the cell migration after 24 h (Fig. 13). CH did not show superior wound healing properties compared to NE3. The wound closure of CH and NE3 was 70 and 69%, respectively. NE2, in turn, resulted in a wound closure percentage of 41%, which may be explained by its lower content of CH (Fig. 14).

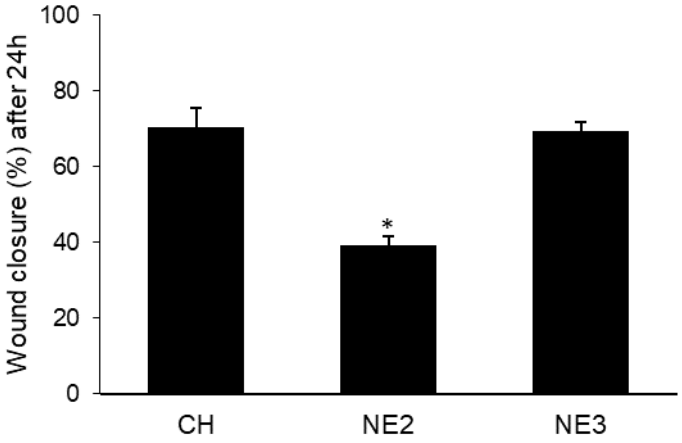

Figure 13. Wound closure percentage in SHED cells after 24 h of treatment with pure chaulmoogra oil (25 µg mL^{-1}), NE2 (without chaulmoogra oil) and NE3 (25 µg mL^{-1} of chaulmoogra oil; n=3). *p<0.05

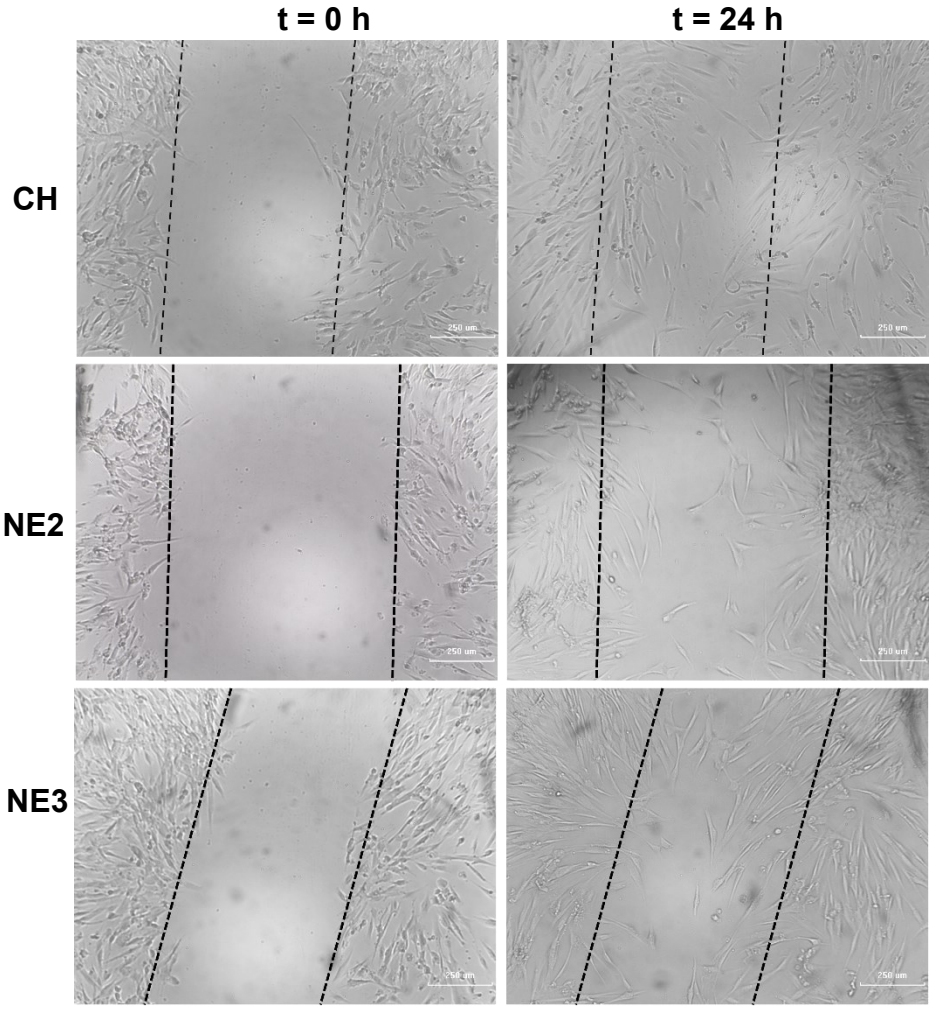

Figure 14. Microscopy images of artificial wound after treatment with CH free (25 µg mL^{-1}), NE2 (without CH) and NE3 (25 µg mL^{-1} of chaulmoogra oil). Left side: before treatment; right side - after 24 h of exposure with the different samples.

4. DISCUSSION

The oral administration of DAP has shown high clinical relevance in leprosy treatment and dermatological diseases. In contrast, it has been accompanied by various adverse effects and its topical application emerges as an alternative. In case of leprosy, the disease-causing bacillus is preferentially distributed in skin layers and peripheral nerves, which would be more easily accessed by using this administration route. Moreover, leprosy causes lesions and loss of skin pigmentation. The association of anti-leprosy drugs with other active compounds may also be considered to improve the efficacy and patient adherence to treatment, particularly in cases of microbial resistance or multiple disease symptoms are found.

Considering that CH was one of the first therapeutic agents used in leprosy patients [38] as well as its effect in wound healing processes [39–41], topical NEs containing DAP and CH were developed in this new study. Formulation studies were initially performed to obtain an effective topical delivery system for the DAP. The oil droplet size of NEs increased with the CH. The PHO, which is emulsifying system composed of phosphatidylcholine and safflower oil [42], also positively affected the oil droplet size when its concentration was changed. An increase in the droplet size of approximately 1.22 times was observed when the PHO concentration ranged from 5 to 8% (NE1 versus NE2; Table 1). The range of particle size found for DAP-loaded NEs (154.4-225.5 nm) is similar to other literature studies performed with topical NEs [43,44]. Almeida (2020), for example, prepared NEs containing PHO, polysorbate and pentyl cinnamate, and found particles with a mean diameter similar to this study [45].

Encapsulation efficiency values higher than 99% were found for all NEs, demonstrating that DAP was successfully incorporated into NEs. Its log P of 0.97 [31] indicates a greater affinity for the oil phase of NEs. FTIR analyses also suggest an internal distribution of DAP in NEs as its characteristic bands (bending vibration of -NH_2 groups at 1,596 cm^{-1} and vibration of *p*-disubstituted aromatic ring at 828 cm^{-1}) were not found.

DAP-loaded NEs presented PDI values lower than 0.3 and thus they can be considered monodisperse systems (DANAEI et al., 2018). Low PDI and high ZP values are important for kinetic stability of the systems. High ZP values (> ± 30 mV) reflect a strong force of repulsion between oil droplets, preventing coalescence or flocculation phenomena [23]. The negative charge of the oil droplets may be attributed to the presence of anionic groups in the PHO and free fatty acids of CH [47]. PHO impacted more significantly on particle surface charge than CH since formulations containing higher concentrations of PHO presented higher difference in ZP values.

All formulations showed to be stable after a storage of 60 days at room temperature without significant changes in surface charge, droplet diameter and PDI. pH values were also maintained close to 4.5, which are compatible with a topical application [48]. The surface of the skin has an acidic pH, known as the 'acid mantle', which is necessary for homeostasis, metabolism of the lipid barrier as well as skin microbiota control [49,50]. Hydrolases responsible for the restoration of the skin barrier exhibit an optimal activation at acidic pH, an important event observed in leprosy patients [51,52].

Unlike the long-term stability tests, instability phenomena were observed in accelerated stability assays, which can be justified by the more drastic conditions of the test. On the other hand, accelerated stability assays can be more interesting to discriminate the formulations from the point of view of their stability. The presence of CH was crucial to increase the stability of formulations. In fact, NE3-DAP and NE4-DAP were more stable than NE2-DAP (without CH). In this way, CH resulted in an improved thermal stability for NEs.

Conventional topical formulations usually have poor patient compliance as they require many applications per day [53]. NEs, in turn, are able to provide a sustained drug release as these systems can increases the contact time and/or maintain drug delivery at the site of action, forming a drug depot on the skin [54]. Indeed, release profiles of DAP followed a biphasic drug release pattern. A fast drug release was observed at the first hour (between 58 and 78% of DAP released) followed by a sustained drug release until 6 h. The initial burst may be attributed to the release of DAP close to the interface of the NEs since the drug can be rapidly solubilized by the surfactants (phosphatidylcholine and polysorbate 80). Subsequently, DAP incorporated into the oily nucleus was slowly released by diffusion to the aqueous phase. The NE with the highest content of oil showed a higher release rate of DAP, which was attributed to the lower solubility of the drug in the CH compared to the release medium. The Korsmeyer-Peppas kinetic model indicated a non-Fickian diffusion behavior for DAP release, which may be explained by the fast DAP release at the beginning of kinetic study.

The NE4-DAP provided a higher retention of DAP in the epidermis compared to other formulations, which was also corroborated by the detection of the drug in the receptor fluid at the end of the assay. The amount of DAP retained in the skin layers were above the minimum inhibitory concentration (MIC = 0.025 μg mL^{-1}) for *M. leprae* [55], suggesting that the purposed formulation would be effective in leprosy. The presence of a greater amount of CH in NE4-DAP could explain these results. Fatty acids such as hydnocarpic, chaulmugric and gorlic acid would play a role as chemical permeation enhancer. They would interact with lipids of the skin

bilayer, affecting the structure of the SC and its fluidity [56,57]. Indeed, FTIR analysis indicated a greater lipid disorder and extraction after skin treatment with formulation containing 6% CH.

Considering that cytotoxicity data of DAP are already reported, only blank formulations were tested. The cytotoxic concentration of DAP in peritoneal macrophages of rats is approximately 350 μg mL^{-1} [58]. Therefore, no dermal toxicity events would be expected during its transport through the skin. Once the pure CH showed very low cytotoxicity (IC_{50} = 7.861 mg mL^{-1}), *in vitro* cytotoxicity assays were performed only with NEs containing higher concentration of surfactants (NE2 and NE3). The NE without the oil showed to be more cytotoxic; suggesting that surfactants are the main responsible for NE cytotoxicity. Another hypothesis is that CH could exhibit an effect on cell proliferation.

With this in mind, the effect of pure CH and encapsulated on wound healing processes was also studied by considering the scratch assay. After creating an artificial gap into a confluent cell monolayer, the cell migration was monitored. Interestingly, both free and encapsulated CH enhanced the cell migration to the artificially damaged area, which was not observed for NE2 (without CH). CH also demonstrated an effect on collagenation and strength of the scar tissue in a literature study with Wistar rats. These findings were attributed to the double bond of cyclopentene acids of oil, which would act by scavenging free radicals [40]. Oommen (2000) also found a significant reduction in the period of epithelialization without wound contraction after treatment with CH [41]. Ulcers were reduced after topical and oral administration of *Hydnocarpus* extract in diabetic mice. After two weeks, no more lesions were [39]. Taken together, these results support the application of nanocarriers with CH in leprosy due to both activity against both *Mycobacterium lepra* and cutaneous lesions.

5. CONCLUSION

Topical administration of DAP represents a promising alternative to the oral route due to the possibility of reducing the drug dose and toxic adverse effects. The addition of CH in NEs intended for the treatment of leprosy provides a number of advantages. Hot-stage and accelerated stability studies revealed that the CH improve both physical and thermal stability. The incorporation of CH in NEs resulted in monodisperse systems (PDI<0.3). The formulation with higher CH content showed greater interaction with human skin in spectroscopic analyses, which was later confirmed in permeation studies. Fatty acids from the CH would play a role as chemical permeation enhancers, disrupting the cutaneous lipid domains. They also would

contribute to increasing DAP retention in the skin. Another positive effect achieved with CH-based NEs was an enhanced cell migration. Currently, none of the drugs used in the treatment of leprosy have been reported to have a positive effect on wound healing. Therefore, the use of CH may be a favorable choice for all benefits mentioned here. Many literature reports also suggest that CH has activity against *M. leprae* and thus it could act synergistically with DAP. Further studies should be performed in this context.

Funding Statement

Bianca da Costa Bernardo Port thank the Brazilian governmental agency CAPES for her scholarship.

Declaration of Competing Interest

The authors declare that they have no known competing financial interests or personal relationships that could have appeared to influence the work reported in this paper.

Acknowledgments

The authors thank the company Lipid (Campinas) and also FURP (Fundação para o Remédio Popular) for the donation of Phosal 50+® and dapsone, respectively.

References

[1] G. Barbeito-Castiñeiras, B. Mejuto, A.C. Nieto, M.J.D. Santalla, A.A. Guirao, M.L.P. del Molino, Leprosy in the twenty-first century: a microbiological, clinical, and epidemiological study in northwestern Spain, Eur. J. Clin. Microbiol. Infect. Dis. (2020). https://doi.org/10.1007/s10096-020-03911-x.

[2] Leprosy (Hansen's disease), ([s.d.]). https://www.who.int/news-room/fact-sheets/detail/leprosy (acessado 26 de julho de 2021).

[3] A. Máquina, A. Catarino, L. Silva, G. Catorze, L. Ferreira, I. Viana, Lepra: Da Antiguidade aos Nossos Tempos, J. Port. Soc. Dermatology Venereol. 77 (2020) 323–338. https://doi.org/10.29021/spdv.77.4.1116.

[4] Brasil, Guia prático sobre a hanseníase, 2017.

[5] P.V. Uaska Sartori, G.O. Penna, S. Bührer-Sékula, M.A.A. Pontes, H.S. Gonçalves, R. Cruz, M.C.L. Virmond, I.M.F. Dias-Baptista, P.S. Rosa, M.L.F. Penna, V. Medeiros Fava, M.M.A. Stefani, M. Távora Mira, Human Genetic Susceptibility of Leprosy Recurrence, Sci. Rep. 10 (2020) 1–5. https://doi.org/10.1038/s41598-020-58079-3.

[6] J. Parascandola, Chaulmoogra oil and the treatment of leprosy., Pharm. Hist. (2003).

[7] S.A. Norton, Useful plants of dermatology. I. Hydnocarpus and chaulmoogra, J. Am. Acad. Dermatol. 31 (1994) 683–686. https://doi.org/10.1016/S0190-9622(08)81744-6.

[8] M.R. Sahoo, S.P. Dhanabal, A.N. Jadhav, V. Reddy, G. Muguli, U. V. Babu, P. Rangesh, Hydnocarpus: An ethnopharmacological, phytochemical and pharmacological review, J. Ethnopharmacol. 154 (2014) 17–25. https://doi.org/10.1016/j.jep.2014.03.029.

[9] P.L. Jacobsen, L. Levy, Mechanism by which hydnocarpic acid inhibits mycobacterial multiplication., Antimicrob. Agents Chemother. 3 (1973) 373–379. https://doi.org/10.1128/AAC.3.3.373.

[10] L. Levy, The activity of chaulmoogra acids against Mycobacterium leprae, Amer.Rev.Resp.Dis. 111 (1975) 703–705. https://doi.org/10.1164/arrd.1975.111.5.703

[11] F.S.D. Dos Santos, L.P.A. De Souza, A.C. Siani, Chaulmoogra oil as scientific knowledge: the construction of a treatment for leprosy, Hist Cienc Saude-Manguinhos. 15 (2008) 29–47. https://doi.org/10.1590/S0104-59702008000100003

[12] K. V. Desikan, Multi-drug regimen in leprosy and its impact on prevalence of the disease, Med. J. Armed Forces India. 59 (2003) 2–4. https://doi.org/10.1016/S0377-1237(03)80092-8.

[13] H.K. Kar, R. Gupta, Treatment of leprosy, Clin. Dermatol. 33 (2015) 55–65. https://doi.org/10.1016/j.clindermatol.2014.07.007.

[14] OMS, Chagas disease (American trypanosomiasis) Epidemiology, OMS. (2018).

[15] WHO, Leprosy elimination, Leprosy. (2020). https://www.who.int/news-room/fact-sheets/detail/leprosy.

[16] E. Molinelli, M. Paolinelli, A. Campanati, V. Brisigotti, A. Offidani, Metabolic, pharmacokinetic, and toxicological issues surrounding dapsone, Expert Opin. Drug Metab. Toxicol. 15 (2019) 367–379. https://doi.org/10.1080/17425255.2019.1600670.

[17] I.M. Bernades Goulart, G. Leonel Arbex, M. Hubaide Carneiro, M. Scalia Rodrigues, R. Gadia, Efeitos adversos da poliquimioterapia em pacientes com hanseníase: Um levantamento de cinco anos em um Centro de Saúde da Universidade Federal de Uberlândia, Rev. Soc. Bras. Med. Trop. 35 (2002) 453–460. https://doi.org/10.1590/s0037-86822002000500005.

[18] F.R. Oliveira, M.C. Pessoa, R.F.V. Albuquerque, T.R. Schalcher, M.C. Monteiro, Clinical applications and methemoglobinemia induced by dapsone, J. Braz. Chem. Soc. 25 (2014) 1770–1779. https://doi.org/10.5935/0103-5053.20140168.

[19] Y.I. Zhu, M.J. Stiller, Dapsone and sulfones in dermatology: Overview and update, J. Am. Acad. Dermatol. 45 (2001) 420–434. https://doi.org/10.1067/mjd.2001.114733.

[20] T.W. Wong, Electrical, magnetic, photomechanical and cavitational waves to overcome skin barrier for transdermal drug delivery, J. Control. Release. 193 (2014) 257–269. https://doi.org/10.1016/j.jconrel.2014.04.045.

[21] C. Puglia, F. Bonina, Lipid nanoparticles as novel delivery systems for cosmetics and dermal pharmaceuticals, Expert Opin. Drug Deliv. 9 (2012) 429–441. https://doi.org/10.1517/17425247.2012.666967.

[22] B. Clares, A.C. Calpena, A. Parra, G. Abrego, H. Alvarado, J.F. Fangueiro, E.B. Souto,

Nanoemulsions (NEs), liposomes (LPs) and solid lipid nanoparticles (SLNs) for retinyl palmitate: effect on skin permeation, Int. J. Pharm. 473 (2014) 591–598. https://doi.org/10.1016/j.ijpharm.2014.08.001.

[23] Y. Singh, J.G. Meher, K. Raval, F.A. Khan, M. Chaurasia, N.K. Jain, M.K. Chourasia, Nanoemulsion: Concepts, development and applications in drug delivery, J. Control. Release. 252 (2017) 28–49. https://doi.org/10.1016/j.jconrel.2017.03.008.

[24] V. Vichai, K. Kirtikara, Sulforhodamine B colorimetric assay for cytotoxicity screening, Nat. Protoc. 1 (2006) 1112–1116. https://doi.org/10.1038/nprot.2006.179.

[25] P. Pandey, N. Gulati, M. Makhija, D. Purohit, H. Dureja, Nanoemulsion: A Novel Drug Delivery Approach for Enhancement of Bioavailability, Recent Pat. Nanotechnol. 14 (2020) 276–293. https://doi.org/10.2174/1872210514666200604145755.

[26] G.O. Ildiz, S. Akyuz, Conformational analysis and vibrational spectroscopic studies on dapsone, Opt. Spectrosc. (English Transl. Opt. i Spektrosk. 113 (2012) 495–504. https://doi.org/10.1134/S0030400X12110033.

[27] L.L. Chaves, A.C.C. Vieira, D. Ferreira, B. Sarmento, S. Reis, Rational and precise development of amorphous polymeric systems with dapsone by response surface methodology, Int. J. Biol. Macromol. 81 (2015) 662–671. https://doi.org/10.1016/j.ijbiomac.2015.08.009.

[28] T.M.N. dos Santos, Extração e purificação dos ciclopentênicos presentes nas amêndoas de Carpatroche brasiliensis Endl, UESB, 2019.

[29] H. Possolo, O Óleo De Chaulmugra Na Farmacopeia Brasileira Helena, (1898).

[30] M. Alhreez, D. Wen, Controlled releases of asphaltene inhibitors by nanoemulsions, Fuel. 234 (2018) 538–548. https://doi.org/10.1016/j.fuel.2018.06.079.

[31] L.M. Monteiro, V.F. Lione, F.A. do Carmo, L.H. do Amaral, J.H. da Silva, L.E. Nasciutti, C.R. Rodrigues, H.C. Castro, V.P. de Sousa, L.M. Cabral, Development and characterization of a new oral dapsone nanoemulsion system: Permeability and in silico bioavailability studies, Int. J. Nanomedicine. 7 (2012) 5175–5182. https://doi.org/10.2147/IJN.S36479.

[32] R.L. Pereira, F.I. Leites, K. Paese, R.M. Sponchiado, C.B. Michalowski, S.S. Guterres, E.E.S. Schapoval, Hydrogel containing adapalene- and dapsone-loaded lipid-core nanocapsules for cutaneous application: development, characterization, in vitro irritation and permeation studies, Drug Dev. Ind. Pharm. 42 (2016) 2001–2008. https://doi.org/10.1080/03639045.2016.1188110.

[33] M. Cotte, P. Dumas, M. Besnard, P. Tchoreloff, P. Walter, Synchrotron FT-IR microscopic study of chemical enhancers in transdermal drug delivery: Example of fatty acids, J. Control. Release. 97 (2004) 269–281. https://doi.org/10.1016/j.jconrel.2004.03.014.

[34] F. Shakeel, S. Baboota, A. Ahuja, J. Ali, S. Shafiq, Skin permeation mechanism of aceclofenac using novel nanoemulsion formulation, Pharmazie. 63 (2008) 580–584. https://doi.org/10.1691/ph.2008.8036.

[35] I. Vashisth, A. Ahad, M. Aqil, S.P. Agarwal, Investigating the potential of essential oils as penetration enhancer for transdermal losartan delivery: Effectiveness and mechanism of action, Asian J. Pharm. Sci. 9 (2014) 260–267. https://doi.org/10.1016/j.ajps.2014.06.007.

[36] P. Garidel, Mid-FTIR-microspectroscopy of stratum corneum single cells and stratum corneum tissue, Phys. Chem. Chem. Phys. 4 (2002) 5671–5677. https://doi.org/10.1039/b207478h.

[37] R. Panchagnula, P.S. Salve, N.S. Thomas, A.K. Jain, P. Ramarao, Transdermal delivery of naloxone: Effect of water, propylene glycol, ethanol and their binary combinations on permeation through rat skin, Int. J. Pharm. 219 (2001) 95–105. https://doi.org/10.1016/S0378-5173(01)00634-2.

[38] J.M. Barbosa-Filho, F.A. Do Nascimento Júnior, A.C. De Andrade Tomaz, P.F. De Athayde-Filho, M.S. Da Silva, E.V.L. Da Cunha, M.F.V. De De Souza, L.M. Batista, M.F.F.M. Diniz, Natural products with antileprotic activity, Brazilian J. Pharmacogn. 17 (2007) 141–148. https://doi.org/10.1590/S0102-695X2007000100022.

[39] G.S. Lee, J.Y. Choi, Y.J. Choi, D.S. Yim, T.J. Kang, J.H. Cheong, The wound healing effect of hydnocarpi semen extract on ulcer in diabetic mice, Biomol. Ther. 18 (2010) 329–335. https://doi.org/10.4062/biomolther.2010.18.3.329.

[40] S.T. Oommen, M. Rao, C.V.N. Raju, Effect of oil of hydnocarpus on wound healing, Int. J. Lepr. Other Mycobact. Dis. 67 (1999) 154–158.

[41] S.T. Oommen, The effect of oil of hydnocarpus on excision wounds [4], Int. J. Lepr. Other Mycobact. Dis. 68 (2000) 69–70.

[42] Lipoid, Botanical Actives , Botanical We make beauty natural ., ([s.d.]).

[43] N. Salim, N. Ahmad, S.H. Musa, R. Hashim, T.F. Tadros, M. Basri, Nanoemulsion as a topical delivery system of antipsoriatic drugs, RSC Adv. 6 (2016) 6234–6250. https://doi.org/10.1039/c5ra14946k.

[44] M. Elmowafy, K. Shalaby, H.M. Ali, N.K. Alruwaili, A. Salama, M.F. Ibrahim, M.A. Akl, T.A. Ahmed, Impact of nanostructured lipid carriers on dapsone delivery to the skin: in vitro and in vivo studies, Int. J. Pharm. 572 (2019) 118781. https://doi.org/10.1016/j.ijpharm.2019.118781.

[45] A.R. de Almeida, Desenvolvimento e caracterização de formulações larvicidas contendo derivado do ácido cinâmico para o combate ao Aedes aegypti, 2020.

[46] M. Danaei, M. Dehghankhold, S. Ataei, F. Hasanzadeh Davarani, R. Javanmard, A. Dokhani, S. Khorasani, M.R. Mozafari, Impact of particle size and polydispersity index on the clinical applications of lipidic nanocarrier systems, Pharmaceutics. 10 (2018) 1–17. https://doi.org/10.3390/pharmaceutics10020057.

[47] J. Desai, H. Thakkar, Enhanced oral bioavailability and brain uptake of Darunavir using lipid nanoemulsion formulation, Colloids Surfaces B Biointerfaces. 175 (2019) 143–149. https://doi.org/10.1016/j.colsurfb.2018.11.057.

[48] G. Yosipovitch, G.L. Xiong, E. Haus, L. Sackett-Lundeen, I. Ashkenazi, H.I. Maibach, Time-dependent variations of the skin barrier function in humans: Transepidermal water loss, stratum corneum hydration, skin surface pH, and skin temperature, J. Invest. Dermatol. 110 (1998) 20–23. https://doi.org/10.1046/j.1523-1747.1998.00069.x.

[49] S.P. Song, C.Z. Lv, K.R. Feingold, Q.N. Hou, Z.Y. Li, C.Y. Guo, P.M. Elias, M.Q. Man, Abnormalities in stratum corneum function in patients recovered from leprosy, Skin Pharmacol. Physiol. 22 (2009) 131–136. https://doi.org/10.1159/000189802.

[50] M.H. Schmid-Wendtner, H.C. Korting, The pH of the skin surface and its impact on the barrier function, Skin Pharmacol. Physiol. 19 (2006) 296–302. https://doi.org/10.1159/000094670.

[51] H. Lambers, S. Piessens, A. Bloem, H. Pronk, P. Finkel, Natural skin surface pH is on average

below 5, which is beneficial for its resident flora, Int. J. Cosmet. Sci. 28 (2006) 359–370. https://doi.org/10.1111/j.1467-2494.2006.00344.x.

[52] J. Blaak, P. Staib, The Relation of pH and Skin Cleansing, Curr. Probl. Dermatology. 54 (2018) 132–142. https://doi.org/10.1159/000489527.

[53] K. Frederiksen, R.H. Guy, K. Petersson, Formulation considerations in the design of topical, polymeric film-forming systems for sustained drug delivery to the skin, Eur. J. Pharm. Biopharm. 91 (2015) 9–15. https://doi.org/10.1016/j.ejpb.2015.01.002.

[54] G. Cevc, U. Vierl, Nanotechnology and the transdermal route. A state of the art review and critical appraisal, J. Control. Release. 141 (2010) 277–299. https://doi.org/10.1016/j.jconrel.2009.10.016.

[55] A.M. Dhople, In vivo activity of epiroprim, a dihydrofolate reductase inhibitor, singly and in combination with dapsone, against Mycobacterium leprae, Int. J. Antimicrob. Agents. 19 (2002) 71–74. https://doi.org/10.1016/S0924-8579(01)00470-8.

[56] B.J. Aungst, Structure/Effect Studies of Fatty Acid Isomers as Skin Penetration Enhancers and Skin Irritants, Pharm. Res. An Off. J. Am. Assoc. Pharm. Sci. 6 (1989) 244–247. https://doi.org/10.1023/A:1015921702258.

[57] T. Marjukka Suhonen, J. A. Bouwstra, A. Urtti, Chemical enhancement of percutaneous absorption in relation to stratum corneum structural alterations, J. Control. Release. 59 (1999) 149–161. https://doi.org/10.1016/S0168-3659(98)00187-4.

[58] E. Moreno, A. Calvo, J. Schwartz, I. Navarro-Blasco, E. González-Peñas, C. Sanmartín, J.M. Irache, S. Espuelas, Evaluation of skin permeation and retention of topical dapsone in murine cutaneous leishmaniasis lesions, Pharmaceutics. 11 (2019). https://doi.org/10.3390/pharmaceutics11110607.

[59] D.W. Osborne, Compositions and methods for topical applications of theraputic agents, United States Pat. Off. 5,863,560. (1999).

[60] D.W. Osborne, Compositions and methods for topical application of theraputic agentes, 6,060,085 (2000).

[61] D.W. Osborne, Topical dapsone for the treatment of acne., (2002).

[62] D.E. Braun, U.J. Griesser, Supramolecular Organization of Nonstoichiometric Drug Hydrates: Dapsone, Front. Chem. 6 (2018) 1–17. https://doi.org/10.3389/fchem.2018.00031.

[63] V. Patel, O.P. Sharma, T. Mehta, Nanocrystal: a novel approach to overcome skin barriers for improved topical drug delivery, Expert Opin. Drug Deliv. 15 (2018) 351–368. https://doi.org/10.1080/17425247.2018.1444025.

6 DISCUSSÃO GERAL

A administração oral da DAP tem sido considerada para o tratamento de várias patologias infecciosas. Apesar da alta eficácia antimicrobiana e anti-inflamatória, a rota oral vem acompanhada de vários efeitos adversos, o que tem motivado estudos com rotas alternativas como a pele. Géis tópicos de DAP, com indicação para acne, já tem sido comercializados em concentrações de 5 e 7,5%. Nesses produtos, acredita-se que a fração da DAP dissolvida no veículo é responsável por sua passagem através do estrato córneo, enquanto, a não dissolvida (cristalina) alcança folículos pilosos e outros anexos da pele, formando verdadeiros reservatórios que permitem uma liberação sustentada. Estes géis são sistemas bifásicos compostos por uma *solução orgânica* com DAP e uma *solução aquosa* em que um polímero formador de gel e conservantes estão presentes. As formulações são preparadas através de um método de cristalização por adição de antissolvente. As patentes desta formulação (OSBORNE, 1999, 2000, 2002) mencionam o uso de diferentes proporções de água/solvente orgânico para solubilizar a DAP. Por outro lado, ainda não haviam estudos ou relatos do

impacto destes solventes no tamanho e morfologia do cristal de DAP que seria obtido, tampouco a proporção de fármaco dissolvido/cristalino. Neste contexto, a primeira etapa deste estudo se concentrou na investigação do efeito de solventes orgânicos (DEGEE, PEG e MPR) sobre estes aspectos. Secundariamente, mas não menos importante, buscou-se encontrar novas formas cristalinas multicomponentes para a DAP.

Inicialmente, preparam-se diagramas de fase com várias combinações binárias de solventes, a considerar: DEGEE: água, PEG: água e MPR: água. Tais estudos são úteis no controle do tipo e quantidade de cristais de fármacos resultantes de diferentes proporções de solventes utilizados na composição das formulações. Os diagramas de fase mostram um limiar de atividade do solvente a partir do qual a natureza do cristal muda caso haja um controle termodinâmico do sistema. As formas sólidas de DAP presente no precipitado das soluções do diagrama de fase foram analisadas por difração de raios X e a quantidade de DAP dissolvida foi quantificada por espectroscopia UV-Vis.

Os resultados obtidos em DEGGE: água foram inconsistentes e dominados "cineticamente" à medida que hidrato e a forma III anidra cristalizaram alternadamente. É possível que estas formas de DAP tenham diferenças significativas tanto na cinética de nucleação quanto do crescimento do cristal. De fato, a literatura mostra que a cinética realmente desempenha um papel importante na cristalização da DAP anidra em soluções aquosas (BRAUN; GRIESSER, 2018). No caso das misturas PEG: água e MPR: água, duas regiões foram claramente identificadas nos diagramas de fases, cada qual com sua forma estável. Em ambos os casos, os resultados mostraram que a DAP tende a cristalizar com PEG ou MPR em concentrações de solvente superiores a 10%, resultando em um cocristal e solvato, respectivamente. A existência de um solvato de DAP com MPR ainda não tinha sido relatada. A estrutura foi depositada no *Cambridge Crystallographic Data Center* (CCDC) e hoje encontra-se disponível para toda a comunidade científica, uma importante contribuição deste estudo. Diferentemente do DEGEE, PEG e MPR mostraram ser mais apropriados para formular géis como o componente cinético não parece ser predominante no equilíbrio das formas hidrato e solvato de DAP. Do ponto de vista prático, a composição DEGEE: água pode resultar em uma forma sólida que é mais difícil de ser controlada tanto durante a produção quanto armazenagem do produto, tornando desafiante a obtenção de um produto que possui sempre as mesmas características (importante para formulações medicamentosas).

Como o grau de supersaturação é outro aspecto que afeta as transformações de fase da DAP, além da identidade da forma sólida, diagramas de fase também podem ser construídos

para estimar as quantidades de fármaco que se encontram nas formas dissolvida e cristalina. Embora a quantidade de DAP dissolvida é maior em altas concentrações de DEGEE em relação a PEG e MPR, as solubilidades são similares no intervalo entre 10 e 25% (concentrações que aparecem nas patentes) para as três composições de solvente.

As formulações foram preparadas pelo método descrito nas patentes, fixando-se a concentração do solvente orgânico em 25% (m/m). A quantidade de DAP dissolvida também foi quantificada por espectrofotometria UV/VIs. Os resultados mostraram que as formulações com DEGEE e PEG (FDE e FPE, respectivamente) resultaram em maior quantidade de cristais de DAP em relação à formulação com MPR (FMP). FMP mostrou uma quantidade dissolvida de fármaco, que foi quatro vezes maior em relação às outras formulações. FDE e FMP mostraram maior quantidade de DAP dissolvida quando comprado àquelas obtidas no diagrama de fase na mesma proporção de água: solvente, sugerindo que essas formulações se encontram em um estado supersaturado.

A forma sólida da DAP presente nas formulações foram identificadas por difração de raios X. Os difratogramas relativos à amostra FDE mostraram um padrão de reflexões que sinaliza a presença de hidrato de DAP, o que foi confirmado pela análise de Rietveld. Embora a presença da forma III de DAP fosse esperada na FDE, a presença do hidrato confirma que o equilíbrio entre a forma III/hidrato é afetado cineticamente e é difícil de controlar. Na FPE, o cocristal de PEG foi encontrado, como já previsto na análise do diagrama de fases. A FMP resultou em mistura de hidrato e solvato MPR, o que poderia justificar a alta quantidade de DAP dissolvida neste meio.

A análise microscópica mostrou partículas heterogêneas em termos de tamanho e morfologia. Diferentes tipos de partículas na mesma formulação indicam que um sólido pode gerar várias formas cristalinas, que a mesma forma sólida pode ter diferenças nas características de superfície, ou o material sólido é composto por uma mistura de fases que apresentam diferentes características morfológicas. O refinamento de Rietveld mostrou a presença de uma mistura de fases somente na formulação FMP. Embora misturas de fases não foram encontradas na FPE e FDE, não é possível descartar esta hipótese já que concentrações de fases cristalinas abaixo de 5% podem não ser detectadas neste tipo de análise.

As formulações apresentaram diferentes características macroscópicas, porém, a FPE resultou em um gel menos viscoso em relação às outras formulações. Curiosamente, os cristais de DAP podem ter afetado negativamente a viscosidade neste caso. A distribuição dos géis na pele humana foi avaliada com auxílio de um estereoscópio. Imagens foram coletadas logo após

a aplicação do gel e depois de 2 h. As formulações se distribuíram em diferentes regiões da pele, particularmente as que continham cristais de DAP, sugerindo que a natureza do cristal pode afetar tal comportamento. Acredita-se que a viscosidade dos géis e o tipo de solvente também afetem a interação com o estrato córneo e a taxa de liberação/permeação da DAP. Estudos de permeação poderiam ter sido considerados para esclarecer estas diferenças em termos da distribuição do fármaco. Há relatos na literatura de uma distribuição preferencial de cristais nas regiões dos apêndices, particularmente nos folículos pilosos (PATEL et al., 2018).

A análise estrutural dos materiais cristalinos estudados revelou diferenças tanto no arranjo espacial das moléculas do cossolvente nos cristais bem como no volume ocupado por eles. A água ocupa cerca de 0,4% do cristal, a MPR 32,6% e o PEG 52,2%. Essas diferenças no empacotamento são estavelmente mantidas pela presença de diferentes interações intermoleculares. Embora a presença de partículas, a natureza do solvente e a composição sejam conhecidas por afetar as propriedades da formulação final, a relação das características específicas da estrutura do cristal também podem desafiar o desempenho de produtos tópicos contendo cristais. Grupos funcionais expostos nas superfícies dos cristais podem afetar interações intermoleculares entre si, com o veículo e com a pele. O uso de formas cristalinas multicomponentes para formular aumenta a diversidade de interações possíveis; permitindo selecionar formas de cristais com propriedades específicas e com uma ação direcionada. Pelo que se conhece até hoje, as características da forma sólida e de superfície ainda não foram exploradas como estratégia tecnológica para a entrega de cristais na pele.

Além da indicação na acne, a DAP tem sido historicamente utilizada para tratar hanseníase, uma doença negligenciada crônica altamente contagiosa descrita em detalhes na revisão bibliográfica deste trabalho. Uma das justificativas para desenvolver uma formulação de aplicação tópica é que o bacilo causador desta doença se distribui preferencialmente nas diferentes camadas da pele e nervos periféricos.

A hanseníase também causa lesões na pele e perda da pigmentação. Frente a isto, a segunda etapa deste trabalho envolveu o desenvolvimento de um sistema nanoemulsionado deste fármaco. Para facilitar a permeação na pele e conferir propriedades adicionais, óleo de chaulmoogra (CH) foi adicionado. Este óleo foi um dos primeiros agentes terapêuticos utilizados em pacientes com hanseníase (BARBOSA-FILHO et al., 2007) e seu efeito em processos de cicatrização de feridas já tem sido documentado em alguns trabalhos (OOMMEN et al., 1999; OOMMEN, 2000; LEE et al., 2010).

Formulações brancas foram inicialmente preparadas para determinar as concentrações do agente emulsificante PHO e do CH. A presença e o aumento da concentração do CH resultaram em um maior tamanho de partícula. O PHO, que é um sistema emulsificante composto por fosfatidilcolina e óleo de cártamo (LIPOID), também aumentou o tamanho da gota de óleo com a concentração. Este agente aumentou de 127,9 para 155,6 nm o tamanho da gota quando sua concentração variou de 5 para 8%. A partir desta triagem inicial, três formulações foram selecionadas para a incorporação da DAP, levando-se em conta os parâmetros destas formulações brancas tais como o tamanho, PDI e carga de superfície.

Alta eficiência de encapsulação foi encontrada para as três formulações (>99%). Análises de FTIR também sugeriram uma distribuição interna da DAP nas nanopartículas, uma vez que nenhuma banda característica do fármaco (vibração de flexão dos grupos -NH2 em 1.596 cm^{-1} e vibração do anel aromático *p*-dissubstituído em 828 cm^{-1}) foi encontrada nos espectros das formulações. A NE com maior conteúdo de CH mostrou maior redução das bandas de IR, sugerindo interação entre seus componentes.

As NEs com DAP apresentaram valores de PDI inferiores a 0,3, indicando que os sistemas são monodispersos [46]. Os valores de carga de superfície foram negativos, o que pode ser atribuído à presença de grupamentos aniônicos do PHO e dos ácidos graxos livres do CH (DESAI; THAKKAR, 2019). Os valores de carga de superfície encontrados para as formulações variaram entre -24,8 e -30,0 mV, sugerindo uma estabilização das partículas por mecanismos eletrostáticos.

Não foram encontradas mudanças significativas na carga de superfície, tamanho de partícula e PDI para as formulações armazenadas a temperatura ambiente durante 60 dias, sugerindo que os sistemas são estáveis. Os valores de pH também foram mantidos próximos a 4,5, o que é compatível com uma aplicação tópica (YOSIPOVITCH et al., 1998). A superfície da pele tem um pH ácido, conhecido como manto ácido, necessário para a homeostase, organização/metabolismo da barreira lipídica e controle da microbiota da pele (SCHMID-WENDTNER; KORTING, 2006; SONG et al., 2009). Ainda, hidrolases responsáveis pela restauração da barreira cutânea em processos cicatriciais possuem atividade ótima em pH ácido (LAMBERS et al., 2006; BLAAK; STAIB, 2018).

Diferentemente dos testes de estabilidade de longa duração, fenômenos de instabilidade foram observados em testes de estabilidade acelerada, o que pode ser justificado pelas condições mais severas do teste. Por outro lado, ensaios de estabilidade acelerada podem ter

maior utilidade na discriminação de formulações do ponto de vista da estabilidade. A presença de CH nas nanoemulsões foi crucial para a melhoria deste aspecto.

Em geral, as preparações medicamentosas tópicas convencionais resultam em baixa adesão terapêutica já que requerem várias aplicações diárias (FREDERIKSEN et al., 2015). NEs são bem conhecidas pela sua capacidade de proporcionar uma liberação sustentada do fármaco. Esses sistemas podem aumentar o tempo de contato e/ou manter a liberação do fármaco no local de ação, formando uma espécie de "depósito" na pele (CEVC; VIERL, 2010). Os perfis de liberação de DAP seguiram um padrão de liberação bifásico, onde se observou uma liberação rápida do fármaco na primeira hora (entre 58 e 78% do DAP liberado), seguido de uma liberação sustentada até 6 h. O "*burst*" inicial pode ser atribuído à liberação de DAP próximo à interface das NEs uma vez que o fármaco seria rapidamente solubilizado pelos tensoativos fosfatidilcolina e polissorbato 80. Subsequentemente, a DAP incorporada ao núcleo oleoso se difundiu mais lentamente para a fase aquosa. A maior quantidade de óleo reduziu a afinidade da DAP pela NE, explicando a liberação mais rápida. De fato, o fármaco mostra uma maior solubilidade no meio de liberação em relação ao CH (1,4 *versus* 1,9 mg/mL).

Ensaios de permeação cutânea realizados em células de difusão de Franz e com pele humana mostraram que a formulação com maior quantidade de CH (NE4-DAP) proporcionou uma maior retenção da DAP na epiderme, o que também foi confirmado pela detecção de fármaco no fluido receptor ao final do ensaio. A quantidade de DAP retida na pele encontra-se acima da concentração inibitória mínima (CIM = 0,025 μg mL^{-1}) para o *M. leprae* (DHOPLE, 2002), sugerindo que a formulação proposta seria eficaz na hanseníase. Ácidos graxos do CH como hidnocárpico, chaulmúgrico e ácido górlico poderiam atuar como promotores de absorção, justificando a maior atividade das formulações com CH. Eles interagiriam com os lipídios da bicamada da pele, afetando a estrutura do SC e sua fluidez (AUNGST, 1989; MARJUKKA SUHONEN et al., 1999). Análises de FTIR da pele tratada com a formulação que tinha maior quantidade de CH indicaram uma maior perturbação e extração lipídica, corroborando com os achados do estudo de permeação/retenção.

Considerando que a concentração citotóxica de DAP em macrófagos peritoneais murinos é de aproximadamente 350 μg/mL (MORENO et al., 2019), eventos de toxicidade dérmica não seriam observados durante seu transporte através da pele. Por outro lado, constituintes da NE poderiam causar certa citotoxicidade. Uma vez que o CH puro apresentou uma citotoxicidade muito baixa (IC_{50} = 7,861 mg mL^{-1}), NEs com maior concentração de tensoativo (NE2 e NE3) foram consideradas para esse ensaio como estes agentes têm sido

frequentemente associados a problemas de toxicidade. NEs sem CH foram mais citotóxicas; sugerindo que os tensoativos são os principais responsáveis pela citotoxicidade da NE. Outra hipótese é que o CH poderia apresentar um efeito positivo na proliferação celular.

Por esta razão, estudou-se também o efeito do CH puro e nanoencapsulado na migração celular através do ensaio de "strach". Ainda, lesões cutâneas são comuns em pacientes com hanseníase. Após a criação de uma ferida artificial em uma monocamada de células confluentes, avaliou-se o percentual de migração celular para esta região em diferentes intervalos. Tanto o CH livre quanto o encapsulado aumentaram a migração celular para a área artificialmente danificada, o que não foi observado para NE2 (sem CH). Estudo prévio em ratos Wistar já tinha mostrado o efeito deste óleo na colagenação e resistência do tecido cicatricial. Isto foi atribuído à dupla ligação dos ácidos ciclopentênicos que compõe o óleo, os quais atuariam na eliminação de radicais livres (OOMMEN et al., 1999). Oommen (2000) encontrou uma redução significativa no período de epitelização sem contração da ferida após o tratamento com CH (OOMMEN, 2000). Em outro estudo, úlceras foram reduzidas após a administração tópica e oral do extrato de *Hydnocarpus* (planta de onde é extraído o óleo) em camundongos diabéticos. Após duas semanas, não foram encontradas mais lesões (LEE et al., 2010).

Em resumo, a via dérmica se mostrou promissora como alternativa à rota oral para a administração da DAP. Sua associação com CH se torna vantajosa na hanseníase não só pela possibilidade de um sinergismo de ação como também por melhorias no processo de cicatrização (é bem comum se encontrarem lesões cutâneas nestes pacientes). O CH traz também vantagens tecnológicas, tornando as formulações mais estáveis. As nanoemulsões trazem como benefícios a melhoria da solubilidade da DAP e CH, além de uma liberação sustentada. Estudos de atividade *in vivo* devem ser realizados para ajustes da dose que seria utilizada e comprovação dos benefícios aqui sugeridos.

7 CONSIDERAÇÕES FINAIS

-O estudo de diagrama de fase permitiu identificar novas formas cristalinas da DAP tal como o solvato deste fármaco com a MPR;

-Trocas dos agentes solubilizantes (DEEG, PEG e MPR) resultaram em diferenças nas formas cristalinas de DAP, impactando tanto no tamanho do cristal como na proporção de DAP cristalina/dissolvida;

-A FMP resultou em 4x mais DAP dissolvida no gel comparativamente as outras formulações;

-O cocristal de PEG na FDE impactou negativamente na viscosidade do gel;

-Os géis reproduzidos a partir da patente apresentam diferentes perfis de distribuição na pele, sugerindo que as características da superfície dos cristais são críticas para a interação com este sítio de aplicação;

-A técnica de emulsificação espontânea foi efetiva para o preparo de nanoemulsões de DAP;

-O tensoativo Phosal® permitiu obter nanoemulsões com reduzido tamanho de gota, baixa polidispersão e alta carga de superfície;

-Nanoemulsões apresentaram-se estáveis durante 60 dias a 25ºC já que não houve variação no tamanho de partícula, índice de polidispersão, potencial zeta e pH;

-Formulações contendo CH se mostraram mais estáveis no estudo de estabilidade acelerada;

-A formulação com maior quantidade de CH (4%) resultou em maior permeação e retenção da DAP em pele humana abdominal;

-Formulações sem CH foram mais citotóxicas que aquelas que continham este agente;

-A nanoencapsulação não afetou as propriedades do óleo de CH sobre a migração celular.

REFERÊNCIAS

ALHREEZ, M.; WEN, D. Controlled releases of asphaltene inhibitors by nanoemulsions. **Fuel**, v. 234, n. June, p. 538–548, 2018. Elsevier.

ALMEIDA, A. R. DE. **Desenvolvimento e caracterização de formulações larvicidas contendo derivado do ácido cinâmico para o combate ao Aedes aegypti**. 2020.

AUNGST, B. J. Structure/Effect Studies of Fatty Acid Isomers as Skin Penetration Enhancers and Skin Irritants. **Pharmaceutical Research: An Official Journal of the American Association of Pharmaceutical Scientists**, 1989.

BARBEITO-CASTIÑEIRAS, G.; MEJUTO, B.; NIETO, A. C.; et al. Leprosy in the twenty-first century: a microbiological, clinical, and epidemiological study in northwestern Spain. **European Journal of Clinical Microbiology and Infectious Diseases**, 2020. European Journal of Clinical Microbiology & Infectious Diseases.

BARBOSA-FILHO, J. M.; NASCIMENTO JÚNIOR, F. A. DO; ANDRADE TOMAZ, A. C. DE; et al. Natural products with antileprotic activity. **Brazilian Journal of Pharmacognosy**, v. 17, n. 1, p. 141–148, 2007.

BERNADES GOULART, I. M.; LEONEL ARBEX, G.; HUBAIDE CARNEIRO, M.; SCALIA RODRIGUES, M.; GADIA, R. Efeitos adversos da poliquimioterapia em pacientes com hanseníase: Um levantamento de cinco anos em um Centro de Saúde da Universidade Federal de Uberlândia. **Revista da Sociedade Brasileira de Medicina Tropical**, v. 35, n. 5, p. 453–460, 2002.

BLAAK, J.; STAIB, P. The Relation of pH and Skin Cleansing. **Current Problems in Dermatology (Switzerland)**, v. 54, p. 132–142, 2018.

BRASIL. **Guia prático sobre a hanseníase**. 2017.

BRAUN, D. E.; GRIESSER, U. J. Supramolecular Organization of Nonstoichiometric Drug Hydrates: Dapsone. **Frontiers in Chemistry**, v. 6, n. February, p. 1–17, 2018.

CEVC, G.; VIERL, U. Nanotechnology and the transdermal route. A state of the art review and critical appraisal. **Journal of Controlled Release**, v. 141, n. 3, p. 277–299, 2010. Elsevier B.V.

CHAVES, L. L.; VIEIRA, A. C. C.; FERREIRA, D.; SARMENTO, B.; REIS, S. Rational and precise development of amorphous polymeric systems with dapsone by response surface methodology. **International Journal of Biological Macromolecules**, v. 81, p. 662–671, 2015. Elsevier B.V.

CLARES, B.; CALPENA, A. C.; PARRA, A.; et al. Nanoemulsions (NEs), liposomes (LPs) and solid lipid nanoparticles (SLNs) for retinyl palmitate: effect on skin permeation. **International journal of pharmaceutics**, v. 473, n. 1–2, p. 591–598, 2014. Elsevier B.V.

COTTE, M.; DUMAS, P.; BESNARD, M.; TCHORELOFF, P.; WALTER, P. Synchrotron FT-IR microscopic study of chemical enhancers in transdermal drug delivery: Example of fatty acids. **Journal of Controlled Release**, v. 97, n. 2, p. 269–281, 2004.

DANAEI, M.; DEHGHANKHOLD, M.; ATAEI, S.; et al. Impact of particle size and polydispersity index on the clinical applications of lipidic nanocarrier systems. **Pharmaceutics**, v. 10, n. 2, p. 1–17, 2018.

DESAI, J.; THAKKAR, H. Enhanced oral bioavailability and brain uptake of Darunavir using lipid nanoemulsion formulation. **Colloids and Surfaces B: Biointerfaces**, v. 175, n. August 2018, p. 143–149, 2019. Elsevier.

DESIKAN, K. V. Multi-drug regimen in leprosy and its impact on prevalence of the disease. **Medical Journal Armed Forces India**, v. 59, n. 1, p. 2–4, 2003. Director General, Armed Forces Medical Services.

DHOPLE, A. M. In vivo activity of epiroprim, a dihydrofolate reductase inhibitor, singly and in combination with dapsone, against Mycobacterium leprae. **International Journal of Antimicrobial Agents**, v. 19, n. 1, p. 71–74, 2002.

ELMOWAFY, M.; SHALABY, K.; ALI, H. M.; et al. Impact of nanostructured lipid carriers on dapsone delivery to the skin: in vitro and in vivo studies. **International Journal of Pharmaceutics**, v. 572, n. May, p. 118781, 2019. Elsevier.

FREDERIKSEN, K.; GUY, R. H.; PETERSSON, K. Formulation considerations in the design of topical, polymeric film-forming systems for sustained drug delivery to the skin. **European Journal of Pharmaceutics and Biopharmaceutics**, v. 91, p. 9–15, 2015. Elsevier B.V.

GARIDEL, P. Mid-FTIR-microspectroscopy of stratum corneum single cells and stratum corneum tissue. **Physical Chemistry Chemical Physics**, v. 4, n. 22, p. 5671–5677, 2002.

ILDIZ, G. O.; AKYUZ, S. Conformational analysis and vibrational spectroscopic studies on dapsone. **Optics and Spectroscopy (English translation of Optika i Spektroskopiya)**, v. 113, n. 5, p. 495–504, 2012.

JACOBSEN, P. L.; LEVY, L. Mechanism by which hydnocarpic acid inhibits mycobacterial multiplication. **Antimicrobial agents and chemotherapy**, v. 3, n. 3, p. 373–379, 1973.

KAR, H. K.; GUPTA, R. Treatment of leprosy. **Clinics in Dermatology**, v. 33, n. 1, p. 55–65, 2015. Elsevier Inc.

LAMBERS, H.; PIESSENS, S.; BLOEM, A.; PRONK, H.; FINKEL, P. Natural skin surface pH is on average below 5, which is beneficial for its resident flora. **International Journal of Cosmetic Science**, v. 28, n. 5, p. 359–370, 2006.

LEE, G. S.; CHOI, J. Y.; CHOI, Y. J.; et al. The wound healing effect of hydnocarpi semen extract on ulcer in diabetic mice. **Biomolecules and Therapeutics**, v. 18, n. 3, p. 329–335, 2010.

Leprosy (Hansen's disease). .Disponível em: <https://www.who.int/news-room/fact-sheets/detail/leprosy>. Acesso em: 26/7/2021.

LEVY, L. The activity of chaulmoogra acids against Mycobacterium leprae. **Amer.Rev.Resp.Dis.**, v. 111, n. 5, p. 703–705, 1975.

LIPOID. Botanical Actives , Botanical We make beauty natural . .

MÁQUINA, A.; CATARINO, A.; SILVA, L.; et al. Lepra: Da Antiguidade aos Nossos Tempos. **Journal of the Portuguese Society of Dermatology and Venereology**, v. 77, n. 4, p. 323–338, 2020.

MARJUKKA SUHONEN, T.; A. BOUWSTRA, J.; URTTI, A. Chemical enhancement of percutaneous absorption in relation to stratum corneum structural alterations. **Journal of Controlled Release**, v. 59, n. 2, p. 149–161, 1999.

MOLINELLI, E.; PAOLINELLI, M.; CAMPANATI, A.; BRISIGOTTI, V.; OFFIDANI, A. Metabolic, pharmacokinetic, and toxicological issues surrounding dapsone. **Expert Opinion on Drug Metabolism & Toxicology**, v. 15, n. 5, p. 367–379, 2019.

MONTEIRO, L. M.; LIONE, V. F.; CARMO, F. A. DO; et al. Development and characterization of a new oral dapsone nanoemulsion system: Permeability and in silico bioavailability studies. **International Journal of Nanomedicine**, v. 7, p. 5175–5182, 2012.

MORENO, E.; CALVO, A.; SCHWARTZ, J.; et al. Evaluation of skin permeation and retention of topical dapsone in murine cutaneous leishmaniasis lesions. **Pharmaceutics**, v. 11, n. 11, 2019.

NORTON, S. A. Useful plants of dermatology. I. Hydnocarpus and chaulmoogra. **Journal of the American Academy of Dermatology**, v. 31, n. 4, p. 683–686, 1994. American Academy of Dermatology, Inc.

OLIVEIRA, F. R.; PESSOA, M. C.; ALBUQUERQUE, R. F. V.; SCHALCHER, T. R.; MONTEIRO, M. C. Clinical applications and methemoglobinemia induced by dapsone. **Journal of the Brazilian Chemical Society**, v. 25, n. 10, p. 1770–1779, 2014.

OMS. Chagas disease (American trypanosomiasis) Epidemiology. .

OOMMEN, S. T. The effect of oil of hydnocarpus on excision wounds [4]. **International Journal of Leprosy and Other Mycobacterial Diseases**, v. 68, n. 1, p. 69–70, 2000.

OOMMEN, S. T.; RAO, M.; RAJU, C. V. N. Effect of oil of hydnocarpus on wound healing. **International Journal of Leprosy and Other Mycobacterial Diseases**, v. 67, n. 2, p. 154–158, 1999.

OSBORNE, D. W. **Compositions and methods for topical applications of theraputic agents.** Depositante: ViroTex Corporation. MU: 5863560. Depósito: 26 jan, 1999.

OSBORNE, D. W. **Compositions and methods for topical applications of theraputic agents.** Depositante: ViroTex Corporation. MU: 6060085. Depósito: 9 mai, 2000.

OSBORNE, D. W. **Topical dapsone for the treatment of acne**. Depositante: Allergan, INC., US. Agente: Gowling Lafleur Henderson LLP. MU: 2776702. Depósito: 18 mar, 2002. Concessão: 02 set, 2014.

PANCHAGNULA, R.; SALVE, P. S.; THOMAS, N. S.; JAIN, A. K.; RAMARAO, P. Transdermal delivery of naloxone: Effect of water, propylene glycol, ethanol and their binary combinations on permeation through rat skin. **International Journal of Pharmaceutics**, v. 219, n. 1–2, p. 95–105, 2001.

PANDEY, P.; GULATI, N.; MAKHIJA, M.; PUROHIT, D.; DUREJA, H. Nanoemulsion: A Novel Drug Delivery Approach for Enhancement of Bioavailability. **Recent Patents on Nanotechnology**, v. 14, n. 4, p. 276–293, 2020.

PARASCANDOLA, J. Chaulmoogra oil and the treatment of leprosy. **Pharmacy in history**, 2003.

PATEL, V.; SHARMA, O. P.; MEHTA, T. Nanocrystal: a novel approach to overcome skin barriers for improved topical drug delivery. **Expert Opinion on Drug Delivery**, v. 15, n. 4, p. 351–368, 2018. Taylor & Francis.

PEREIRA, R. L.; LEITES, F. I.; PAESE, K.; et al. Hydrogel containing adapalene- and dapsone-loaded lipid-core nanocapsules for cutaneous application: development, characterization, in vitro irritation and permeation studies. **Drug Development and Industrial Pharmacy**, v. 42, n. 12, p. 2001–2008, 2016.

POSSOLO, H. O Óleo De Chaulmugra Na Farmacopeia Brasileira Helena. , 1898.

PUGLIA, C.; BONINA, F. Lipid nanoparticles as novel delivery systems for cosmetics and dermal pharmaceuticals. **Expert Opinion on Drug Delivery**, v. 9, n. 4, p. 429–441, 2012.

SAHOO, M. R.; DHANABAL, S. P.; JADHAV, A. N.; et al. Hydnocarpus: An ethnopharmacological, phytochemical and pharmacological review. **Journal of Ethnopharmacology**, v. 154, n. 1, p. 17–25, 2014.

SALIM, N.; AHMAD, N.; MUSA, S. H.; et al. Nanoemulsion as a topical delivery system of antipsoriatic drugs. **RSC Advances**, v. 6, n. 8, p. 6234–6250, 2016. Royal Society of Chemistry.

SANTOS, F. S. D. DOS; SOUZA, L. P. A. DE; SIANI, A. C. Chaulmoogra oil as scientific knowledge: the construction of a treatment for leprosy. **Hist Cienc Saude-Manguinhos**, v. 15, n. March 2006, p. 29–47, 2008.

SANTOS, T. M. N. DOS. **Extração e purificação dos ciclopentênicos presentes nas amêndoas de Carpatroche brasiliensis Endl**, 2019. Jequié: UESB.

SCHMID-WENDTNER, M. H.; KORTING, H. C. The pH of the skin surface and its impact on the barrier function. **Skin Pharmacology and Physiology**, v. 19, n. 6, p. 296–302, 2006.

SHAKEEL, F.; BABOOTA, S.; AHUJA, A.; ALI, J.; SHAFIQ, S. Skin permeation mechanism of aceclofenac using novel nanoemulsion formulation. **Pharmazie**, v. 63, n. 8, p. 580–584, 2008.

SINGH, Y.; MEHER, J. G.; RAVAL, K.; et al. Nanoemulsion: Concepts, development and applications in drug delivery. **Journal of Controlled Release**, v. 252, p. 28–49, 2017. Elsevier B.V.

SONG, S. P.; LV, C. Z.; FEINGOLD, K. R.; et al. Abnormalities in stratum corneum function in patients recovered from leprosy. **Skin Pharmacology and Physiology**, v. 22, n. 3, p. 131–136, 2009.

UASKA SARTORI, P. V.; PENNA, G. O.; BÜHRER-SÉKULA, S.; et al. Human Genetic Susceptibility of Leprosy Recurrence. **Scientific Reports**, v. 10, n. 1, p. 1–5, 2020.

VASHISTH, I.; AHAD, A.; AQIL, M.; AGARWAL, S. P. Investigating the potential of essential oils as penetration enhancer for transdermal losartan delivery: Effectiveness and mechanism of action. **Asian**

Journal of Pharmaceutical Sciences, v. 9, n. 5, p. 260–267, 2014. Elsevier Ltd.

VICHAI, V.; KIRTIKARA, K. Sulforhodamine B colorimetric assay for cytotoxicity screening. **Nature Protocols**, v. 1, n. 3, p. 1112–1116, 2006.

WHO. Leprosy elimination. Disponível em: <https://www.who.int/news-room/fact-sheets/detail/leprosy>. .

WONG, T. W. Electrical, magnetic, photomechanical and cavitational waves to overcome skin barrier for transdermal drug delivery. **Journal of Controlled Release**, v. 193, p. 257–269, 2014. Elsevier B.V.

YOSIPOVITCH, G.; XIONG, G. L.; HAUS, E.; et al. Time-dependent variations of the skin barrier function in humans: Transepidermal water loss, stratum corneum hydration, skin surface pH, and skin temperature. **Journal of Investigative Dermatology**, v. 110, n. 1, p. 20–23, 1998. Elsevier Masson SAS.

ZHU, Y. I.; STILLER, M. J. Dapsone and sulfones in dermatology: Overview and update. **Journal of the American Academy of Dermatology**, v. 45, n. 3, p. 420–434, 2001.

APÊNDICE

Este apêndice é destinado ao material suplementar do artigo do capítulo II: The effect of vehicle composition on the preparation of different types of dapsone crystals for topical drug delivery

THE EFFECT OF VEHICLE COMPOSITION ON THE PREPARATION OF DIFFERENT TYPES OF DAPSONE CRYSTALS FOR TOPICAL DRUG DELIVERY

Bianca da Costa Bernardo Port,[a] Gabriela Schneider-Rauber,[a] Debora Fretes Argenta,[a] Mihails Arhangelskis,[b] Carlos Eduardo Maduro de Campos,[c] Adailton João Bortoluzzi,[d] Thiago Caon[a]**

[a] Postgraduate Program in Pharmacy (PGFAR); [c] Department of Physics; [d] Department of Chemistry; Federal University of Santa Catarina, Trindade, Florianopolis, 88040-900, Brazil

[b] Faculty of Chemistry, University of Warsaw, 1 Pasteura Street, Warsaw, 02-093, Poland

*Corresponding authors: gabisrauber@gmail.com; caon.thiago@ufsc.br

Table of Contents

Additional Characterization Methods

1.1 Methods

1.1.1 Differential scanning calorimetry (DSC)

Differential scanning calorimetry (DSC) measurements were performed using the DSC-60 (Shimadzu, Kyoto, Japan) in a temperature range of 30-200 °C. Samples were weighed, sealed (non-hermetically) in an aluminum crucible and thermal properties were monitored at a heating rate of 10 °C min^{-1} under a nitrogen atmosphere.

1.1.2 Thermogravimetric analysis (TGA)

Thermogravimetric analyses were performed in a TGA-50 equipment (Shimadzu, Kyoto, Japan). Approximately 15 mg of each sample was weighed and placed in platinum pans. The thermograms were recorded in the range of 25–600 °C, with a heating rate of 10 °C min^{-1}, under a nitrogen atmosphere.

1.1.3 Hot stage microscopy (HSM)

For hot-stage microscopic (HSM) investigations, an Olympus BX50 microscope equipped with a Mettler Toledo FP-82 hot-stage (Ohio, USA) was used. Photographs were collected with an Olympus DP7 digital camera (Olympus, Tokyo, Japan).

1.1.4 ATR-FT-IR spectroscopy

The spectra were obtained in a FT-IR/NIR Frontier spectrometer (PerkinElmer, Waltham, USA). Samples were placed directly to the ATR sample holder. The FT-IR spectra were recorded at room temperature from 600 to 4000 cm^{-1}, with a resolution of 4 cm^{-1}.

1.1.5 Single crystal X-ray diffraction

The X-ray diffraction analysis was carried out on a Bruker APEX II DUO diffractometer using radiation generated by a molybdenum sealed tube (MoKα λ = 0.71073 Å) and graphite monochromator. During analyses the sample were sustained at 150 K. The crystal structure was

solved by dual space with SHELXT and refined by the least squares method with full matrix with SHELXL-2018. ORTEP plot was generated with PLATON software. Full crystallographic tables (including structure factors) have been deposited with the Cambridge Crystallographic Data Centre as supplementary publication number CCDC-2129304. These data can be obtained free of charge from the Cambridge Crystallographic Data Centre at **www.ccdc.cam.ac.uk.**

2 CHARACTERIZATION OF DAPSONE USED AS RAW PRODUCT

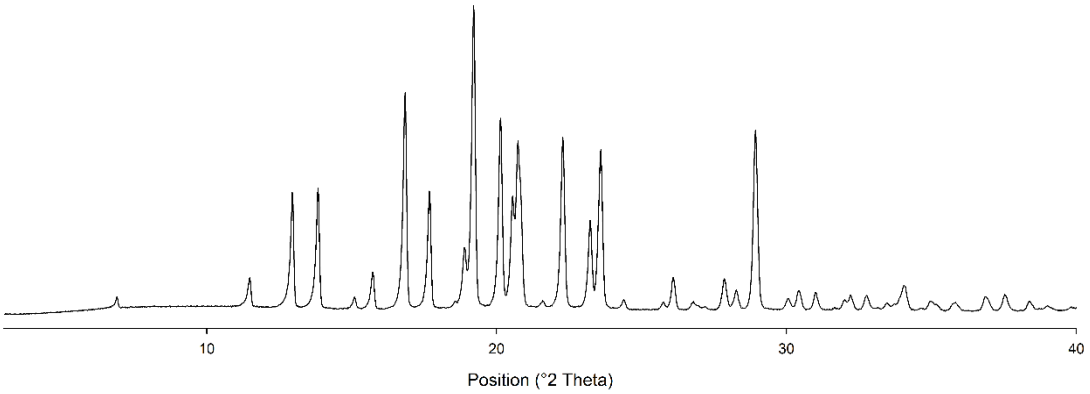

Supplementary Figure S1. PXRD pattern of dapsone raw product (characteristic of Form III; DAPSUO13[30]).

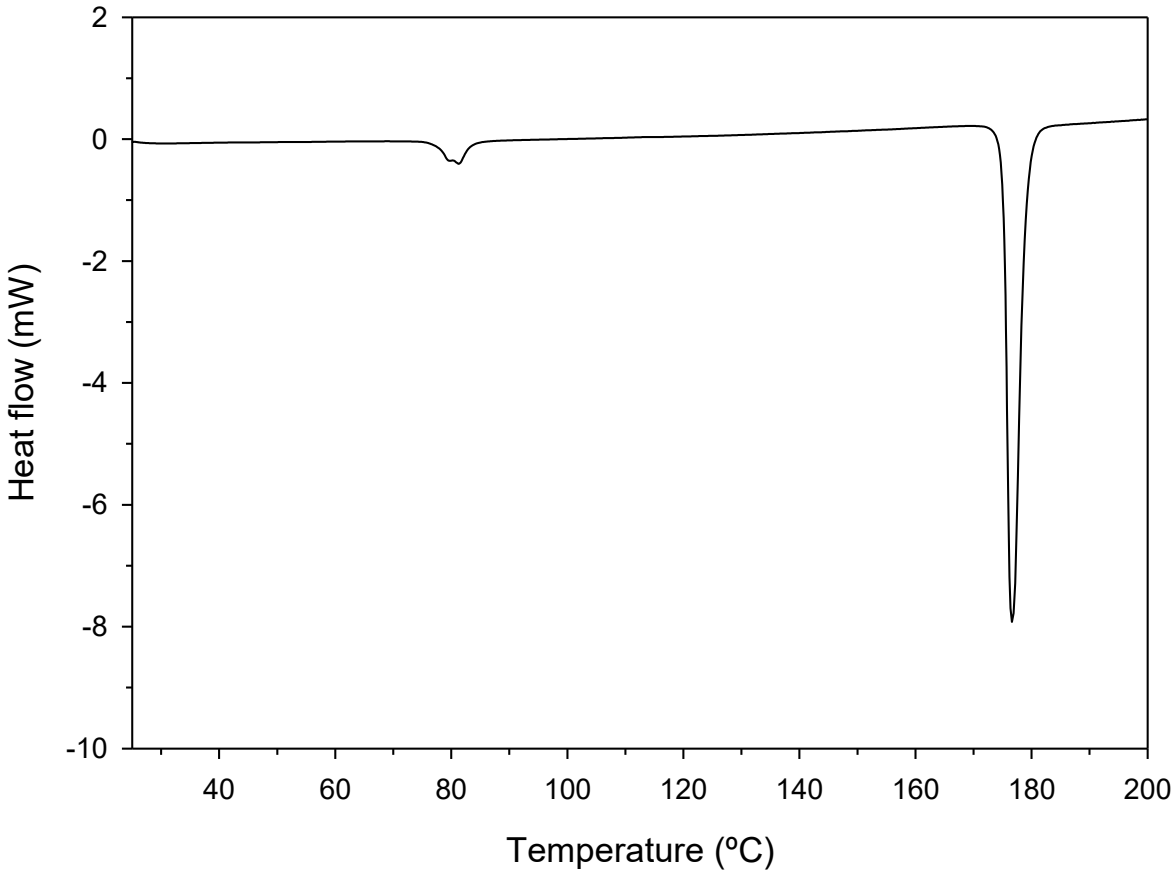

Supplementary Figure S2. DSC curve of dapsone (raw material). The small endothermic event in about 80 °C corresponds to the well-known conversion of Form III to Form II [29]. Form II melts at T_{peak}= 176,63 °C (T_{onset}= 174,09 °C, ΔH= -7,92 J/g) [3].

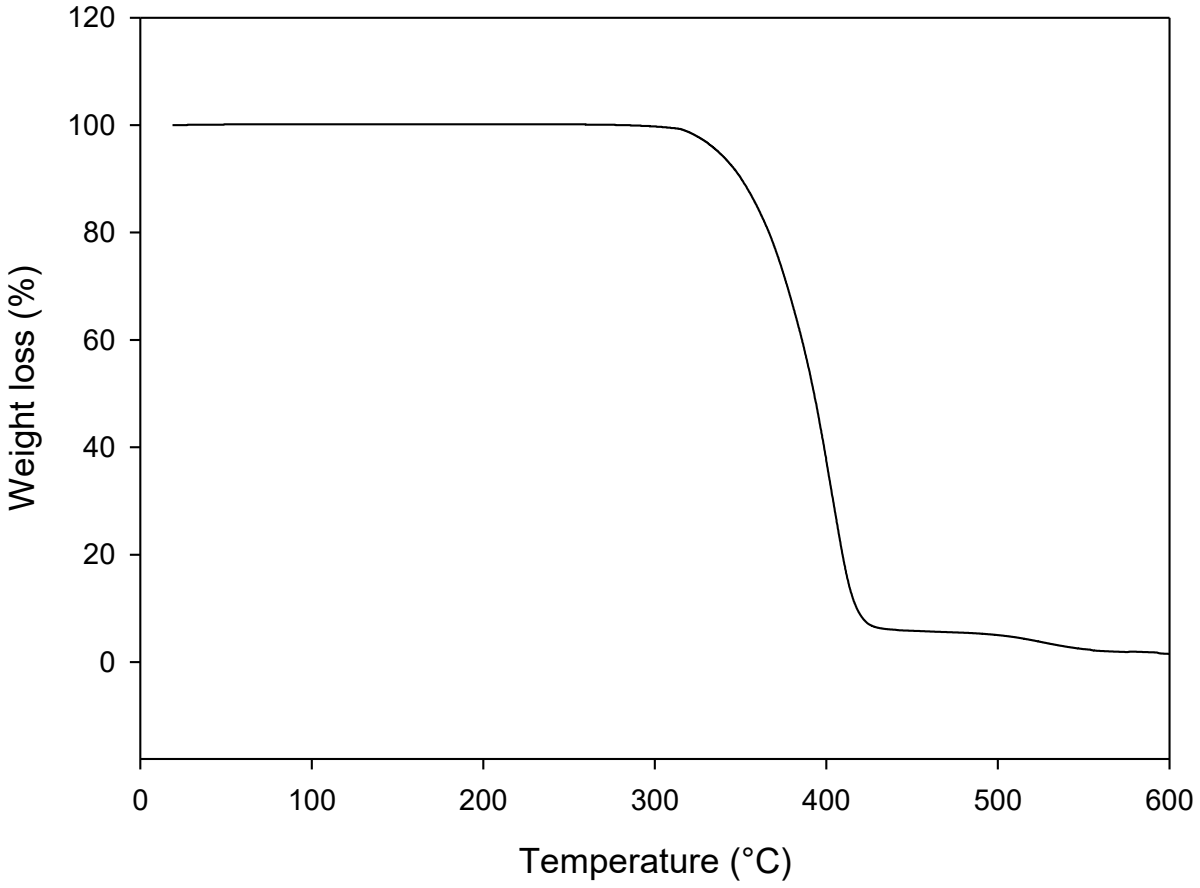

Supplementary Figure S3. TGA curve of dapsone showing no weight loss below melting.

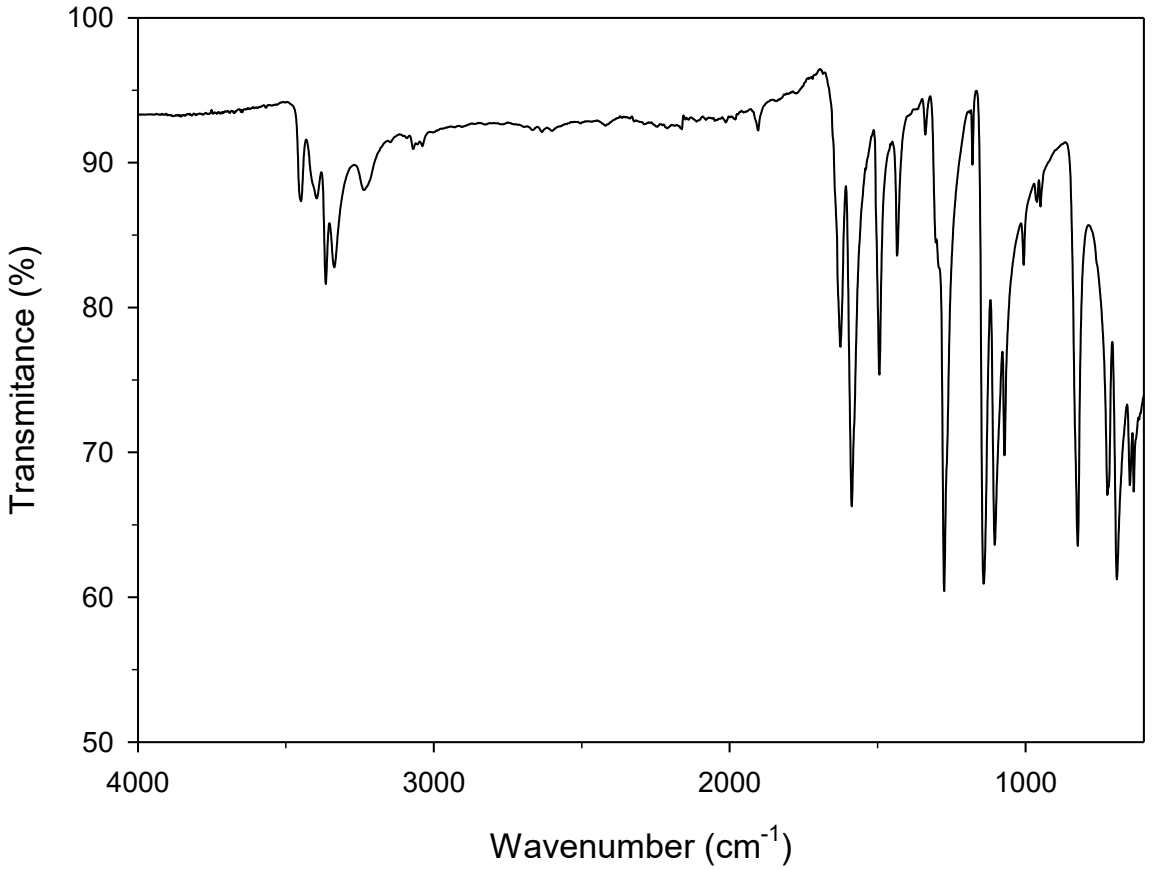

Supplementary Figure S4. Infrared spectrum of dapsone (raw material).

1 CRYSTAL DATA

Supplementary Table S1 – Crystallographic data of dapsone crystal forms discussed in this study.

Crystal form	DAP FORM III	3DAP·H_2O	DAP·PEG	DAP·MPR*
Formula	($C_{12}H_{12}N_2O_2S$)	($C_{12}H_{12}N_2O_2S$)$_3$ (H_2O)	($C_{12}H_{12}N_2O_2S$) ($C_8H_{16}O_4$)$_n$	($C_{12}H_{12}N_2O_2S$) (C_5H_9NO)
MW/g.mol^{-1}	248.30	762.90	424.50	347.44
T/K	343	120	100	RT
Crystal system	Orthorhombic	Monoclinic	Orthorhombic	Monoclinic
Space group	$P2_12_12_1$	$C2/c$	$Pbca$	$P2_1/n$
a/Å	8.0652(8)	48.5832(9)	20.0328(6)	6.2152(2)
b/Å	25.550(2)	11.4183(2)	13.6815(5)	12.8023(4)
c/Å	5.7886(5)	13.0035(2)	15.4710(5)	21.3333(7)
α/º	90	90	90	90
β/º	90	92.2789(10)	90	95.867(1)
γ/º	90	90	90	90
V/Å^3	1192.83	7207.82	4240.27	1688.57
Z/Z’	4/1	24/3	8/1	4/1
ρ/g.cm^{-3}	1.383	1.406	1.33	
R-factor/%	4.32	4.89	6.2	
CSD refcode	DAPSUO13	ANSFON02	YIPMIW	-
Reference	Braun *et al.* (2017)[1]	Yathirajan *et al.* (2004)[4]	Chappa *et al.* (2018)[5]	This work

* Structurally related to the tetrahydrofuran solvate, CSD refcode HASSEB (P21/n, a=5.8587 (3), b=12.6787 (7), c=21.8078 (12), β= 91.3350 (10)) [6].

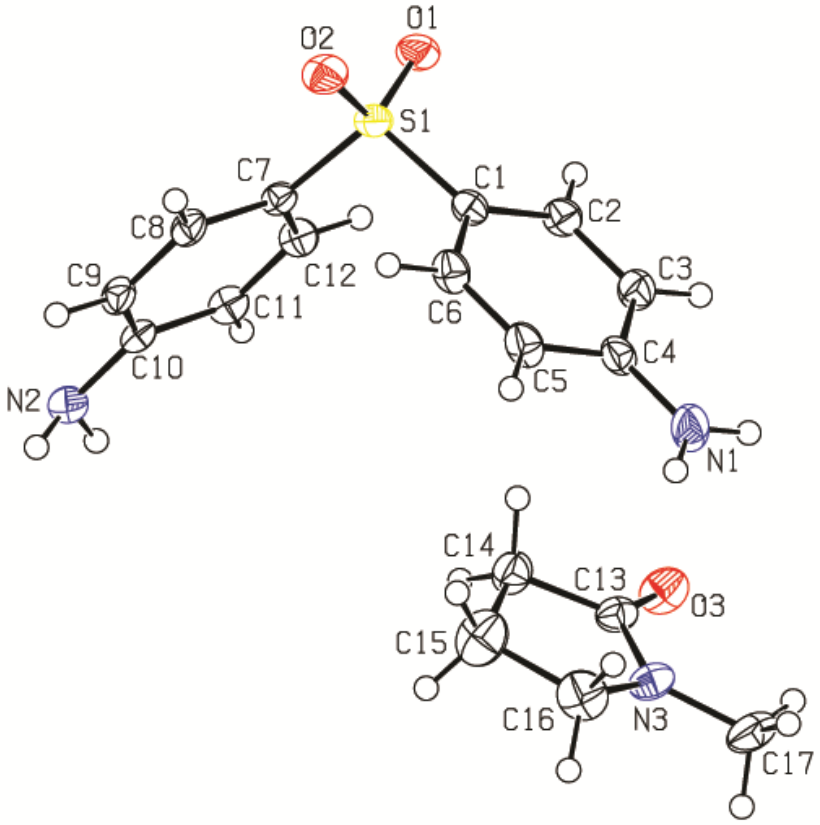

Supplementary Figure S5. ORTEP diagram of the single crystal structure of dapsone·1-methyl-2-pyrrolidone as determined by X-ray crystallography.

4 X-RAY DIFFRACTION PATTERNS USED AS REFERENCE

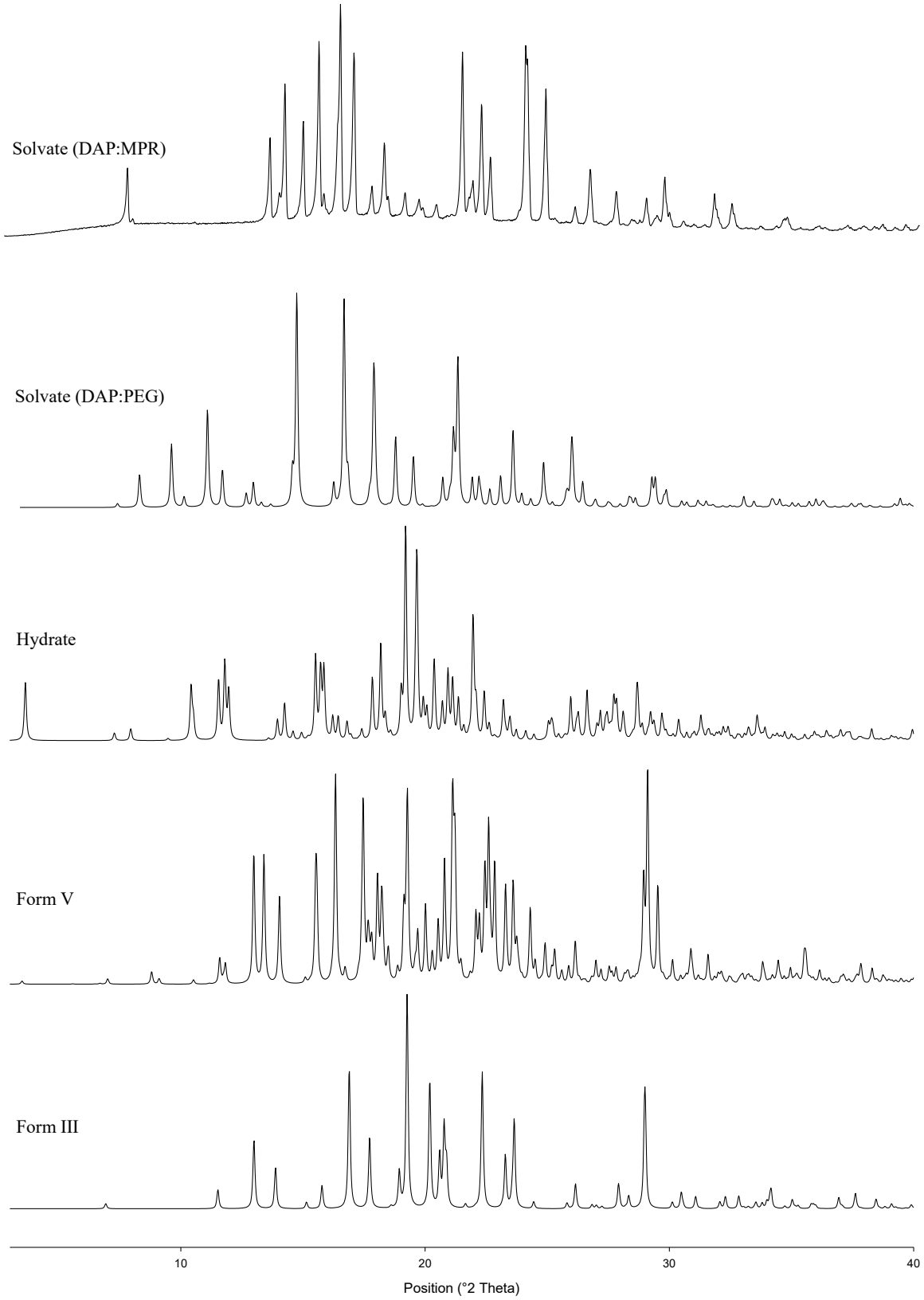

Supplementary Figure S6. PXRD patterns of the crystal forms of dapsone described in Table S1.

5 ADDITIONAL CHARACTERIZATION OF THE NEW DAPSONE·1-METHYL-2-PYRROLIDONE SOLVATE

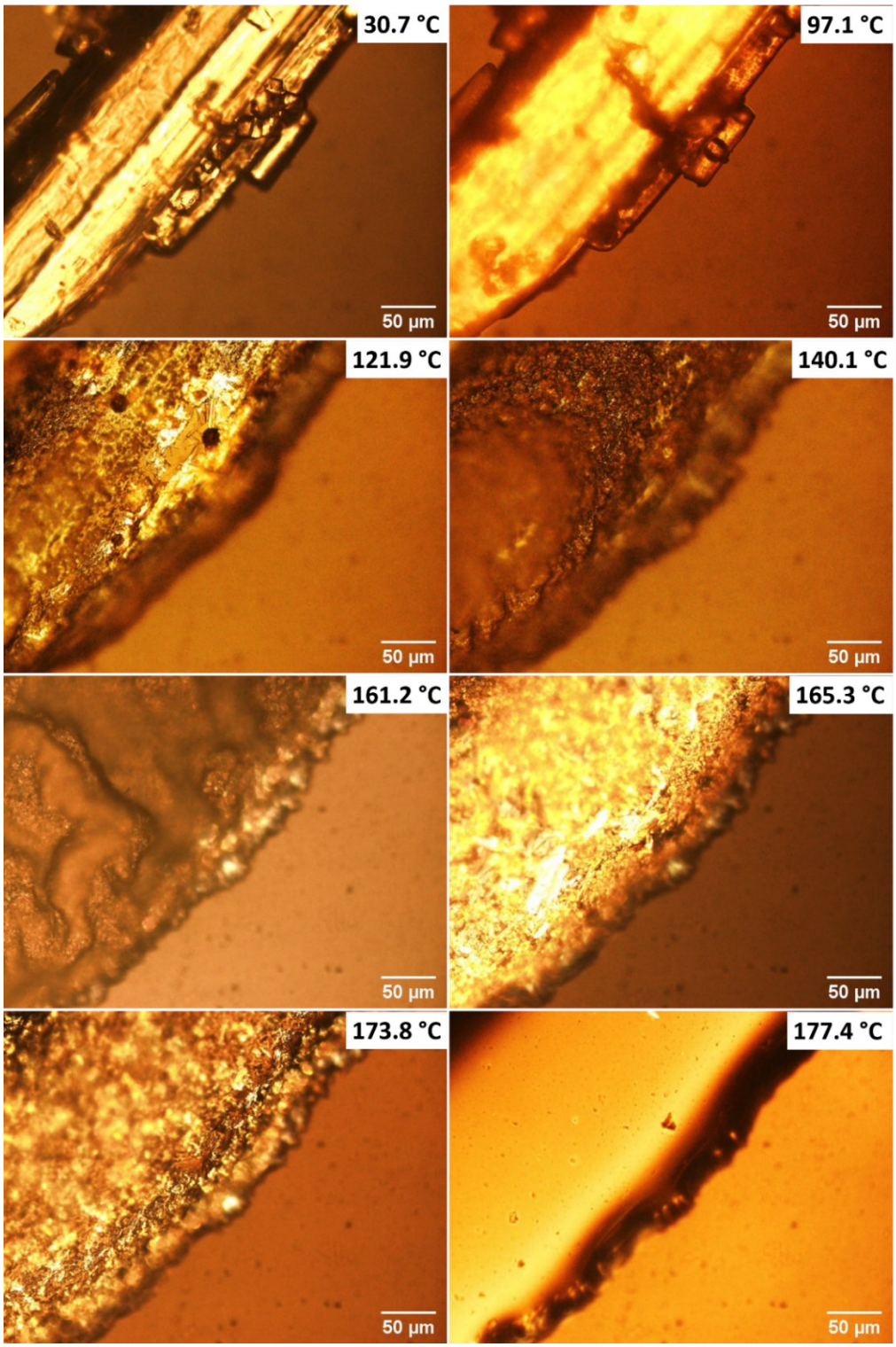

Supplementary Figure S7. Optical micrographs of the new crystal form of dapsone·1-methyl-2-pyrrolidone at different temperatures under polarized light (heating rate of 10 $^{o}C.min^{-1}$).

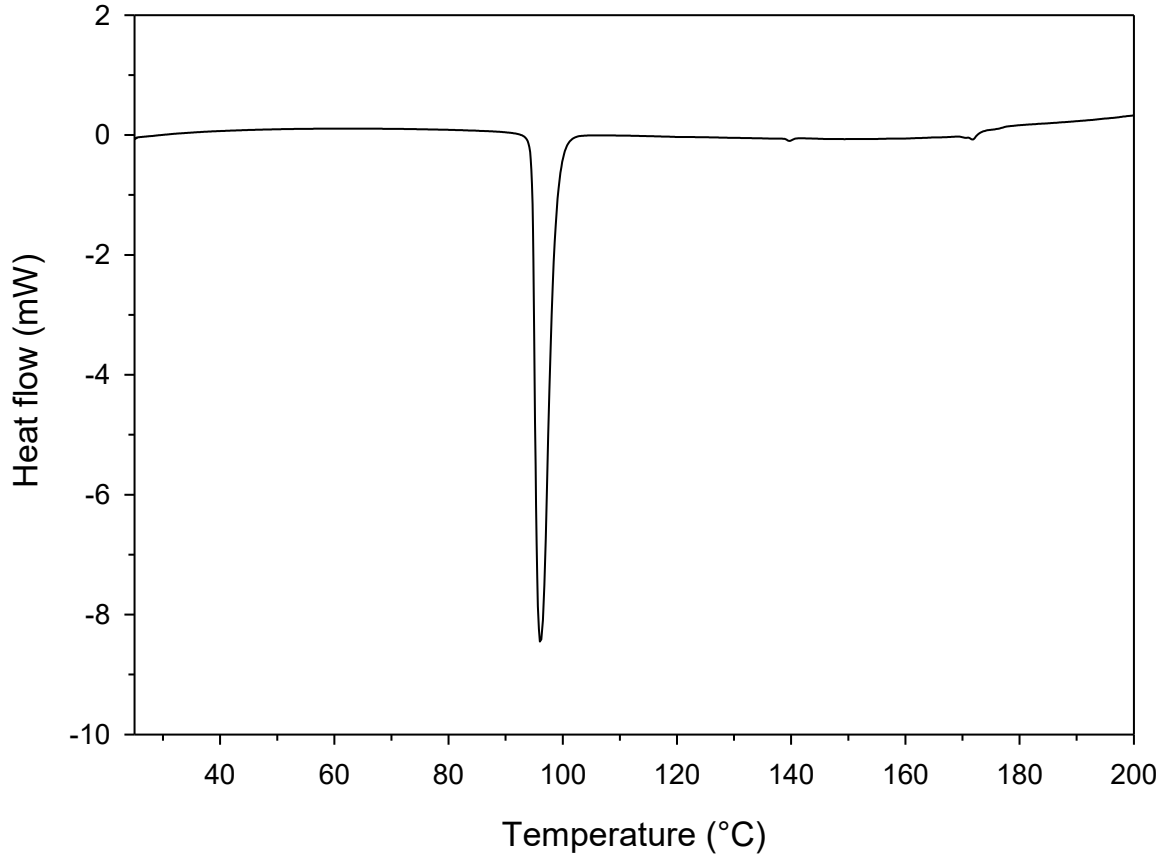

Supplementary Figure S8. DSC curve of the 1-methyl-2-pyrrolidone.solvate of dapsone showing one single event of desolvation/peritectic formation (T_{peak}= 96.01 °C; T_{onset}= 92.83 °C, ΔH= -8.45 J/g). Heating rate of 10 °C.min^{-1}, non-hermetically closed pan, N_2 atmosphere.

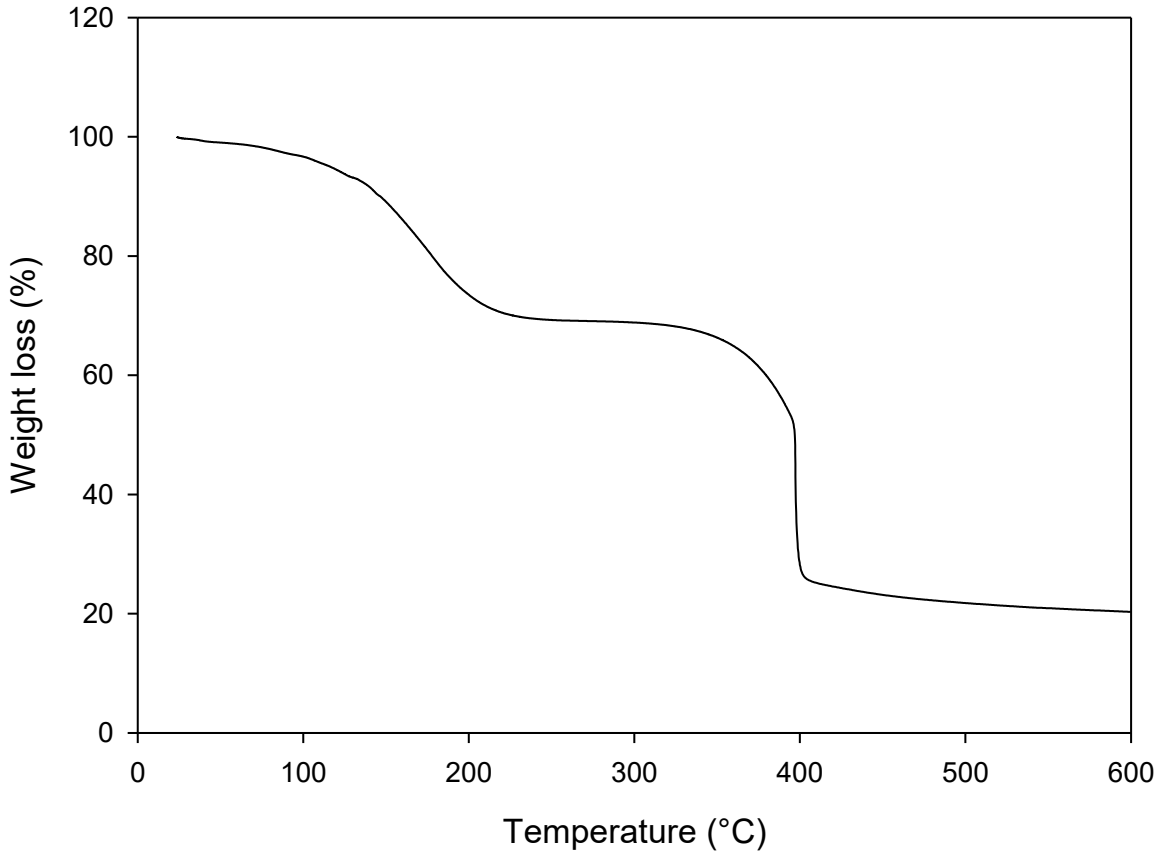

Supplementary Figure S9. TGA curve of the 1-methyl-2-pyrrolidone solvate of dapsone showing one main event of weight loss bellow 300 °C, which corresponds to 30.8 wt% of the initial sample. The theoretical weight loss related to the release of 1-methyl-2-pyrrolidone from the lattice is 28.5 wt%.

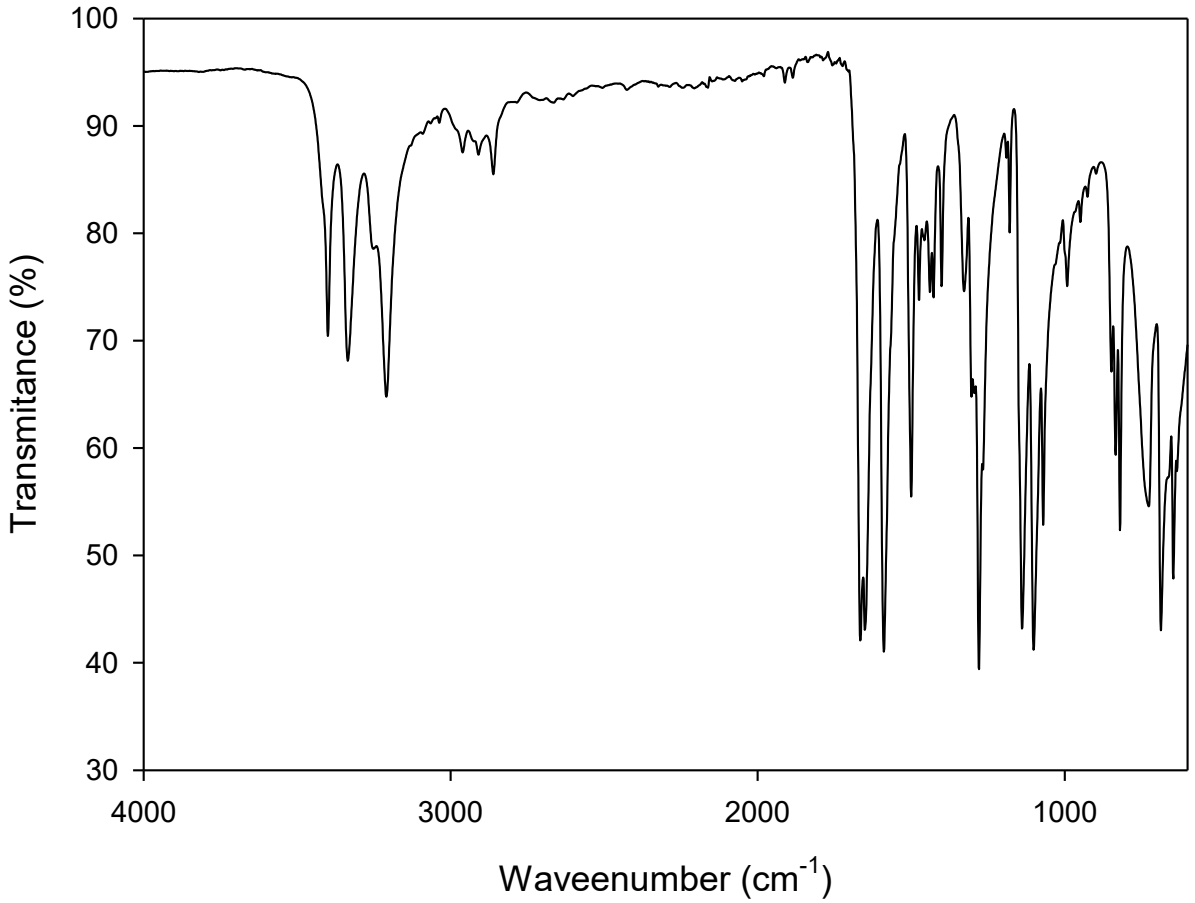

Supplementary Figure S10. Infrared spectrum of the new crystal form of dapsone·1-methyl-2-pyrrolidone.

Supplementary Table S2 - Comparison of infrared peaks present in form III with those of the solvate with 1-methyl-2-pyrrolidone.

	Form III	**MPR Solvate**
N-H stretch (amine)	3449	3400
N-H stretch (amide)	-	3335
C-H stretch (aromatic)	3336	3209
C=O stretch	-	1666
C=C stretch (aromatic)	1587/1494	1589/1500
C-N stretch	1275	1279
SO2	1141/1104	1139/1101
C=O bend	-	726
C-S	691	687

6 ADDITIONAL ANALYSES OF THE STUDIES DIAGRAM

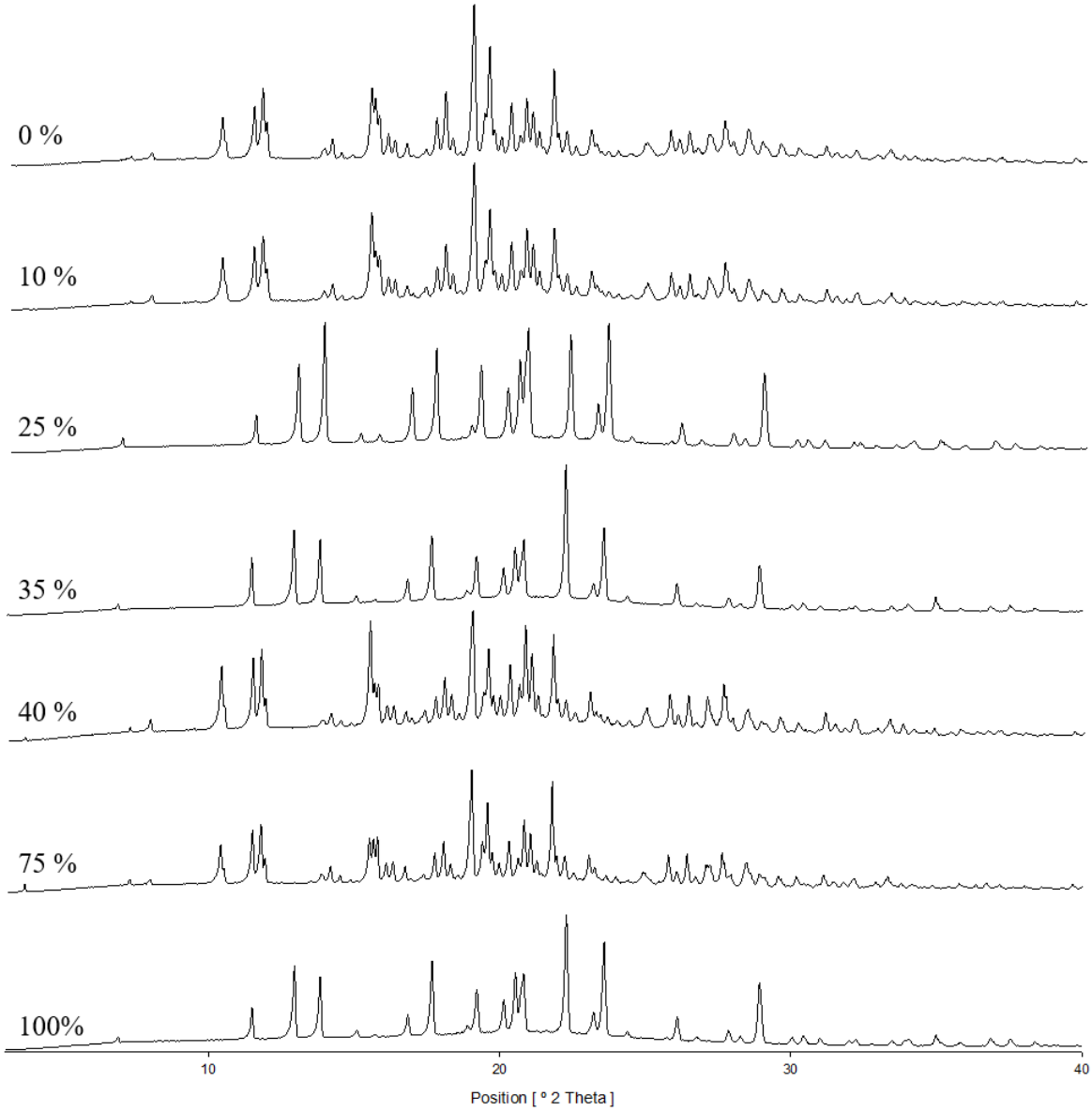

Supplementary Figure S11. X-ray diffractograms of each point on the phase diagram of the system DEGEE:water.

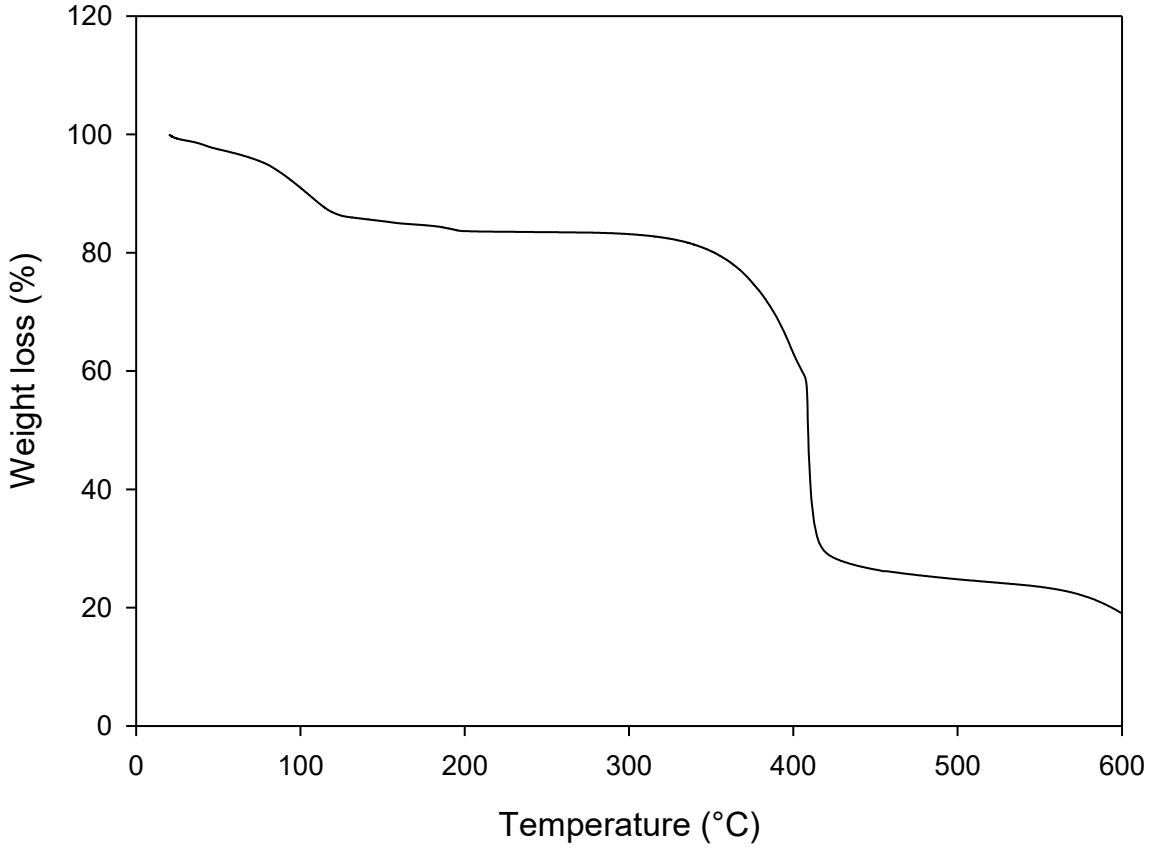

Supplementary Figure S12. TGA curve of the 40% DEGEE point of the phase diagram showing weight loss around 100°C indicating the presence of the hydrate at this point (and not the dehydrate). This is in agreement with the PXRD in Figure S11.

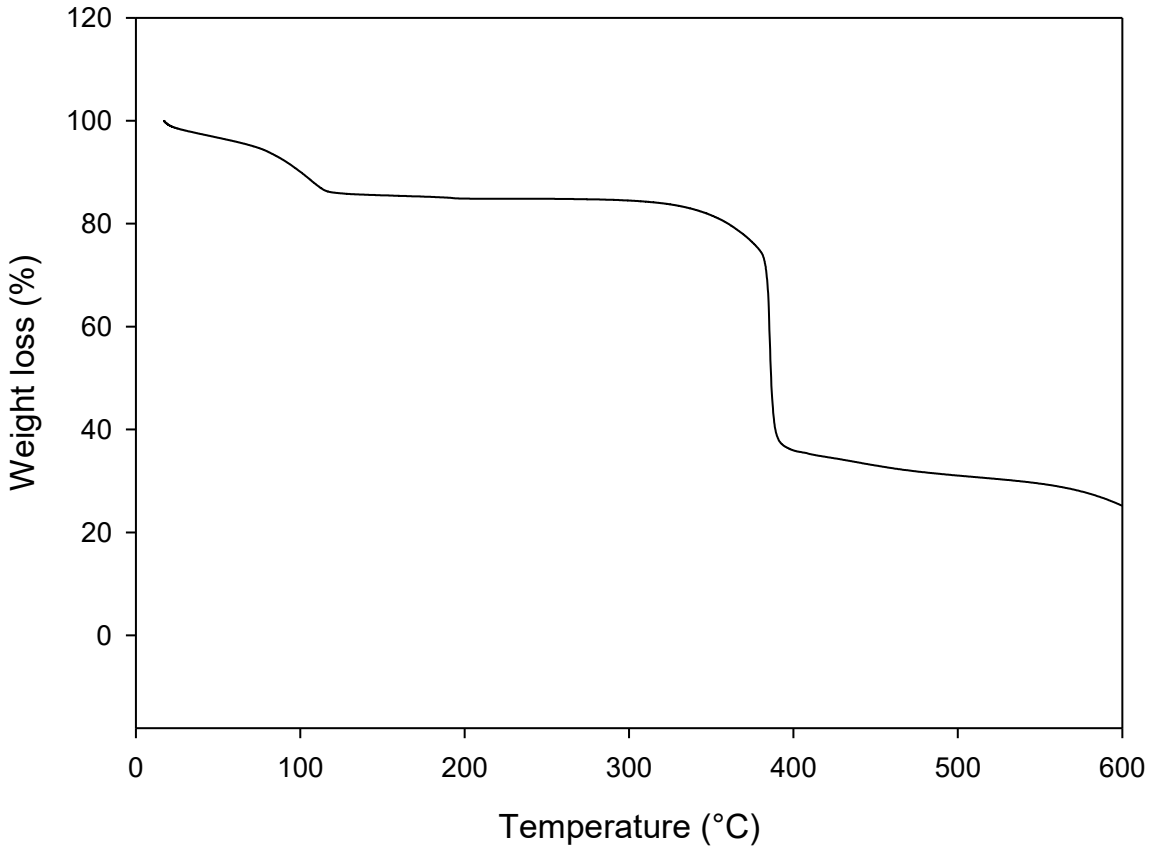

Supplementary Figure S13. TGA curve of the 75% DEGEE point of the phase diagram showing weight loss around 100°C indicating the presence of hydrate at this point (and not the dehydrate). This is in agreement with the PXRD in Figure S11.

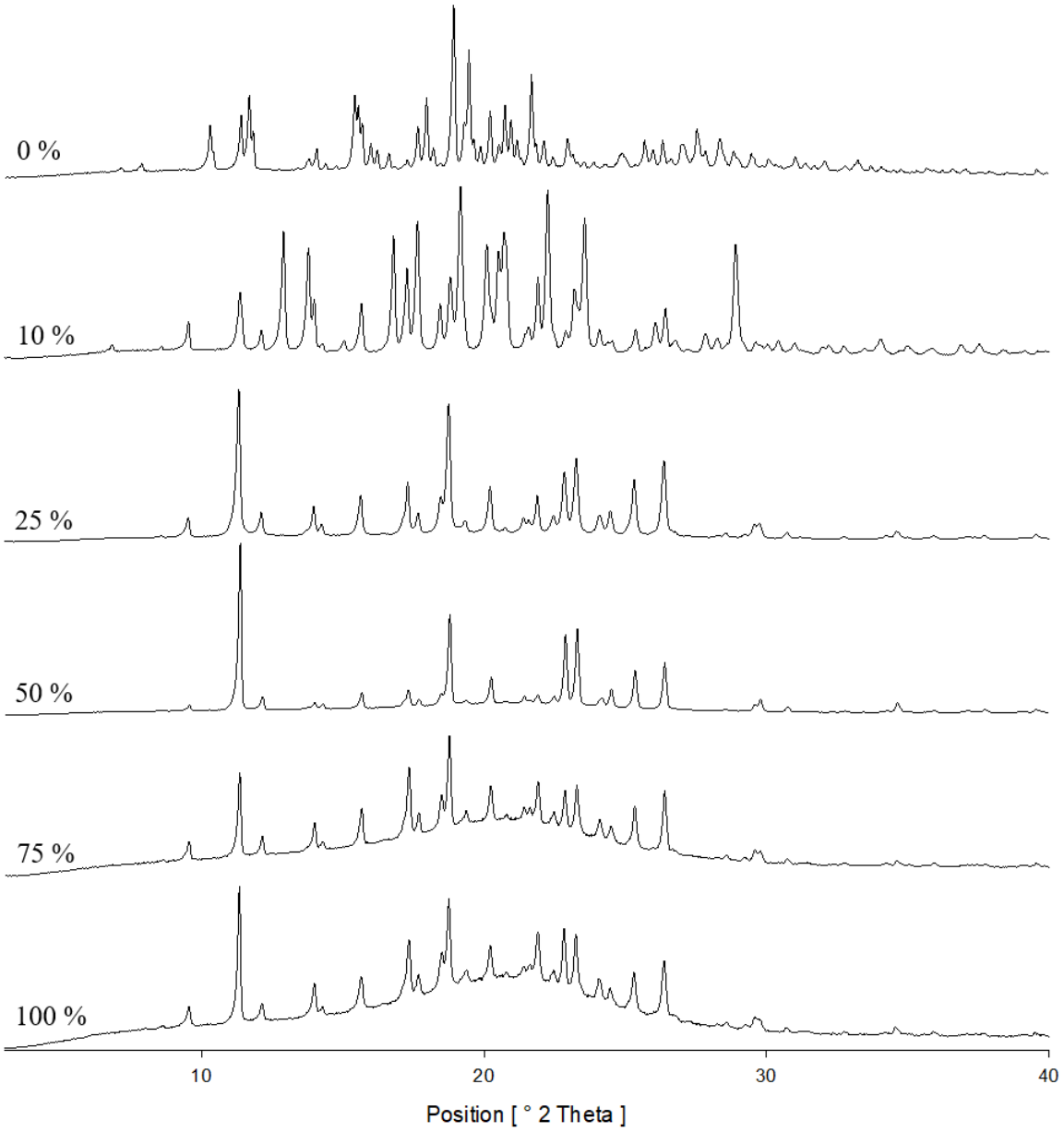

Supplementary Figure S14. X-ray diffractograms of each point on the phase diagram of the system PEG:water.

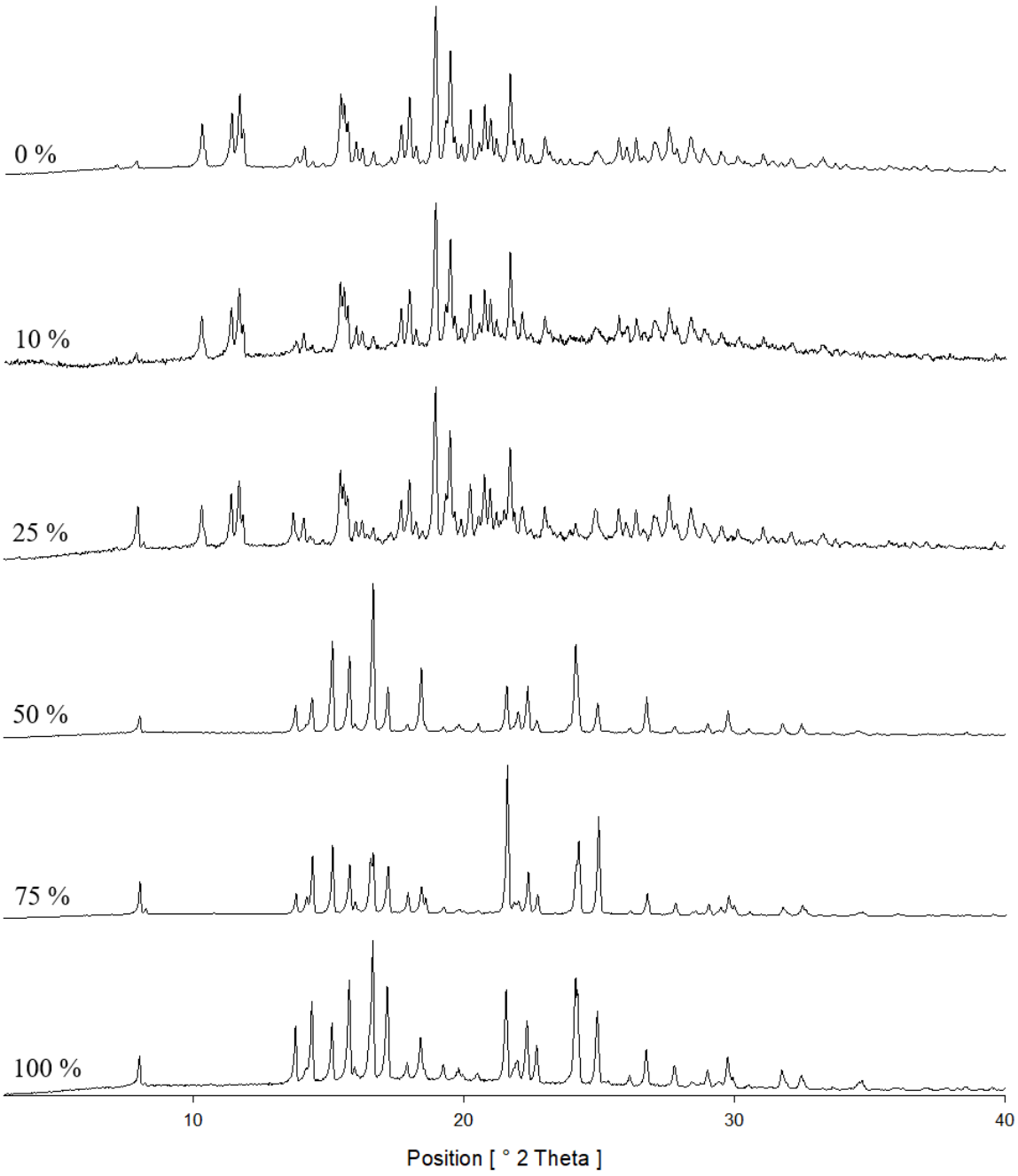

Supplementary Figure S15. X-ray diffractograms of each point on the phase diagram of the system 1-methyl-2-pyrrolidone:water.

7 ADDITIONAL PXRD ANALYSES OF THE FORMULATIONS

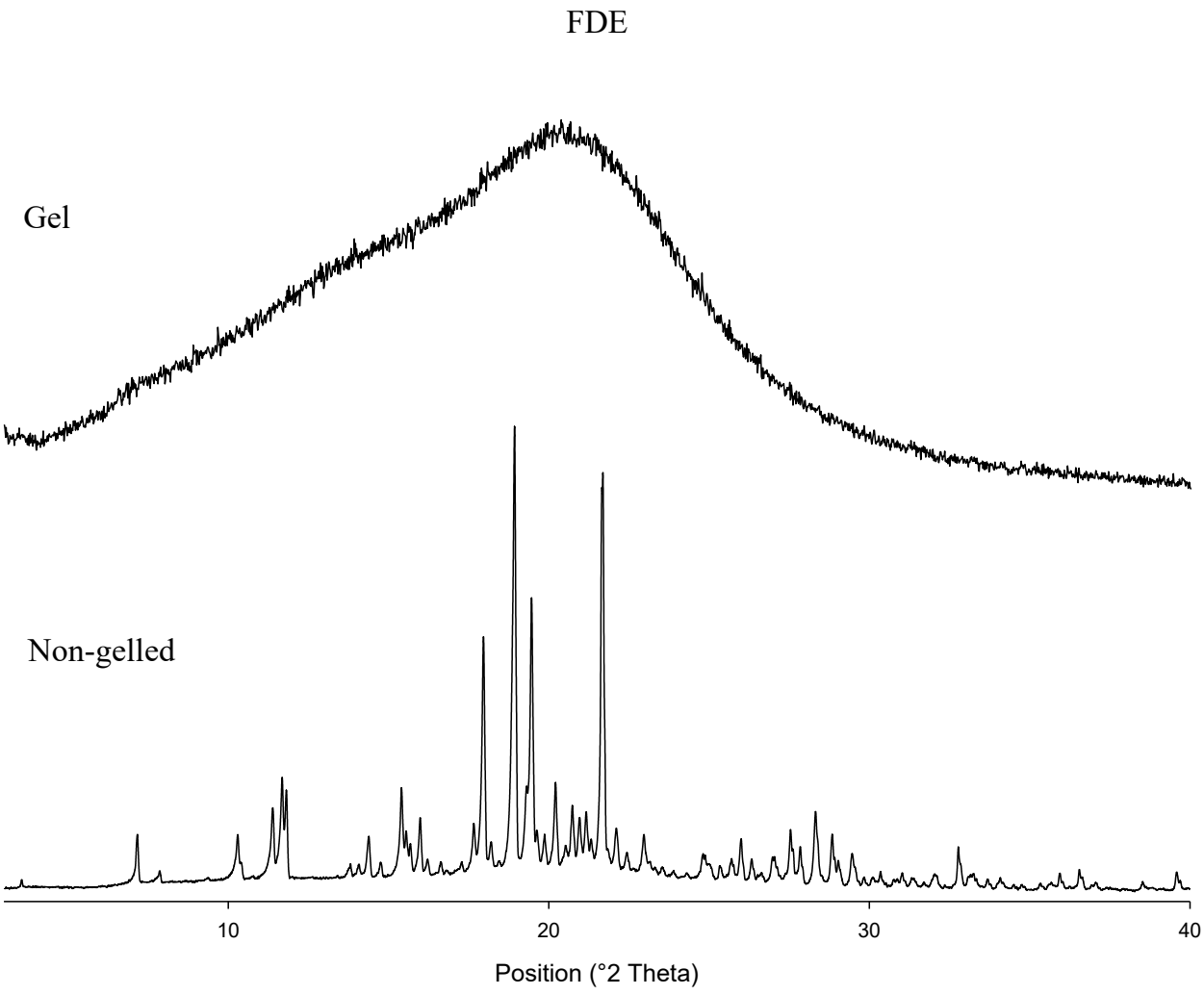

Supplementary Figure S16. PXRD patterns of FDE formulation (DEGEE:water) before and after gelation.

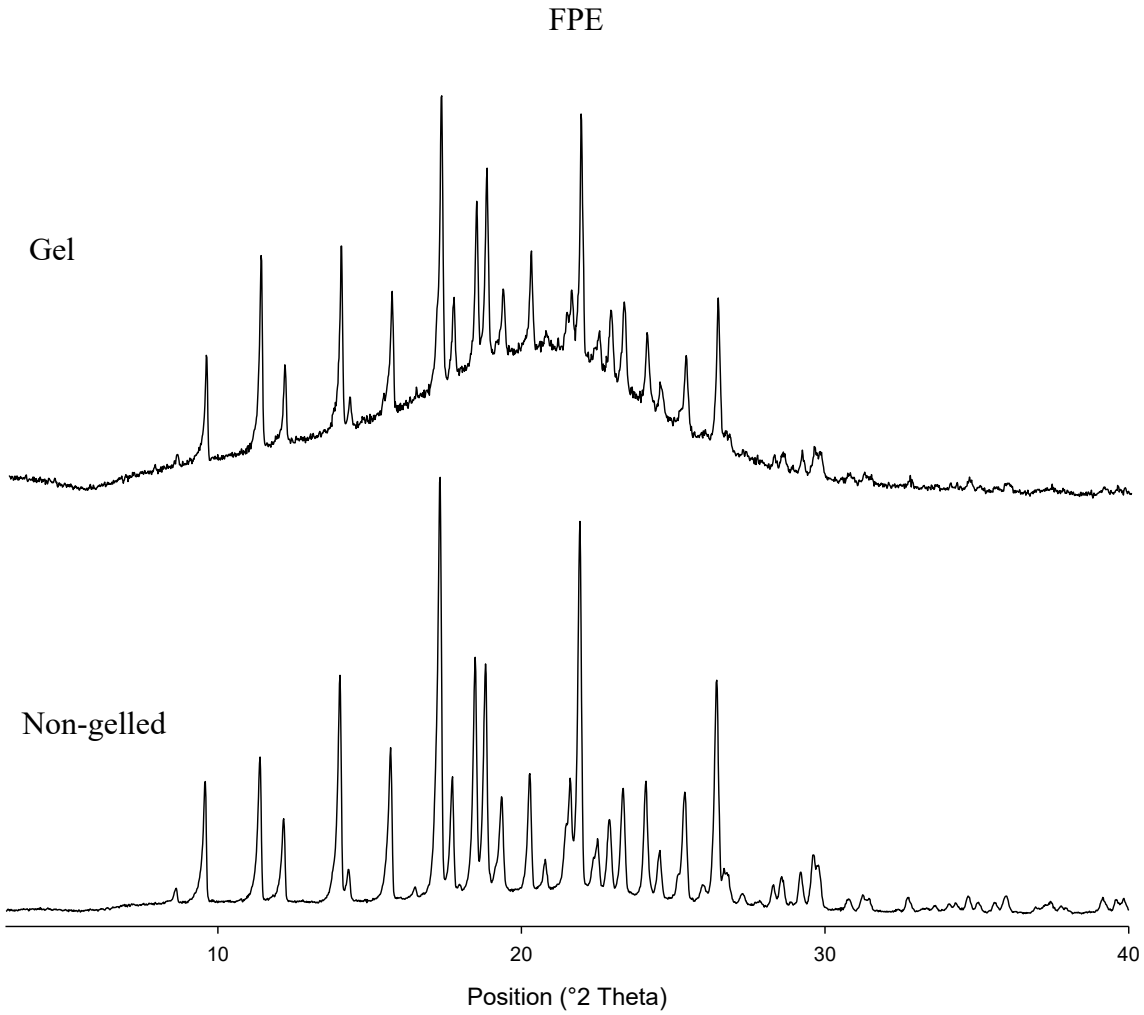

Supplementary Figure S17. PXRD patterns of FPE formulation (PEG 600:water) before and after gelation.

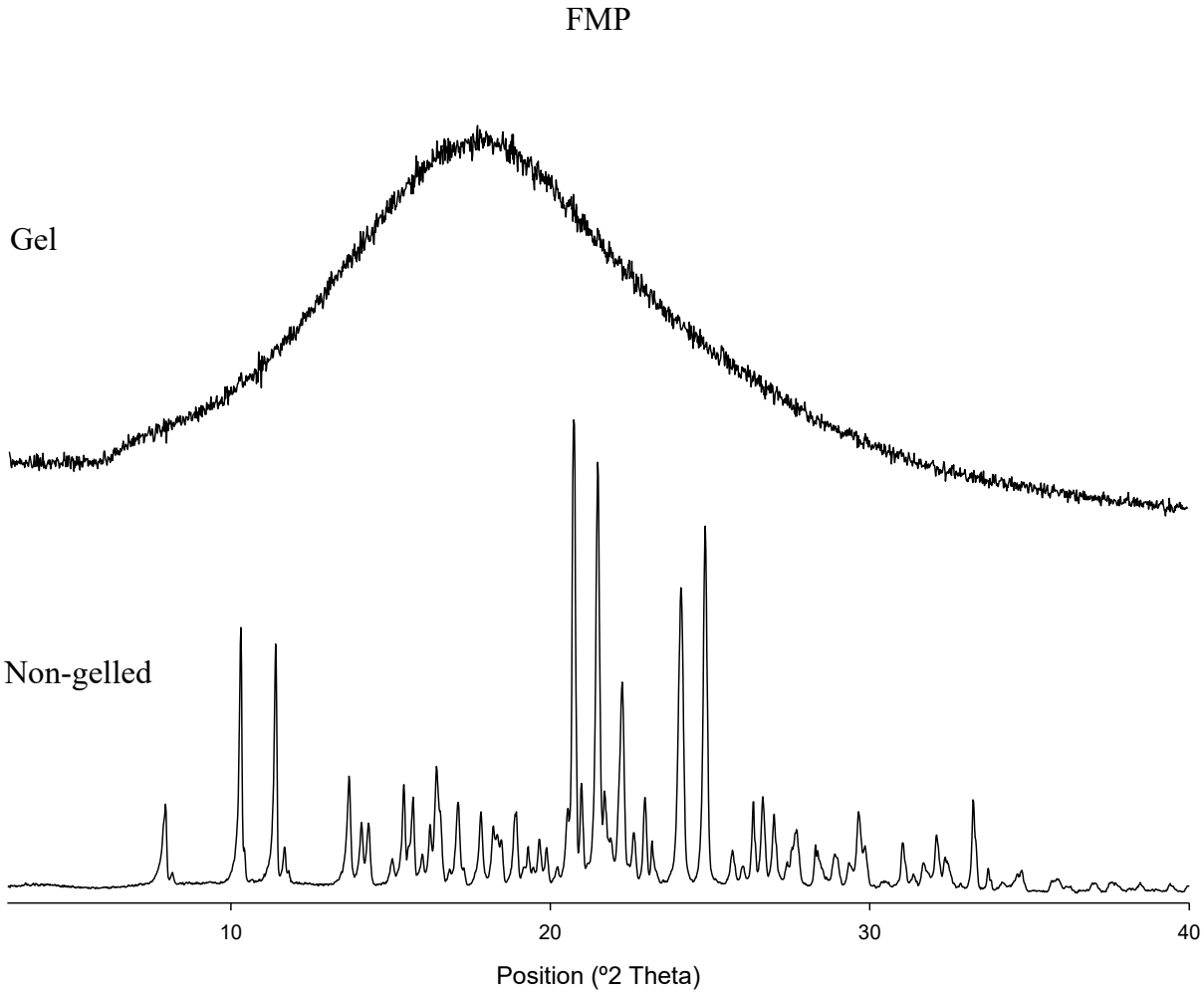

Supplementary Figure S18. PXRD patterns of FMP formulation (1-methyl-2-pyrrolidone:water) before and after gelation.

8 CHARACTERIZATION OF FORMULATIONS AFTER STORAGE

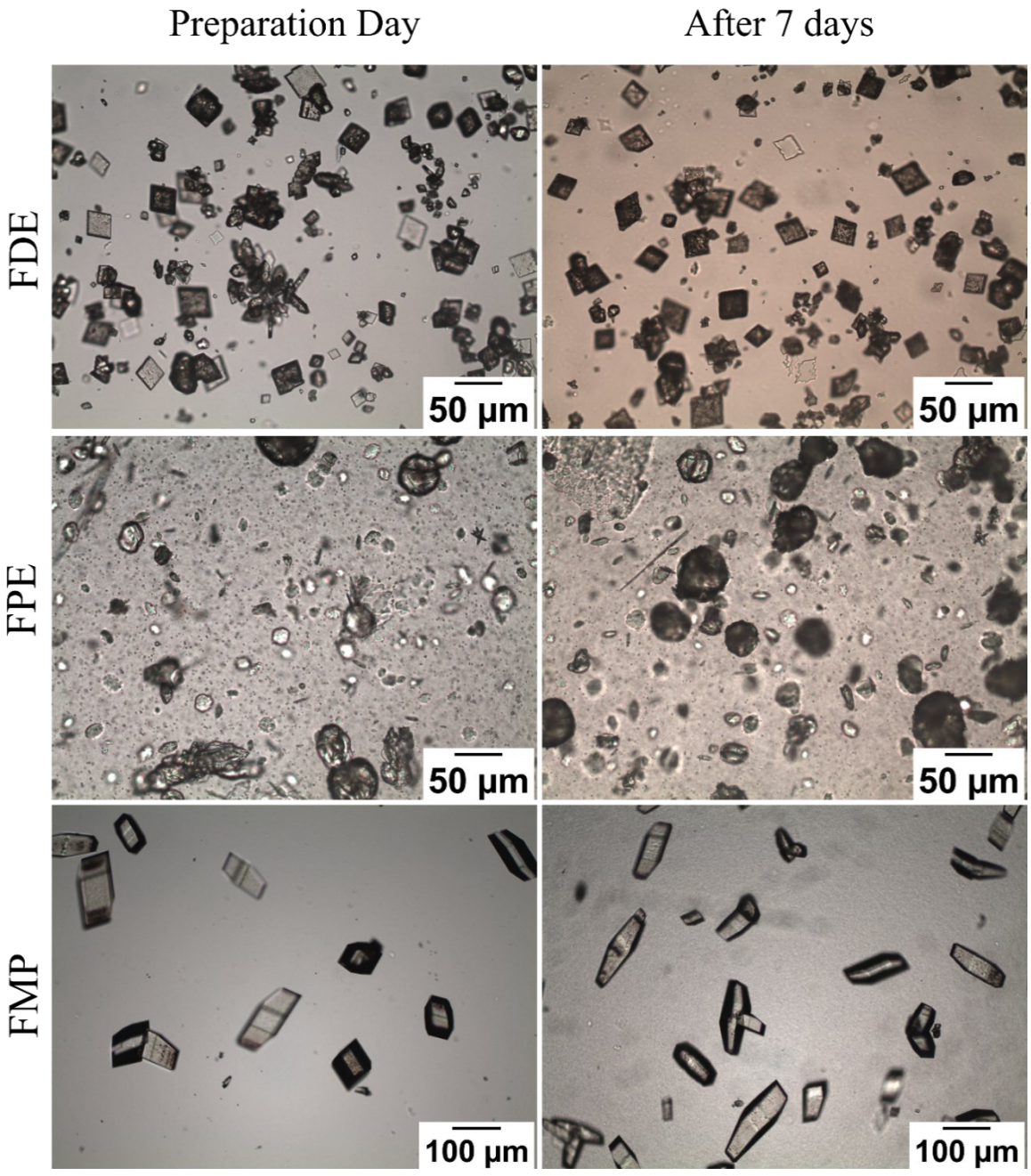

Supplementary Figure S19. Microscopy of the formulations immediately after preparation and after a 7-day storage. FDE, DEGEE:water; FPE, PEG 600:water; FMP, 1-methyl-2-pyrrolidone:water.

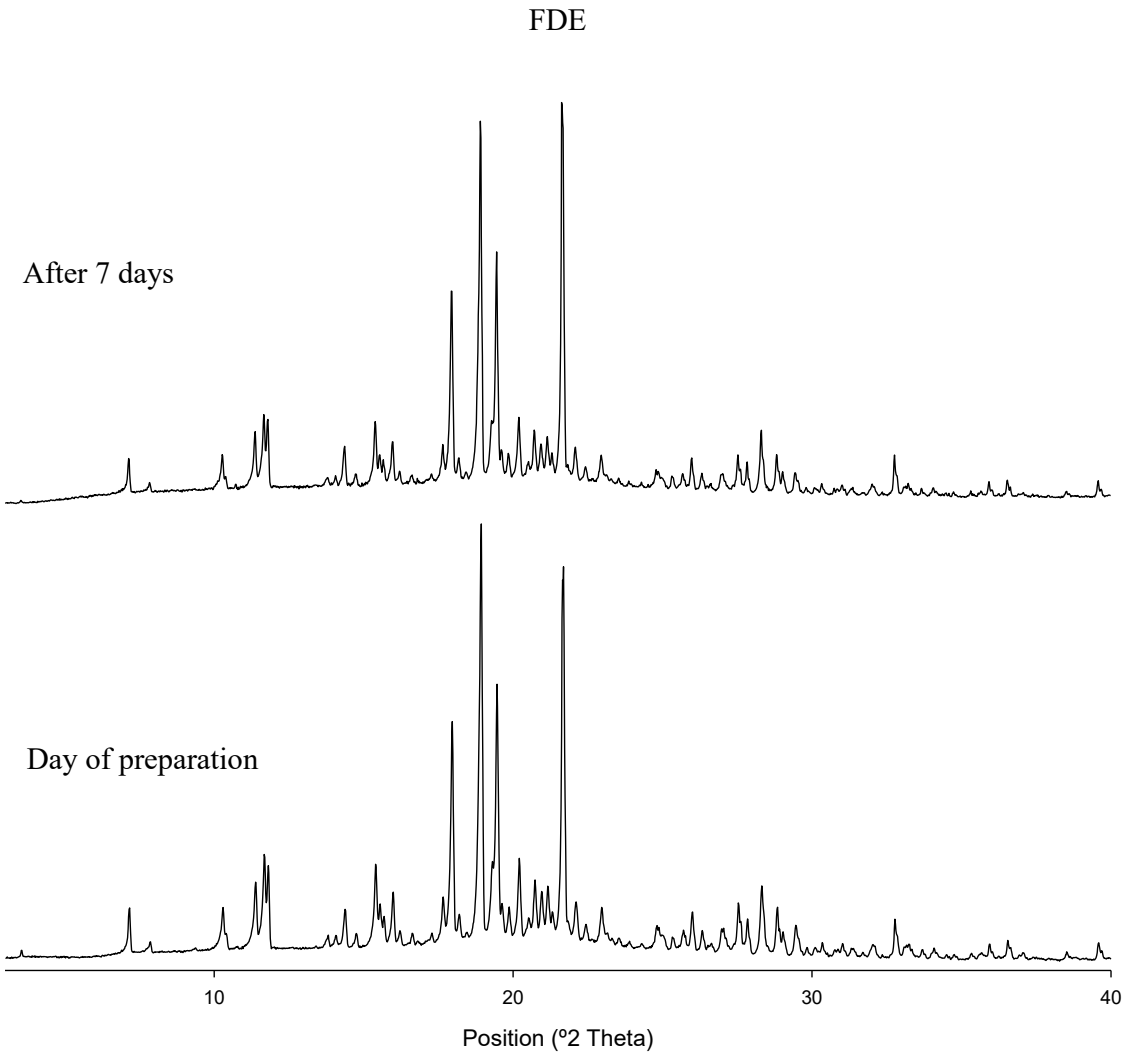

Supplementary Figure S20. PXRD patterns of FDE formulation (DEGEE:water) on the day of preparation compared to patterns collected after a 7-day storage.

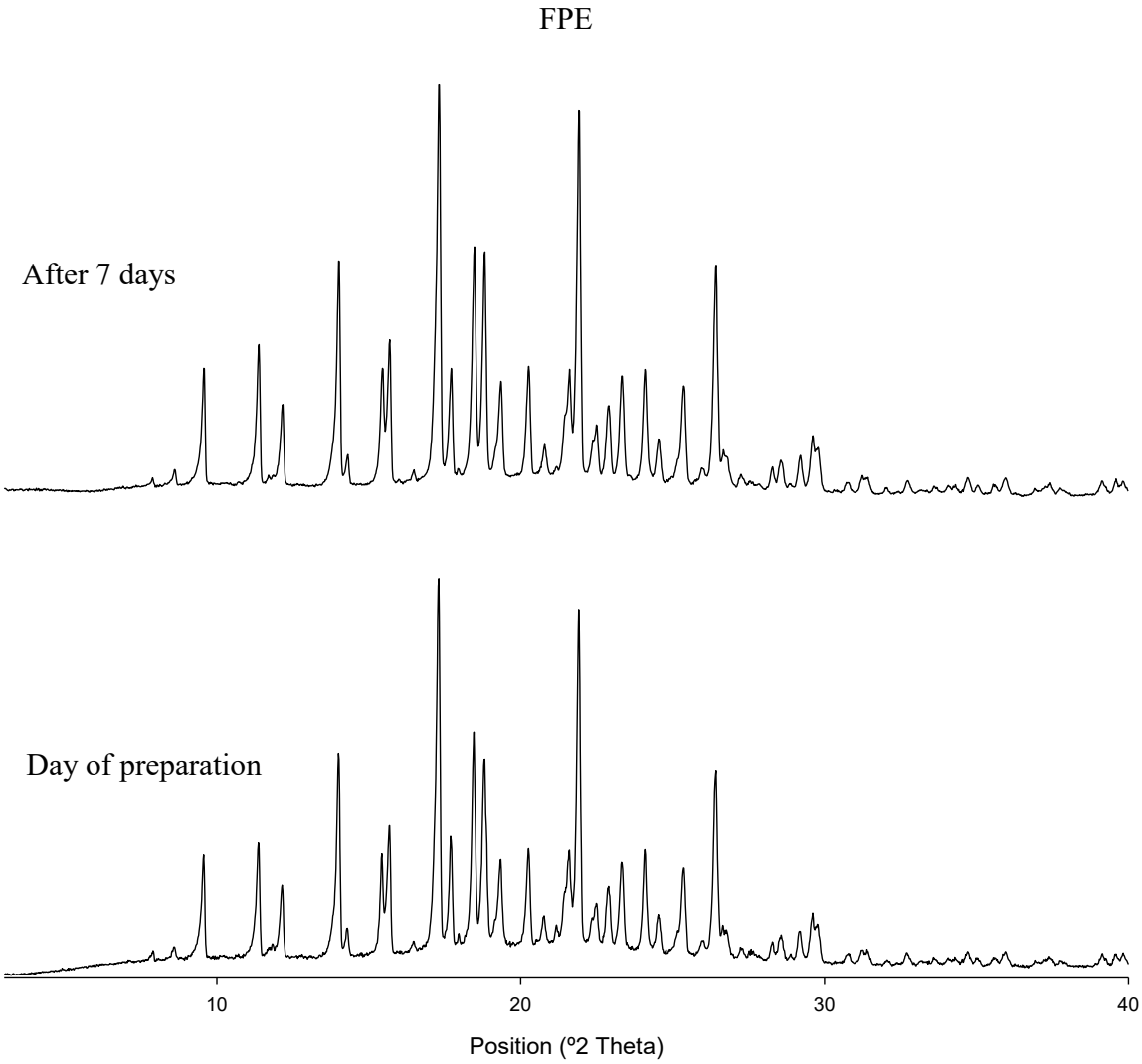

Supplementary Figure S21. PXRD patterns of FPE formulation (PEG 600:water) on the day of preparation compared to patterns collected after a 7-day storage.

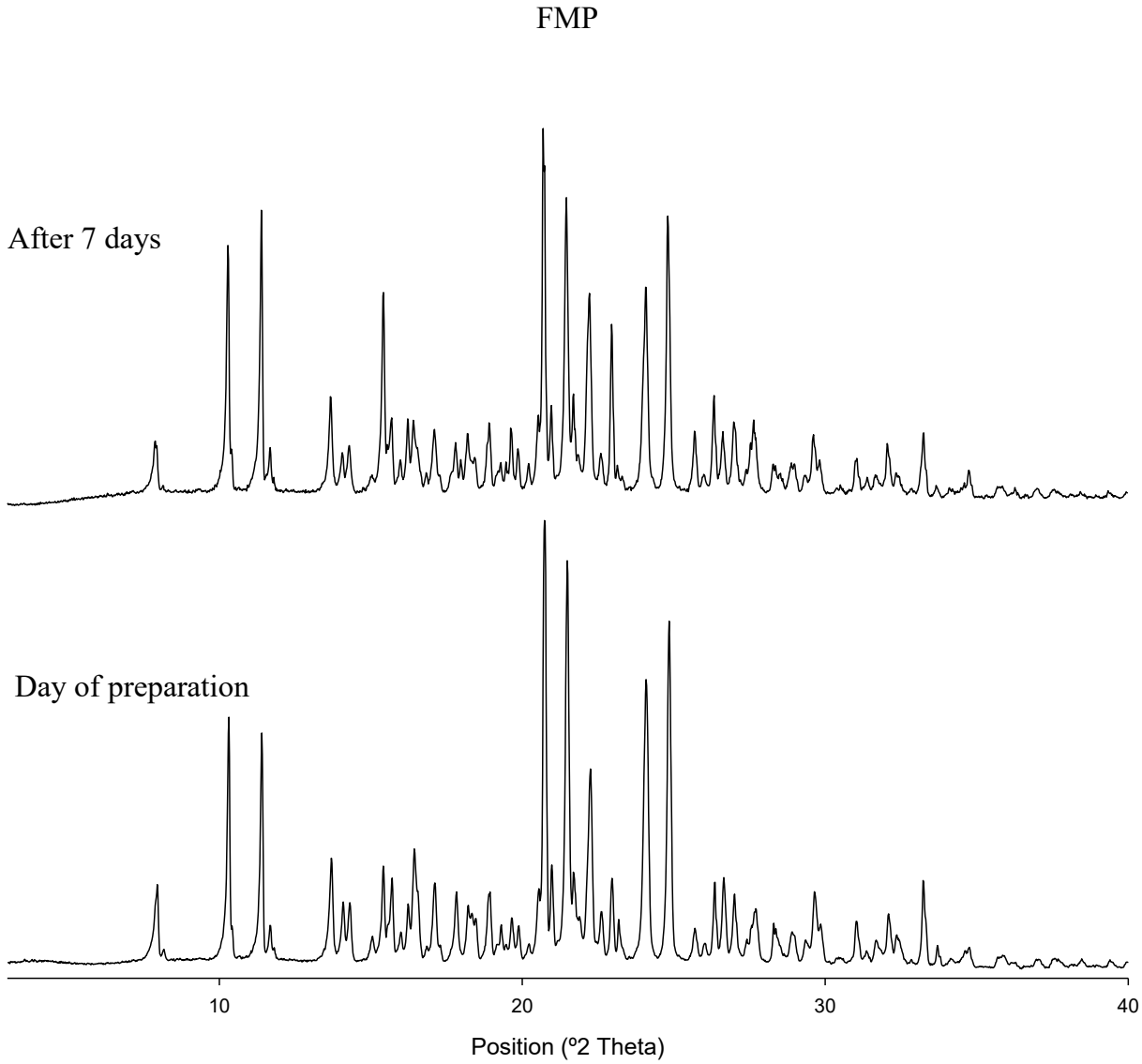

Supplementary Figure S22. PXRD patterns of FMP formulation (1-methyl-2-pyrrolidone:water) on the day of preparation compared to patterns collected after a 7-day storage.

References

(1) D.E. Braun, H. Krüger, V. Kahlenberg, U.J. Griesser, Molecular level understanding of the reversible phase transformation between forms III and II of dapsone, Cryst. Growth Des. 17 (2017) 5054–5060.

(2) M. Kuhnert-Brandstatter, I. Moser, Polymorphism of Dapson and ethambutoldihydrochloride, Microchim. Acta. 71 (1979) 125–136.

(3) A. Brandstaetter-Kuhnert, M. Kofler, R. Hoffmann, Microscopic characterization and identification of pharmaceuticals, IV. Sci. Pharm. 31 (1963) 140–148.

(4) H.S. Yathirajan, P. Nagaraja, B. Nagaraj, B.L. Bhaskar, D.E. Lynch, Experimental Crystal Structure Determination, CSD Commun. (2004).

(5) P. Chappa, A. Maruthapillai, R. Voguri, A. Dey, S. Ghosal, M.A. Basha, Drug-Polymer Co-Crystals of Dapsone and Polyethylene Glycol: An Emerging Subset in Pharmaceutical Co-Crystals, Cryst. Growth Des. 18 (2018) 7590–7598.

(6) H. Lemmer, N. Stieger, W. Liebenberg, M.R. Caira, Solvatomorphism of the antibacterial dapsone: X-ray structures and thermal desolvation kinetics, Cryst. Growth Des. 12 (2012) 1683–1692.